DEVELOPMENT OF POLYELECTROLYTE COMPLEX THIN FILMS FOR POLYMER SURFACE FUNCTIONALIZATION

A Dissertation

by

RYAN JOSEPH SMITH

Submitted to the Office of Graduate and Professional Studies of
Texas A&M University
in partial fulfillment of the requirements for the degree of

DOCTOR OF PHILOSOPHY

Chair of Committee,	Jaime C. Grunlan
Committee Members,	Lei Fang
	Sarbajit Banerjee
	Jeffrey Cirillo
Head of Department,	Simon North

August 2018

Major Subject: Chemistry

ABSTRACT

Polyelectrolyte complexes (PEC) are composites of two or more polyelectrolytes, that when processed appropriately, can create thin films. These films can have a wide array of properties and can serve to functionalize a wide variety of surfaces. This dissertation discusses the functionalization of polymeric surfaces with polyelectrolyte complexes. The layer-by-layer assembly method was used to sequentially build up the PEC on the substrate. This process generally requires several steps to manufacture a film of sufficient thickness and/or surface coverage. In an effort to reduce the number of processing steps to form PEC thin films, development of a single step deposition method was also developed.

Halloysite-based multilayer composites were found to significantly reduce the flammability of polyurethane foam. There was a 60% reduction in the peak heat release rate and total smoke release, and coated foam self-extinguished in open flame testing. This coating worked by forming a physical barrier that reduces heat and mass transfer during combustion, eventually leading to the flame extinguishing. Because of the environmentally-benign nature of the ingredients used, this coating provides a safe alternative to traditional flame retardant materials.

Polyelectrolyte complex multilayers were applied to polyester fabric and bacterial adhesion was significantly reduced after a simple water rinse. >99% of deposited bacteria was removed after rinsing. Bioluminescent *Staphylococcus aureus* was used to evaluate viable bacteria on the fabric surface. Electrostatic repulsion

between the negatively charged surface and the negatively charged bacteria combined with increasing surface roughness is believed to be the reason for reduced bacterial adhesion.

Polyelectrolyte complexes were deposited to polyester fabric and film in a single step. Film structure and morphology are dependent on how the film is cured (i.e. formation of electrostatic network). Rough aggregated films were found to form when the coating is cured while it is still wet on the substrate surface, and is ideal for coating complex substrates (e.g. fabric). This coating was found to reduce bacterial adhesion and >95% of deposited bacteria is removed after a simple rinse with water. When the PEC coatings are cured after the film is dried to the surface of the substrate, a conformal relatively smooth coating is formed, and when applied to PET film, reduces oxygen transmission by two orders of magnitude. The transparency of this coating was found to be dependent on the concentration and ionic strength of the buffer in which the films are cured. These processes significantly reduce processing steps required to deposit films with similar properties using layer-by-layer.

DEDICATION

I would like to dedicate this dissertation to my parents, Hugh and Carrie, the girls, my grandparents, Robert and Constance, and Eleasa for their constant support and love during this journey.

AKNOWLEDGEMENTS

I would like to thank my research adviser and committee chair, Dr. Jaime Grunlan, for providing the foundation (both financial and intellectual) to succeed as a graduate student. I thank Dr. Lei Fang, Sarbajit Banerjee, and Jeffrey Cirillo, for serving as my committee members, and for their help and advice throughout this process.

I would like to thank several people from Texas A&M: Dr. Wilson Serem of the Materials Characterization Facility, Michael Douglas and Jason Charanza of the Mechanical Engineering Department, Sandy Horton, Valerie McLaughlin, and Dr. Joanna Goody Pellois from the Chemistry Department.

I am grateful for the support and friendship from the members of the Polymer Nanocomposites Lab that I have worked with for the last 4 years. In particular, I would like to acknowledge Dr. Merid Haile, Dr. Bart Stevens, Dr. Yixuan Song, Shuang Qin, Simone Lazar, Dr. Chungyeon Cho, Dr. Marcus Leistner, Dan Stevens, Carolyn Long, Thomas Kolibaba and Dr. Igor Jordanov for the scientific and general discussion, and really making these last 4 years a pleasant experience. Thank you also to my undergraduate assistants Travis Smith, Danna Knight, Pablo Leon, and Kyle Falke, who have helped generate some of the data in this dissertation.

On a personal note I would like to thank Kevin Holder, Luke Johnson and Alex Kosanovich for their friendship.

NOMENCLATURE

AFM	Atomic Force Microscopy
ATR-FTIR	Attenuated Total Reflectance Fourier Transform Infrared Spectroscopy
BL	Bilayer
BPEI	Branched Polyethylenimine
HNT	Halloysite
LbL	Layer-by-layer
OTR	Oxygen Transmission Rate
PAA	Poly(acrylic acid)
PDDA	Poly(diallydimethylammonium chloride)
PEC	Polyelectrolyte Complex
PET	Poly(ethylene terephthalate)
pkHRR	Peak Heat Release Rate
PM	Polyelectrolyte Mixture
SEM	Scanning Electron Microscopy
TGA	Thermogravimetric Analysis
TSR	Total Smoke Release
UV-Vis	Ultraviolet-Visible Light Spectroscopy

CONTRIBUTORS AND FUNDING SOURCES

Contributors

This work was supported by a thesis committee consisting of Professor Jaime C. Grunlan as advisor, and Professors Lei Fang and Sarbajit Banerjee of the Department of Chemistry, and Professor Jeffrey Cirillo of the Department of Microbial Pathogenesis and Immunology.

Assistance in data analysis in Chapters IV and V was provided by Professor Jeffrey Cirillo and were published in 2017 in an article listed in Chapter IV.

All other work conducted for this thesis was completed by the student independently.

Funding Sources

Graduate research was supported by the Texas A&M Engineering Experiment Station (TEES).

TABLE OF CONTENTS

Page

LIST OF FIGURES

Page

LIST OF TABLES

Page

CHAPTER I

INTRODUCTION

1.1 Background

Polyelectrolyte complexes (PEC) deposited using layer-by-layer (LbL) assembly have been broadly developed to deposit thin films on a variety of surfaces. Coatings can be applied in ambient conditions and rely on complimentary interactions (e.g. electrostatic, hydrogen bonding, etc.) to sequentially build thin PEC films, which don't adversely affect the desirable properties of the substrate.[1-3] Coatings can be deposited by exposing the substrate to solutions using dipping,[3-5] spraying,[6-9] and spin coating.[10-12] Materials for these composites can included polymers,[13-14] clays,[9, 15] nano-particles,[16-17] dye molecules,[18-19] graphene oxide,[20-21] and carbon nanotubes.[4, 22] A few of the properties of LbL films include: gas barrier,[23-25] anti-reflection,[26-28] super hydrophobicity,[16-17] anti-corrosion,[9, 12, 21] flame retardancy,[29-30] and reduction of bacterial adhesion.[31-32]

Polyurethane foam (PUF) is widely used in the transportation, packaging, and furniture industries. PUF is also highly flammable and during combustion exhibits melt dripping and high heat release rates, both of which contribute to flame spread in a structure fire. Polyurethane decomposes into toxic diisocyanates that contribute to high smoke toxicity and deaths by asphyxiation.[33-34] From 2006-2010, 19% of all home fire deaths and $427 million annually in property damage stemmed from upholstered furniture (containing PUF).[35] Manufacture of flame retardant foam typically incorporates

halogenated compounds, which successfully reduces the danger of PUF in a fire scenario.[36-37] Despite their efficacy, these compounds have come under scrutiny due to suspected adverse effects on human and environmental health.[37-39] Efforts have been made to reduce their use in furniture to limit personal and environmental exposure.[40-41] LbL-assembled coatings have proven to be effective at reducing the flammability of PUF.[29-30] Polymer-only coatings have been evaluated,[42-46] but the most effective and developed are coatings using clay fillers.[47-54] These act by forming physical barriers that reduce heat and mass transfer during combustion. Recently, fillers with tube-morphology have been investigated.[55-56] These materials create a similar physical barrier to clay-containing coatings, but also significantly reduce smoke release during combustion.

Bacterial attachment to surfaces leads to the formation of large bacterial colonies (biofilms) surrounded by an extracellular network that provides structural support and protection from outside influences.[57] Surface-attached biofilms can lead to medical device failure (e.g. catheters, contact lenses, textiles, and implanted devices).[58-59] Biofilm formation can also lead can also lead to dangerous infections.[60-62] There is an immense body of research focused on modifying various surfaces to reduce bacterial adhesion. PEC deposited using layer-by-layer assembly has been shown as a versatile method for combatting bacterial adhesion.[31-32] The two main strategies for reducing adhesion are by modifying the surface to reduce favorable interactions,[63-74] or by creating a surface that kills the bacteria either by releasing bactericidal agents,[75-88] or by direct contact.[89-100]

1.2 Dissertation Outline

Chapter II discusses the properties and applications of polyelectrolyte complexes. Layer-by-layer assembled thin films, which reduce the flammability of polyurethane foam and reduce bacterial adhesion are highlighted. Additionally, other deposition techniques of PEC thin films as an alternative to LbL are discussed.

Chapter III investigates a polyelectrolyte nanocomposite coating using environmentally benign halloysite (HNT) clay to reduce the flammability of polyurethane foam. Deposition of polyelectrolyte stabilized HNT using LbL is investigated. The flame retardant efficacy is evaluated and the composition of the coating after burning is evaluated to elucidate flame retardant mechanism.

Chapter IV explores polyelectrolyte complex coatings to reduce bacterial adhesion to polyester fabric. The effects of morphology and surface wetting are evaluated as a function of deposition cycles. The antifouling is quantified using a bioluminescent assay that can detect living bacteria on the fabric surface.

Chapter V highlights an improvement upon the LbL process by depositing PEC thin films in a single step. Thin film properties are evaluated as a functions of processing parameters, and based on how these films are processed, different properties are explored. Films were evaluated to effectively reduce bacterial adhesion, while the same PEC deposited in a different manner proves to be effective at reducing oxygen transmission through a polyester film.

Chapter VI provides concluding remarks and outlines topics of future research. Improvement of various properties of PEC films is also discussed. Oxygen barrier films can be improved by studying and optimizing the charge compensation within a deposited PEC. Flame retardant coatings for blended fabrics can be improved by modifying amine-containing polymers with melamine. Coatings that reduce bacterial adhesion can be more effective by incorporating ionic bactericidal agents during PEC formation.

CHAPTER II

LITERATURE REVIEW*

2.1 Polyelectrolyte Complexes

Macromolecular in nature, polyelectrolytes exhibit some degree of charge density depending on monomer chemistry and the environment.[101-102] Polycations are usually amine-based, and, depending on pH, can adopt a positive charge in aqueous media and are considered weak polyelectrolytes (e.g. branched polyethylenimine (BPEI), poly(vinyl amine) (PVA), etc.). Quaternary ammonium species in polymer systems are considered strong polyelectrolytes due to lack of charge density dependence on pH (e.g. poly(diallydimethylammonium chloride) (PDDA)). Polyanions are more varied, but typically contain of polycarboxylates, sulphonates, or phosphates (e.g. poly(acrylic acid) (PAA), poly(styrene sulfonate) (PSS), and sodium hexametaphosphate (PSP) respectively). Depending on the pKa of the side group, polyanions can be either weak or strong polyelectrolytes (e.g. PAA and PSS, respectively) in aqueous environments. These polyelectrolytes often have good solubility in water, making them ideal candidates for environmentally-friendly polymer coating systems. Of particular interest are the interactions of oppositely charged polyelectrolytes mixed in aqueous media. **Figure 2.1** shows several examples of polycations and polyanions.

* Reprinted with permission from Smith, R. J.; Holder, K. M.; Ruiz, S.; Hahn, W.; Song, Y.; Lvov Y. M.; Grunlan, J. C. Environmentally-benign halloysite nanotube multilayer assembly significantly reduces polyurethane flammability. *Adv. Funct. Mater*. **2017**, 1703289. Copyright 2017 WILEY-VCH Verlag GmbH & Co. KGaA.

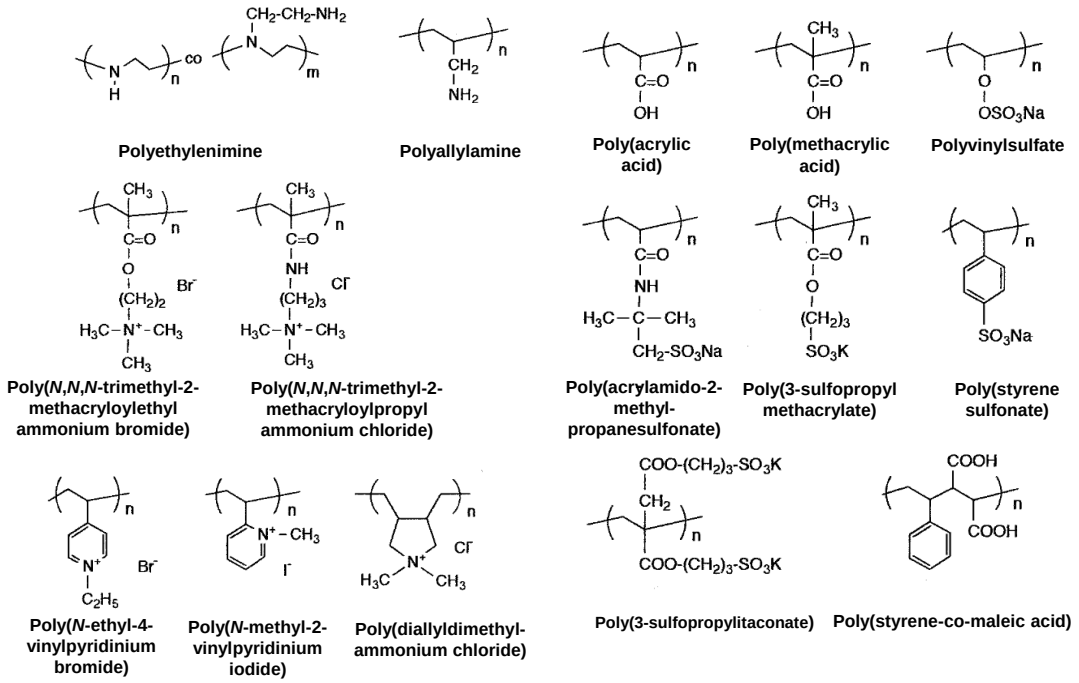

Figure 2.1. Examples of polycations and polyanions.[101] Adapted with permission from Bertrand, P.; Jonas, A.; Laschewsky A.; Legras R. Ultrathin polymer coatings by complexation of polyelectrolytes at interfaces: suitable materials, structure, and properties. *Macromol. Rapid Commun.* **2000**, *21*, 319.

Polyelectrolyte complexation occurs along a spectrum depending on pH and salt concentration, as shown in **Figure 2.2**.[103] Complexes between two polyelectrolytes can form dense liquid-like coacervates,[104] or an insoluble solid precipitate.[105] Coacervates are viscous fluids of loosely interacting and highly hydrated polyelectrolytes. They were first explored in 1929 where their formation, and reaction conditions (including pH and ionic strength) were explored, but there was little evaluation of the coacervate products.[104, 106] Coacervates are formed when the ideal amount of salt is introduced to a polyelectrolyte complex mixture. This causes shielding of the coulombic interactions

and the polyelectrolytes loosely associate with one another. Since there is no expulsion of small ions and water, a solid complex does not form, the coacervate remains hydrated, leading to a viscous liquid-like substance.[107] Coacervates can be formed between two strong polyelectrolytes such as PDDA and PSS by introducing salt.[103, 108] Mixtures of strong and weak polyelectrolytes through, a combination of pH and ionic strength control (e.g. PAH and PAA), can also lead to coacervates and their viscosity can be tuned with salt content and pH.[109-111] Coacervates can also be observed as microscopic phase separations, which will coalesce into a macroscopic, two phase system with time and elevated temperature.[112] Fu *et al*. found that different polyion pairs vary in their association strength based on the concentration of KBr needed to dissolve the formed PEC.[102] They found that more hydrated polyanions like PAA have weaker interactions and are better suited for coacervate formation. Conversely strongly interacting polyelectroltyes like PAH and PSS form strong/glassy complexes that are more resistant to added salt. Since coacervates behave like a liquid, there is significant potential to develop methods to deposit them as functional polyelectrolyte complex (PEC) thin films.

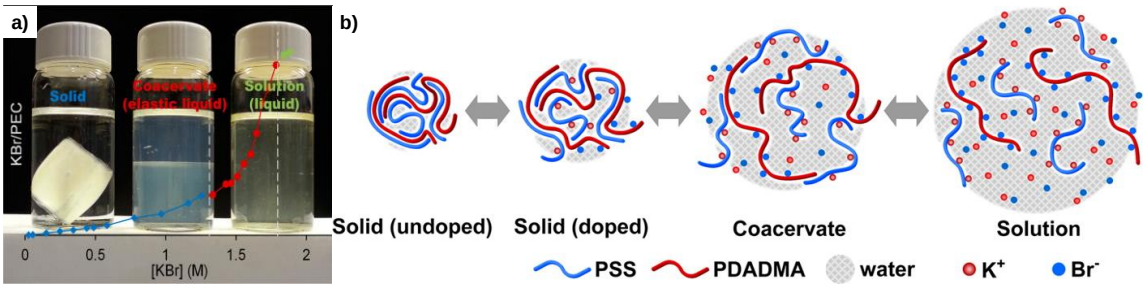

Figure 2.2. Polyelectrolyte complex composition as a function of salt concentration (a). Schematic of PEC phase compositions with increasing salt concentration (b).[103] Adapted with permissions from Wang, Q.; Schlenoff, J. B. The polyelectrolyte Complex/Coacervate Continuum. *Macromolecules*, **20141b** *47* (9), 3108. Copyright 2014 American Chemical Society. https://pubs.acs.org/doi/abs/10.1021/ma500500q Further permissions related to the material excerpted should be directed to the ACS.

The first evaluation of an insoluble polyelectrolyte complex was reported in 1949, where the turbidity was measured of different suspensions of polyacrylate and poly-4-vinyl-*n*-*N*-butylpyridonium bromide complexes.[105] Electrostatic interactions between polycations and polyanions form PEC's which can be insoluble solid materials or suspended microparticles, depending on ionic strength and mixing ratio.[112] These interactions between macromolecules are favored due to the large entropic gains from small counterion and water expulsion during complexation.[113] Formation of complexes can be exothermic or endothermic depending on pH[114] and salt concentration.[115] Alonso *et al*. found that PDDA and PAA complexation became more endothermic as the pH of PAA increased.[114] PAA undergoes more hydration with increasing pH and water coordination with carboxylate groups needs to be disrupted in order for the complex to form. Usually the stoichiometry of the complexed repeat units is 1:1, but studies have shown that this ratio can be changed with added salt, changing the order of mixing, and

differences in molecular weight.[113, 116-117] As functional thin films, polyelectrolyte complexes have a myriad of uses, but deposition of premade complexes is very difficult due to their insoluble nature in aqueous media.[118] The following section will outline the deposition of PEC thin films using layer-by-layer assembly.

2.2 Layer-by-Layer Deposition of Polyelectrolyte Complexes

The most well established method for depositing polyelectrolyte complex thin films is layer-by-layer (LbL) assembly. First reported by Iler at DuPont in 1966, it was suggested that thin films could be assembled on substrates using sequential deposition cycles with oppositely charged colloidal particles.[119] It was observed that discrete thickness increases could be achieved with increased deposition cycles. The technique didn't gain traction until 1992 when Decher reported the assembly of oppositely charged polyelectrolytes.[120] These films were also found to withstand water rinsing, stay relatively smooth during deposition, and were optically transparent. These LbL deposited polyelectrolyte complexes have garnered significant study over the last 30 years.

Layer-by-layer assembly is a relatively simple and environmentally benign technique (usually water-based) in which a substrate is alternately and sequentially exposed to materials with complimentary interactions to sequentially form a PEC.[1-3] A typical deposition starts by adapting substrate to the surface to promote polyelectrolyte adsorption (generally through imparting surface charge). The prepared substrate is then exposed to a polyelectrolyte with the opposite charge of the surface. The polyelectrolyte

adsorbs to the surface, usually through electrostatic and van der Waal's interactions. The loosely adhered/excess polyelectrolyte is typically rinsed and dried (although this isn't always necessary). The substrate is then exposed to a polyelectrolyte of opposite charge. The oppositely charged polyelectrolyte adsorbs through electrostatic interactions and through the entropic gains from the exclusion of small counterions and water. This constitutes the formation of one bilayer (BL) and the process is repeated until the desired thickness is achieved. **Figure 2.3** highlights this process schematically.

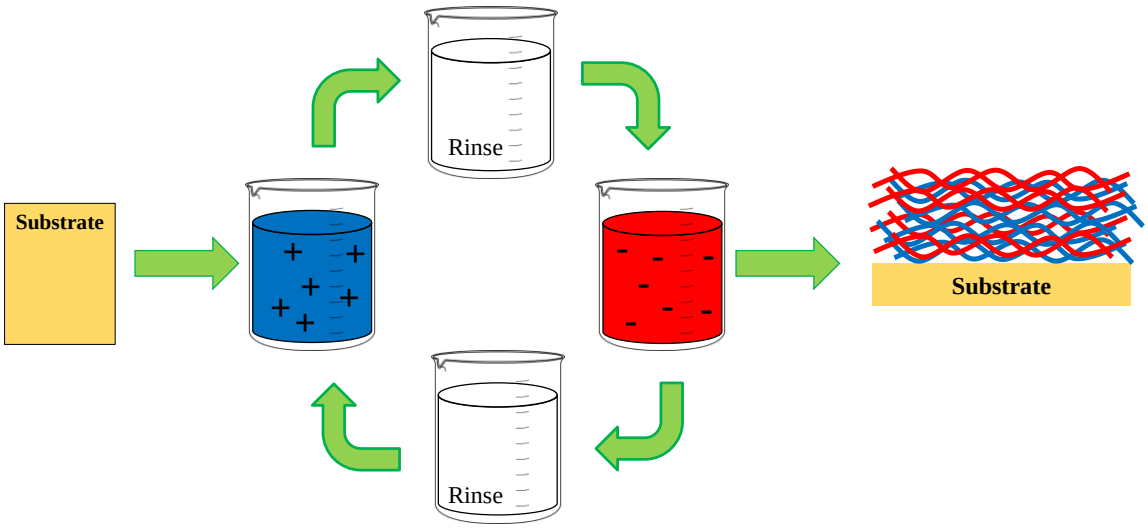

Figure 2.3 Schematic of layer-by-layer assembly.

Substrate exposure can consist of dipping,[3-5] spraying,[6-9] and spin coating.[10-12] The vast majority of these interactions are electrostatic in nature, but other complimentary interactions can be used, such as hydrogen bonding.[121-122] The chemistry

of layering materials is diverse and film properties (e.g. thickness, transparency, roughness etc.) can be tailored by changing temperature,[123-124] pH,[13, 125-126] salt concentration (i.e. ionic strength),[127-128] and buffering capacity.[129-130] Coating materials aren't restricted to just polymeric materials, clays,[9, 15] nano-particles,[16-17] dye molecules,[18-19] graphene oxide,[20-21] and carbon nanotubes,[4, 22] among others, can all be used to construct these nanocomposite coatings. These systems are not restricted to just bilayer assemblies. Trilayer[19, 131-132] and quadlayer[14, 133] assemblies can be constructed, incorporating many chemistries into the final composite coating. Because of the flexibility of the LbL technique there are a wide array of properties and substrates that can be modified. A few of the properties of LbL films include: gas barrier,[23-25] anti-reflection,[26-28] super hydrophobicity,[16-17] and anti-corrosion.[9, 12, 21] The following sections will highlight research focusing on multilayer assemblies that impart flame retardancy to polyurethane foam, and polyelectrolyte complex coatings that reduce bacterial adhesion.

2.2.1 Layer-by-Layer Flame Retardants for Polyurethane Foam

Polyurethane foam (PUF) has many desirable properties (e.g. flexibility, strength, cost, etc.) and is widely used in the transportation, packaging, and furniture industries. PUF is also highly flammable and during combustion exhibits melt dripping and high heat release rates, both of which contribute to flame spread in a structure fire. The polyurethane decomposes into toxic compounds (diisocyanates) that contribute to high smoke toxicity and deaths by asphyxiation.[33-34] From 2006-2010, 19% of all home fire

deaths and $427 million annually in property damage stemmed from upholstered furniture (containing PUF).[35] Manufacture of flame retardant foam typically incorporated halogenated compounds, which successfully reduced the danger of PUF in a fire scenario.[36-37] These halogenated agents form halide radicals that abstract hydrogen. The resulting hydrogen halide reacts with hydrogen or hydroxyl radicals in the gas phase that form hydrogen or water, respectively. This reaction acts to limit the combustible gasses in the flame zone and eventually halts the spread of the fire.[134-135] Despite their efficacy, these compounds have come under scrutiny due to suspected adverse effects on human and environmental health.[37-39] To help reduce the use of these materials in furniture, the California 117B safety bulletin removed the requirements that PUF in furniture needed to resist an open flame.[40-41] While the intentions of minimizing the impact on the environment and human health are good, open flame ignition of upholstered furniture still contributes significantly (either as an ignition source or as a source of flame spread) in ~1/3 of structure fires.[33] As a result, there is a need to develop more environmentally-benign solutions to combat PUF flammability.

Due to its complex geometry, applying a uniform coating to the surface of polyurethane foam is difficult. Layer-by-layer assembly can overcome these difficulties by applying conformal coatings directly to the surface of PUF without impairing the inherent characteristics of the foam (e.g. porosity). LbL coatings have been employed to reduce PUF flammiblity.[29-30] Laufer *et al.* prepared multilayers of chitosan (CH) and poly(vinyl sulfonic acid sodium salt) (PVS). This coating, during combustion, degrades to form SO_2 gas and dilutes/displaces oxygen in the gas phase, slowing combustion and

leading to self-extinguishing behavior.[42] This coating also prevents melt dripping and shows extensive char formation on the surface. Carbohydrate containing coatings are suspected to lead extensive char formation during combustion, which usually shows a significant reduction in the peak heat release rates. This was demonstrated by Wang *et al*. who used CH and sodium alginate multilayers to reduce the peak heat release rate (pkHRR) by 66%.[43] This coating is also a good example of an environmentally and health-friendly coating as it is composed of two naturally abundant and safe polysaccharides. Insulating char can also be formed using an intumescent composite coating. Carosio *et al.* has developed several of these systems, utilizing CH and various phosphorous containing polymers.[44-46] Due to char formation, these coatings typically reduce pkHRR, but do little to preserve the underlying foam and in one case increased the total smoke released during combustion.[44] However they were able to demonstrate the deposition of 2 BL in 2.5 seconds,[46] which if applied correctly and with a more efficient flame retardant system could improve the commercial appeal of the LbL process to flame retard PUF (**Figure 2.4**).

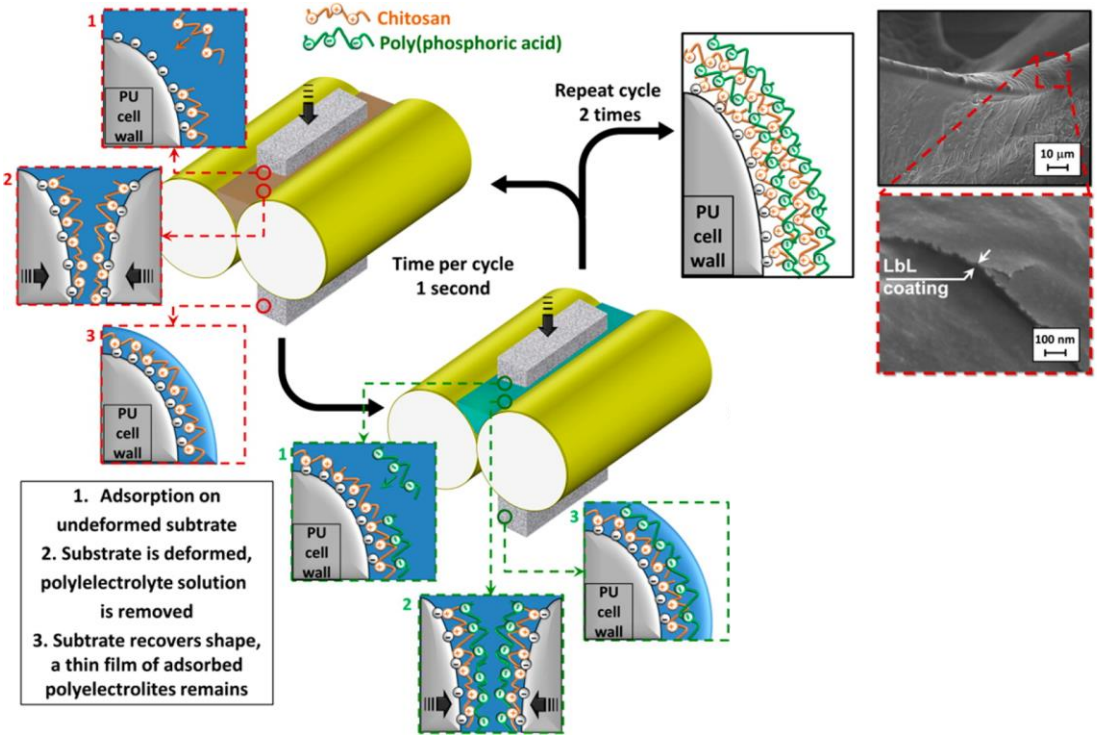

Figure 2.4. Schematic of rapidly deposited FR multilayers onto polyurethane foam. Processes like this highlight the commercial feasibility of the layer-by-layer process.[46] Adapted from Carosio, F.; Alongi J.; Ultra-fast layer-by-layer approach for depositing flame retardant coatings on flexible PU foams within seconds. *ACS Appl. Mater. Interfaces*, 2016, *8* (10), 6315. Copyright 2016 American Chemical Society.

Incorporating clay platelets into a multilayer assembly has proven an effective method for reducing the flammability of polyurethane foam. Laufer *et al*. was the first to explore this concept by combining CH with montmorillonite (MMT) clay.[47] 10 BL reduced pkHRR by 52%, prevented any melt dripping and preserved the interior of the foam. This coating is also completely from naturally abundant sources. A separate studied showed that increasing clay composition during deposition improved flame retardant properties.[48] The same study highlighted the durability of these coatings by

showing only a marginal reduction in flame retardant properties after compression testing. These coatings act by creating a clay-rich char layer on the surface of the foam that acts as a physical barrier, shielding the inner portion from heat and prevents combustion. Cain *et al*. highlighted the importance of char formation by incorporating PSP into trilayers with PAH and MMT (**Figure 2.5**).[49] Compared to the CH/MMT coating, PAH and PSP can promote char formation, while the MMT provides a physical/thermal barrier and required less coating to reduce the pkHRR by 55%. This study showed the synergy between intumescence and clay leading to increased char formation and better flame retardant properties. This combination of materials was expanded by Holder *et al*. by combining 4 bilayers of CH and vermiculite (VMT) with 20 bilayers of CH and ammonium polyphosphate (APP).[50] CH/APP by itself forms a char during combustion through intumescence, but due to the underlying polyurethane foam collapsing, the char collapses as well due to lack of support from the substrate. The clay coating by itself behaved similar to other clay-containing coatings by preserving the interior of the sample during an open flame test. When the two are combined, the resulting coating almost completely resists an open flame and reduces in the pkHRR by 66%. This is due to the underlying VMT-based coating providing structural support for the intumescent char to successfully form. This coating has two drawbacks: the number of processing steps and the increased smoke released from the intumescent coating.

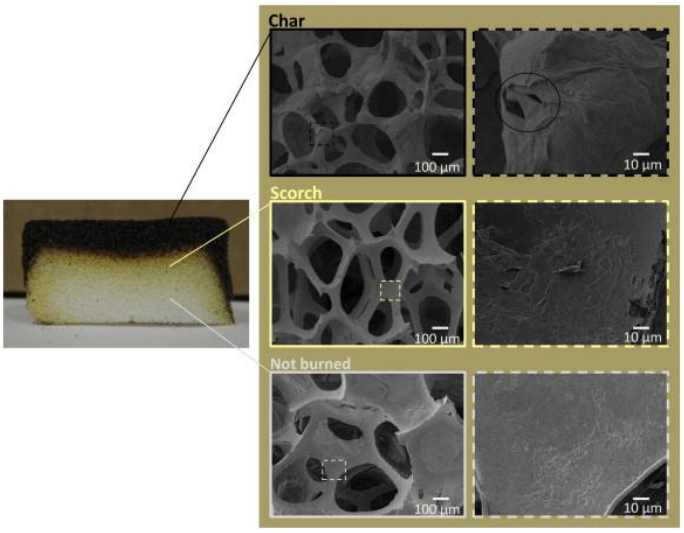

Figure 2.5. Cross section photograph of 10 PSP/PAH/MMT TL on PUF (left). SEM images of coated foam after burning (right).[49] Reproduced with permission from Cain, A. A.; Nolen, C. R.; Li, Y.; Davis, R.; Grunlan, J. C. Phosphorous-filled nanobrick wall multilayer thin film eliminates polyurethane melt dripping and reduces heat release associated with fire. *Polym. Degrad. Stab.* **2013**, *98* (12), 2645. Copyright 2013 Elsevier Ltd.

Due to the success of these clay-based coatings, efforts to reduce the number of processing steps have been made to improve the industrial feasibility of LbL-assembled flame retardants. Kim *et al*. coated a full-size chair with 2 BL of a MMT-based coating.[51] Not only was there a significant reduction in the pkHRR, there was no melt dripping, and the original shape was maintained with significantly reduced processing steps (**Figure 2.6**). This highlights an important aspect of these flame retardant treatments (i.e. they will not keep objects from burning in a structure fire), but they will reduce the spread of a fire, providing more time to escape safely. Cain *et al*. was able to reduce processing steps by depositing1 BL of BPEI and VMT, which significantly reduced pkHRR and TSR (54% and 31% respectively) and prevented melt dripping.[52] It

was suggested that this significant improvement with VMT is due to a larger aspect ratio than MMT, creating a more efficient thermal barrier and reduced mass transfer during combustion due to fewer gaps between platelets.

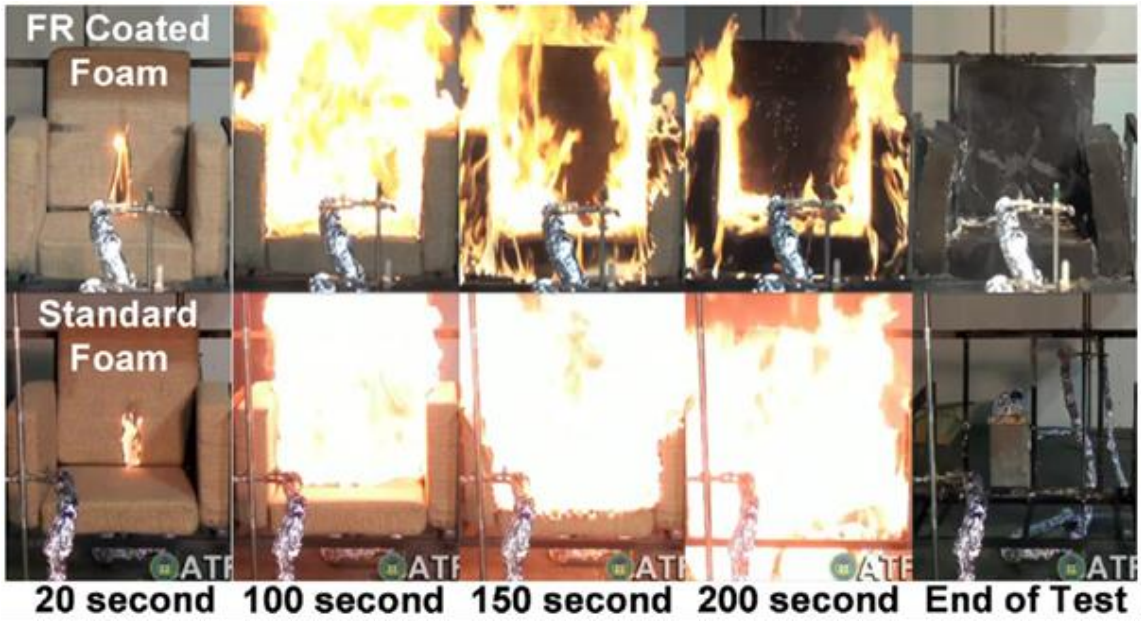

Figure 2.6. Images of full a scale LbL coated foam chair (top) that burns less than an uncoated chair (bottom).[51] Adapted with permission from Kim, Y. S.; Li, Y.; Pitts W. M.; Werrel M.; Davis, R. D. Rapid growing clay coatings to reduce the fire thereat of furniture, *ACS Appl. Mater. Interfaces*, **2014**, *6* (3), 2146. Copyright 2014 American Chemical Society.

Patra *et al*. developed a one bilayer boehmite (BMT) and VMT coating that prevented melt dripping and reduced pkHRR and TSR by 50%.[53] The alumina hydrate in BMT undergoes an endothermic dihydroxylation, which absorbs heat during combustion and leaves behind insulating aluminum oxide. Layered double hydroxides (LDH) were compared to MMT in films containing BPEI and PAA.[54] LDH-containing films decreased the pkHRR by 10% relative to MMT-containing films. LDH also undergoes

an endothermic dehydration, suggesting this mechanism can significantly reduce heat release rates in a flame retardant composite. Aluminum hydroxide based "cooling" FR coatings were further investigated by Haile *et al*. by introducing aluminum trihydrate (ATH) into a LbL assembled film.[136] Incorporation of ATH lead to self-extinguishing of foam during torch testing and a 64% reduction in the pkHRR.

Aside from clay platelets, other nano-fillers have been used in FR multilayers for PUF (nanotubes are of particular interest). Pan *et al*. assembled CH, alginate (AL), and titanate nanotubes in trilayers (TL) on the surface of PUF.[55] 6 TL reduced the pkHRR by 70% and the TSR by 41%, while only adding 5.7wt% to the sample. Analysis of the pyrolosis products using FTIR showed no difference between uncoated and coated samples, suggesting the TNT acts as physical barrier to prevent heat and mass transfer. Carbon nanotubes (CNT) have also been incorporated into multilayers for flame retardation.[56] 6 BL of pyrene-modified BPEI/PAA-stabilized CNT reduced the pkHRR by 67% and TSR by 80%. This study was also significant because at 9 BL, it is the only example of coated foam self-extinguishing during vertical flame testing (VFT). It was suggested that the CNT acts as a foundation for char formation, creating a thermal insulating barrier. It was also suggested in both studies that the fillers with tubular morphology absorb pyrolysis products and combustion products, which help limit combustion and reduce smoke release. TSR was reduced by 31% in TL assemblies of CH, AL, and graphene oxide (GO).[137] Materials with tubular morphology add another dimension of fire safety by reducing smoke and heat release. It would be interesting to see if there is a synergistic effect with coatings containing both platelets and tubes.

2.2.2 Layer-by-Layer Coatings to Reduce Bacterial Adhesion

As one of the oldest living organisms on the planet, bacteria have had millions of years to adapt to adverse environments in order to survive and reproduce. In many cases this is achieved through attachment to surfaces. Attachment leads to the formation of large bacterial colonies (biofilms) surrounded by an extracellular network that provides structural support and protection from outside influences.[57] Surface-attached biofilms can lead to decreased utility of medical devices (e.g. catheters, contact lenses, textiles, and implanted devices).[58-59] Not only can device efficacy be reduced, but dangerous infections can occur as a result of biofilm formation.[60-62] It should be noted that there are cases where bacterial adhesion is desired,[138] including sewage treatment[139] and biofuel production.[140] As a result, there is an immense body of research focused on modifying various surfaces to reduce bacterial adhesion. Zhu *et al*. and Séon *et al.* recently prepared reviews highlighting several of the common strategies using LbL films to fight bacterial adhesion/colonization.[31-32]

Bacteria range from 0.2-5 μm in size and can be treated like colloidal particles when examining their interactions with surfaces. Derjaguin-Landau-Verwey-Overbeek (DLVO) theory, which is generally used to describe these interactions, applies to bacterial surface attachment. Bacterial adhesion to a surface is a typically a two stage process.[141] Basic DLVO theory describes the first stage as initial attraction to a surface through a combination of van der Waal's (always attractive) and coulombic (attractive or repulsive depending on surface charge) forces. During this stage, bacterial cells are still mobile and can undergo Brownian motion and adhesion is reversible. If the only

considerations being made are van der Waal's and electrostatic interactions, DLVO theory does an adequate job of predicting bacterial adhesion (**Figure 2.7a**),[142] but Lewis acid and base interactions (usually in the form of hydrogen bonding)[143] and hydrophilicity (through surface hydration)[144] of the surface play significant roles in predicting bacterial adhesion. As a result, DLVO has been modified to encompass these energies and can often reliably predict/explain the factors for bacterial adhesion. It has also been suggested that a conditioning layer can contribute to adhesion to a surface.[138, 145] This layer is described as the accumulation of particles, organic and inorganic molecules, or anything else present in solution. This accumulation is driven by gravity or Brownian motion and can affect the nature of the bacterial interactions with a surface by changing the conditions considered in a DLVO model. Regardless of the factors considered, the mechanism of bacterial adhesion is exceedingly complicated, and the individual contributions of individual factors (e.g. surface charge, hydrophilicity, etc.) towards adhesion in multifaceted treatments are not well understood.[146] Since this stage of adhesion is reversible, modifying a surface to decrease favorable interactions is a common strategy to prevent permanent adhesion.

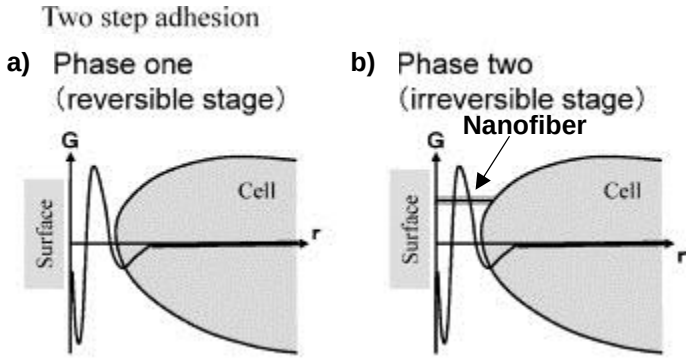

Figure 2.7. Two stage adhesion process of bacteria.[138] Adapted from Hori, K.; Matsumoto, S. Bacterial adhesion: from mechanism to control, *Biochem. Eng. J.*, **2010**, *48* (3). 424. Copyright 2010 Elsevier Ltd.

Device failure from bacterial fouling requires colonies to be permanently adhered to the device surface. In order for this to occur, bacterial cells need to get into close proximity to the surface. Surfaces that facilitate hydration layer formation, or electrostatic repulsion, can be effective at preventing this, but bacteria can use pili (nano fiber appendages) to anchor themselves to the surface (**Figure 2.7b**).[147] Pili can range from nanometers to microns in length, and consist of several protein subunits and often act as adhesins, which help facilitate bacterial adhesion to both biological and non-biological surfaces.[148] They can also promote bacterial motility and aid in the positioning between a bacterial cell and a surface (e.g. flagella).[149] Interactions between pili and a surface can be covalent or non-covalent and are highly dependent on surface chemistry and bacterial species.[150-151] To a lesser extent, the secretion of exopolysaccharides (EPS) can influence adhesion to a surface through non-covalent interactions, but these secreted films also provide protection, and cohesion in a biofilm.[152-154] Once bacteria is firmly

anchored to a surface, accumulation begins through cohesion, which eventually leads to biofilm formation and device failure.[58] Permanent adhesion is a multifaceted process which still requires significant effort to overcome (often with the use of bactericidal agents).

LbL- assemblies can be deposited to alter the surface hydrophilicity/hydrophobicity to create non-adhesive surfaces. Filtration membranes are especially susceptible to biofouling, which causes the membranes to operate inefficiently. LbL has been used to make the surface charge negative and increase the hydrophilicity, to reduce the bacterial adhesion to the surface of the membrane and other surfaces.[63-68] Tang *et al*. deposited PAH/PAA multilayers on polysulfone membranes, that removed 99% of deposited bacteria (*E. coli*) with two 10 minute rinsing cycles of a NaCl solution.[64] It was suggested that the PAA on the surface increased the hydrophilicity and imparted a negative surface charge which limited direct interaction between the membrane and bacteria through electrostatic repulsion and the formation of a hydration layer. LbL assemblies can also be made hydrophobic, through multilayer assembly utilizing polyelectrolytes with hydrophobic side groups,[69-71] or by a post-deposition modification,[72-73] but there are limited studies which explored this as a viable strategy.[71, 74]

Bactericidal multilayer assemblies have been more extensively developed. These coatings, due to the intrinsic variability of LbL, offer a wide array of killing-chemistries that utilize many different mechanisms.[31] An exceedingly popular technique has been to incorporate heavy metals (e.g. silver) into multilayer assemblies to take advantage of

their bactericidal properties.[75-79] Silver has been found to reduce bacterial DNA's ability to replicate and deactivates proteins through reactions with thiol groups.[155] Silver ions have been imbedded into multilayer assemblies. In a notable example, Malcher *et al*. constructed multilayers of poly(L-lysine) and hyaluronic acid (HA) with $AgNO_3$ filled liposome aggregates.[75] The liposome "bins" undergo a phase transformation at ~34 °C releasing the Ag^+ to the surrounding area. This temperature is ideal because ideal growth temperature for bacteria is ~37 °C. After exposure of two hours, there was a four order of magnitude reduction in *E. coli* population (**Figure 2.8**). Direct loading of $AgNO_3$ into the PLL/HA assemblies did not lead to coatings with bactericidal properties. This suggests that loaded bins have sufficient concentrations of Ag^+ to be bactericidal. While silver salts loaded into multilayers after fabrication don't show bactericidal properties, they can be reduced (Ag^+ to Ag^0) *in situ* to form silver nanoparticles.[77-80] Antibacterial multilayer coatings utilizing metals have also incorporated copper[81] and zinc.[82-83]

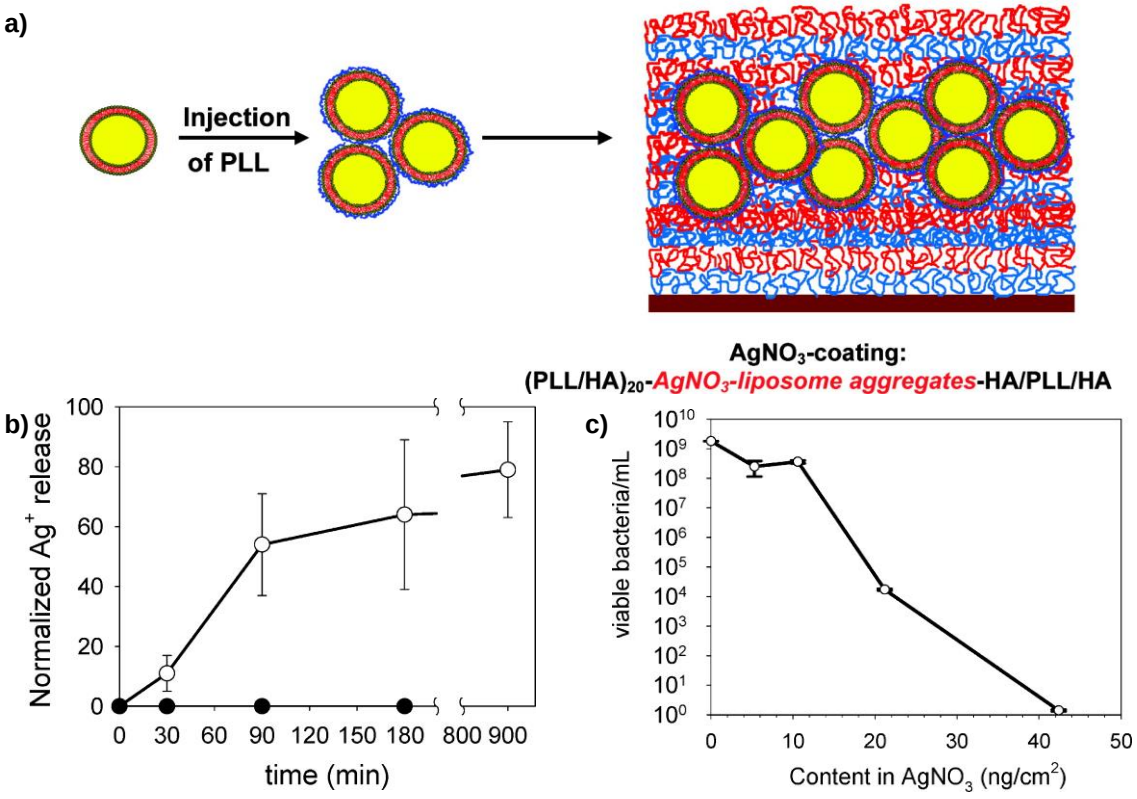

Figure 2.8. Schematic of liposome aggregates filled with $AgNO_3$ incorporated into PLL/HA multilayers (a). Release of Ag^+ as a function of time (b). Viable bacteria as a function of $AgNO_3$ content in multilayers (c).[75] Adapted from Malcher, M.; Volodkin, D.; Heurtault, B.; André, P.; Schaaf, P.; Möhwald, H.; Voegel, J.-C.; Sokolowski, A.; Ball, V.; Boulmedais, F.; Frisch, B., Embedded silver ions-containing liposomes in polyelectrolyte multilayers: cargos films for antibacterial agents, *Langmuir*, **2008**, *24* (18), 10209. Copyright 2008 American Chemical Society.

Multilayer assemblies with a triggered release of antibiotics have been prepared to combat bacterial colonization.[84-88] These films are usually loaded with an ionic antibiotic such as gentamicin which binds to the film through electrostatic interactions. The compound is released through a change in pH which causes a change in charge-state, eliminating electrostatic interactions, and allowing the drug to interact with the

bacteria. Albright *et al*. recently reported on a multilayer assembly of poly(vinyl caprolactam) (PVCL) and poly(methacrylic acid) (PMAA) with either gentamicin or polymyxin (both cationic antibiotics).[88] These films showed a high efficacy of killing adhered bacteria (both *S. aureus* and *E. coli*). Local acidification of the surface by the bacteria was found to trigger the release of antibiotics locally, killing bound bacteria. The coatings were also exposed to multiple sequential assays and did not lose efficacy. This highlights a current research need, which is extending the lifetime of antibiotic releasing coatings. This is a good example of improving lifetime through multiple approaches. Not only does triggered release lead to longer efficacy times, but the amount of gentamycin in the film scales with number of bilayers (i.e. more bilayers leads to longer efficacy time). One thing not addressed in this study is whether or not the antibiotics incorporated deep into the film are accessible through this mostly surface-mediated process.

The last major strategy for killing bacteria is direct contact with the coating surface. Usually these coatings have some high degree of positive charge (usually through a quaternary ammonium salt).[31-32, 156] It has been suggested that a positively charged surface adsorbs bacteria (through electrostatic interactions) and the resulting release of small counterions from the bacteria leads to death and there appears to be a surface charge density threshold to achieve this.[157] Multilayer assemblies utilizing this strategy have been explored.[89-97] Contact killing often leads to dead bacteria forming a conditioning layer,[158-159] which not only blocks killing sites, but also leads to bacterial build up, drastically reducing the coating potency. Methods have been developed to

release bacteria from the surface after they die. Multifunctional LbL coatings have been designed to release dead bacteria before it can form a conditioning layer on the surface.[74, 98-100] Wei *et al*. recently reported a multilayer assembly with quaternary ammonium salt derivatives of β-cyclodextrin (CD-QAS), which is loosely adhered as the top layer.[98] The salt participated in contact killing of *E coli*, which the dead bacteria subsequently adhered. With a simple treatment of sodium dodecylsulphate (SDS), the CD-QAS is removed through swelling of the LbL assembly, taking the bacteria with it. The coating can then be exposed to fresh CD-QAS to restore antibacterial activity. This process was shown to be repeatable over multiple cycles, which demonstrates long term effectiveness of a coating of this nature. Ideally, coatings should be designed where bactericidal and antifouling occurred without external stimulus.

2.3 Other Polyelectrolyte Complex Deposition Methods

Layer-by-layer assemblies have the ability to impart a wide range of properties, uniformly, to many complex surfaces, but the number of processing steps has certainly diminished commercialization of this technique.[2, 160] While not as established as LbL-assembly, methods for the deposition of polyelectrolyte complexes in a single step are being explored. One method, often used in the preparation of PEC membranes, involves controlling charge density of a weak anionic polyelectrolyte (e.g. PAA, hyaluronic acid, sodium alginate, etc.) via pH, mixing them with a polycation (often chitosan). The solution is then cast, and the solvent (usually water) is evaporated away leaving a film comprised of a polymer mixture that forms a PEC when rinsed with deionized water due

to polyanion ionization.[161-163] These polyelectrolyte films are usually in the tens to hundreds of μm thick and usually free standing (well beyond thicknesses required for LbL prepared films).

Controlling the pH of a polyelectrolyte has been used to deposit intumescent PEC thin film coatings onto cotton,[164] polyester-cotton,[165] and nylon-cotton[166] blend fabrics. These coatings consist of a nitrogen containing polycation (e.g. BPEI or PAH) and a polyphosphate (e.g. PSP or APP). The charge density of the polycation was reduced by increasing pH. When mixed with polyphosphates, electrostatic interactions are minimized and both polyelectrolytes are soluble simultaneously. This makes for an ideal coating solution. Upon deposition, coatings are cured in buffer to form an insoluble PEC on the fabric surface. Leistner *et al*. showed that this method could effectively deposit a BPEI-melamine/APP coating in a single step to the surface of a nylon-cotton blend fabric.[166] Following the buffer cure, ~20 wt% was added to the fabric, rendering it self-extinguishing in VFT (due to increased char formation from the melamine), and reduced the pkHRR by 60%.

Complimentary polyelectrolytes can be sprayed simultaneously onto a surface. This forms the polyelectrolyte complexes as the two solutions come into contact with one another. Film thickness increases linearly as a function of spraying time.[167] This technique was extended to deposit inorganic salts, nanoparticles, and small oligo ions (e.g. citric acid).[168] This represents a significant reduction in processing requirements to deposit a thin polyelectrolyte complex, and also highlights that under the correct conditions single step deposition methods can be as versatile as LbL assembly. Spraying

has also been used to make stimuli-responsive PEC containers fabricated in a single step. They can be fabricated to contain magnetic nanoparticles,[169-170] proteins,[171] and fluorescent dyes.[172-173] Typically one polyelectrolyte solution is sprayed into a solution containing a complimentary polyelectrolyte. The capsule formation relies on phase separation of the two solvent systems, and a PEC microcapsule is formed at the liquid-liquid interface of the two solvents. The formed microcapsules can release any stored material upon exposure to the appropriate pH or ionic strength, making them an interesting concept for delivery devices.

Sedimentation of polyelectrolyte complexes has also been investigated. PEC is formed by mixing a polycation and polyanion. The size of the PEC and by extension the rate at which they underwent sedimentation (i.e. film formation) was determined by polymer chemistry, pH and ionic strength (**Figure 2.9a)**.[174-175] Interestingly, these parameters also dictated whether a cohesive film or an aggregated "snow flake" structure formed. Thickness was found to be dependent on the time the substrate was exposed to the sedimentation solution. This idea was used to deposit an intumescent flame retardant PEC onto the surface of cotton fabric.[176] BPEI and PSP were mixed at pH 7 and the complex formed was allowed to settle and deposit onto the cotton surface. The efficacy of the coating was evaluated as a function of sedimentation time. It was found that cotton fabric exposed to the sedimenting PEC for 10 minutes self-extinguished during vertical flame testing and showed a 57% reduction in peak heat release rate (**Figure 2.9b**). This coating was compared to various intumescent LbL deposited PEC coatings and showed comparable open flame testing and calorimetry (i.e. VFT and pkHRR,

respectively) results and reduced processing cycles from 40-64 down to one and reduced time of deposition down from 64-108 minutes to 10. This study is an excellent example of advantages these "one-pot" systems have over similar LbL deposited coatings to deliver desired properties.

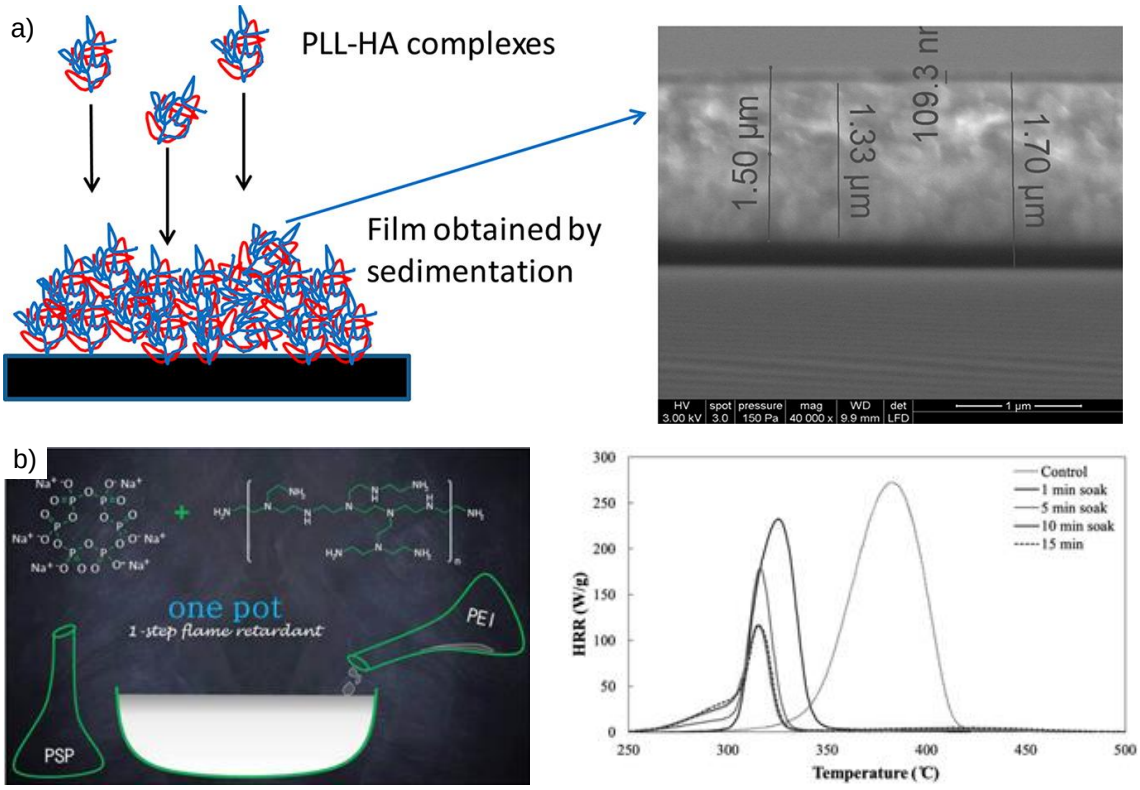

Figure 2.9. Schematic and electron micrograph of PEC coating deposited through sedimentation (a).[174] Schematic and heat release rate as a function of temperature of intumescent PEC coatings deposited through sedimentation (b). [176] Adapted with permission from Ball, V.; Michel, M.; Toniazzo, V.; Ruch, D., The possibility of obtaining films by single sedimentation of polyelectrolyte complexes. *Ind. Eng. Chem. Res.* **2013,** *52* (16), 5691. Copyright 2013 American Chemical Society. And Cain, A. A.; Murray, S.; Holder, K. M.; Nolen, C. R.; Grunlan, J. C., Intumescent nanocoating extinguishes flame on fabric using aqueous polyelectrolyte complex deposited in single step. *Macromol. Mater. Eng.*, **2014,** *299* (10), 1180. Copyright 2014 Wiley-VCH Verlag GmbH & Co. KGaA, Weinheim, respectively.

Coacervates have also received some recent attention for depositing PEC in a single step. Kelly *et al.* created free-standing 15 μm films via spin coating PDDA/PSS coacervates.[108] Increasing rpm reduced coating thickness. Increasing the salt concentration showed the same trend, but increasing spin time also decreased the thickness of the films due to decreased coacervate viscosity. Haile *et al*. deposited a high oxygen barrier coating using a coacervate made from BPEI and PAA. The coating was deposited on the surface of a PET film using a Meyer rod. In order to achieve a transparent PEC coating, the deposited coacervate was cured in citric acid buffer, and humidity treated. The resulting PEC reduced the oxygen transmission rate by two orders of magnitude. Curing the polyelectrolytes reduces free volume through electrostatic interaction, creating an efficient gas barrier coating. Even though there are limited examples of direct coacervate deposition, there is significant potential in mimicking LbL coatings, significantly reducing processing steps and achieving many of the same properties. Because of the broad scope of applications and environmental friendliness nature that PEC coatings provide, there is great potential for commercialization and wide spread implementation. The following chapters highlight polyelectrolyte complexes deposited via LbL assembly to reduce PUF flammability and to reduce bacterial adhesion to polyester fabric. Efforts have also been made to make these coatings more commercially viable by depositing PEC complexes in a single step building on some of the methods described here.

CHAPTER III

ENVIRONMENTALLY-BENIGN HALLOYSITE NANOTUBE MULTILAYER* ASSEMBLY SIGNIFICANTLY REDUCES POLYURETHANE FLAMMABILITY

3.1 Introduction

Halloysite nanotubes (HNT) ($AlSi_2O_5(OH)_4 \cdot nH2O$) are clay nanoparticles comprised of rolled aluminosilicate sheets (**Figure 3.1a**). These safe and naturally abundant alumosilicate clay tubes have a diameter of 50-60 nm, inner lumen of 10-15 nm and a length of about 1 μm.[177-179] The inner lumen has water coordinated within, which after thermal dehydration, is vacated and can be filled with various compounds designed for controlled release.[179-181] Because halloysite is a naturally occurring clay with nanotube morphology, it is a good candidate for incorporation into PEC thin films for flame retardation due to the combination of thermal barrier properties of clay and the smoke reduction properties of nanotubes. Polymer composites with flame retardant filled HNT exhibit reduced flammability.[182-183] It is believed that these composites have reduced mass and energy transfer by forming a physical barrier, and dilution of the gas phase via a dehydration mechanism. Filling of the lumen with volatile organics and other toxins during burning reduces smoke release during combustion. Despite promising properties, halloysite has seen limited use in multilayer assemblies, likely due to poor

* Reprinted with permission from Smith, R. J.; Holder, K. M.; Ruiz, S.; Hahn, W.; Song, Y.; Lvov Y. M.; Grunlan, J. C. Environmentally-benign halloysite nanotube multilayer assembly significantly reduces polyurethane flammability. *Adv. Funct. Mater*. **2017**, 1703289. Copyright 2017 WILEY-VCH Verlag GmbH & Co. KGaA.

stability of dispersions in water.[184-185] Even so, a few thin films have been deposited with various properties.[186-187]

This chapter focuses on the development of an environmentally-benign flame retardant for polyurethane foam (PUF). Layers of halloysite clay nanotubes (HNT) stabilized by branched polyethylenimine (BPEI) or poly(acrylic acid) (PAA) were deposited from aqueous suspensions to create multilayered nanocomposite coatings. PUF is very flammable and widely used in upholstered furniture throughout the world. Foam treated with five BPEI-HNT/PAA-HNT bilayers (BL), deposited using layer-by-layer assembly, was rendered self-extinguishing in open flame testing. Cone calorimetry reveals that this coating reduces the peak heat release rate (pkHRR) by 62%. Due to the tubular morphology of HNT, small volatile gasses given off during combustion are trapped, so total smoke release (TSR) is reduced by 60%. Infrared spectroscopy suggests this multilayer film survives during combustion, forming a HNT-rich barrier that prevents mass and energy transfer during open flame testing and calorimetry. The significant reductions in pkHRR and TSR, along with the self-extinguishing behavior, indicate that these halloysite-based multilayer films have the potential to greatly improve PUF fire safety. The low cost and natural abundance of HNT makes this technology especially amenable to widespread use.

3.2 Experimental Section

3.2.1 Materials

Branched polyethylenimine (25,000 g/mol) and poly(acrylic acid) (100,000 g/mol) were purchased from Sigma Aldrich (Milwaukee, WI.) Halloysite was supplied from Applied Minerals, Inc. (New York, NY). All chemicals were used as received and all solutions were prepared with 18 MΩ deionized water. Solutions of 1.0 wt% PAA, used as a surface treatment for polyurethane foam,[47] were altered to pH 2 with 2 M HNO_3 prior to priming. Halloysite nanotubes (0.5 wt%) were dispersed in 0.1 wt% PAA solutions and 0.1 wt% BPEI solutions (unaltered pH, 3.5 and 9.9, respectively). The suspensions were placed in an ice bath and exposed to two rounds of 15 W tip sonication (Model VCX750; Sonics & Materials, Inc., Newtown, CT) for 30 min each with a 10 min pause in between. Solutions were used for coating immediately after sonication. Silicon wafers (p-doped, single side polished (1 0 0), 500 nm thick) were purchased from University Wafers (South Boston, MA). Flexible open cell polyurethane foam (type 1850, 1.75 lbs/ft^3 density) was purchased from Future Foam (High Point, NC).

3.2.2 Layer-by-Layer Deposition

Films for profilometry and atomic force microscopy were deposited on the polished side of a silicon wafer that was rinsed thoroughly with DI water and methanol and exposed to plasma for 5 minutes to impart a negative surface charge. Using a homebuilt robotic coating system,[188] the substrate was first dipped into the cationic

BPEI-stabilized HNT suspension for 5 minutes followed by a spray rinse with DI water. The substrate was then dipped into the anionic PAA-stabilized HNT suspension for 5 minutes followed by a spray rinse with DI water. This procedure was repeated with dip times reduced to 1 minute until the desired number of bilayers was achieved. For LbL deposition on polyurethane foam, 10.2 cm x 10.2 cm x 2.5 cm thick pieces were cut and rinsed thoroughly with DI water and placed in a 70 °C oven overnight. Prior to LbL deposition, dry pieces of foam were first submerged and were compressed completely 3 times to ensure priming solution uptake into the free volume of the foam. Saturated foam was left for 30 seconds, after which the sample was wrung out using a mechanical roller. The foam was then rinsed with DI water by compression three times to ensure removal of loosely adhered material. The sample was then immersed in the cationic HNT solution by fully compressing it three times and letting it soak for 5 minutes. The foam was wrung out in a mechanical roller and rinsed by compressing three times in a DI water basin. The sample was then exposed to the anionic HNT in the same fashion to form the first bilayer. This process was repeated with one minute immersion times until the desired number of bilayers was deposited. Coated samples were placed in an oven at 70 °C to dry overnight and stored in a dry box prior to testing.

3.2.3 Thin Film Characterization

Film thickness was measured on silicon wafers with a P-6 Profilometer (KLA-Tencor; Milpitas, CA). Coated polyurethane substrates were imaged using a field-emission scanning electron microscope (SEM) (Model JSM-7500, JEOL; Tokyo, Japan).

Samples were placed on an aluminum stub and sputter coated with 4 nm of platinum/palladium alloy prior to imaging. 3 and 5 bilayers of BPEI-HNT/PAA-HNT were deposited on silicon wafers as described previously. Surface topology was imaged using a Dimension Icon Atomic Force Microscope (Bruker, Billerica, MA) in tapping mode before and after two hours in an 800 °C furnace. 20 BL of BPEI-HNT/PAA-HNT were deposited onto a silicon wafer as described above. Infrared spectra were compared before and after thermal treatment at 800 °C for two hours using an Alpha Platinum-ATR FTIR spectrometer (Bruker, Billerica, MA).

3.2.4 Thermal Characterization

Thermal stability of coated and uncoated polyurethane foam samples (~ 30 mg) were evaluated using a Q-50 thermogravimetric analyzer (TA Instruments; New Castle, DE), under a controlled heating ramp of 10 °C min^{-1}, from ambient temperature to an isothermal hold at 100 °C for 60 min and then ramping up to 850 °C. A sample purge flow of 60 mL s^{-1} air and a balance purge flow of 40 mL s^{-1} nitrogen was used. TGA experiments were repeated with a sample purge flow of nitrogen for a non-oxidative atmosphere. Open flame tests were performed on control and coated foam by exposing samples (5 x 5 x 2.5 cm^3) to the direct flame (~ 1400 °C) of a butane hand torch (Triggertorch™ MT-76 K, Master Appliance Corps.; Racine, WI) for 10 s. The torch was adjusted prior to each test so that the inner blue flame length was approximately 2.5 cm and the outer transparent blue flame was approximately 5 cm in total length. The fume hood sash was lowered to 12.5 cm before the start of each test and the samples

were suspended over a wire mesh sheet 25 cm above the benchtop to minimize fume hood ventilation draft influence on the flame. The torch was placed approximately 5 cm from the side face of the foam such that the flame tip contacted the foam. Cone calorimetry experiments were conducted at the University of Dayton Research Institute using a FTT Dual Cone Calorimeter in accordance with a standard testing procedure (ASTM E-1354-12). Samples (10.2 x 10.2 x 2.5 cm^3) were placed in an aluminum foil pan and exposed to a heat flux of 35 kW/m^2 (exhaust flow of 24 L/s).

3.3 Results and Discussion

3.3.1 Layer-by-Layer Assembly of Halloysite Nanocoatings

Halloysite has seen little use in layer-by-layer assemblies due to its poor dispersibility in water. Even after ultrasonication, halloysite suspensions begin to settle almost immediately, making them impractical for use in water-based coatings. Unaltered halloysite has a zeta potential of -25.9 ± 0.8 eV. When sonicated with either BPEI or PAA, a white suspension is formed that shows very little settling for up to 7 hours. The zeta potentials for the BPEI-HNT and PAA-HNT suspensions were measured to be 19.2 ± 1.1 eV and -33.7 ± 1.7 eV, respectively. It is believed that positively-charged BPEI adsorbs onto the surface and stabilizes the suspension through electrostatic repulsive interactions. For PAA, it is believed that it adsorbs onto the surface of HNT through hydrogen-bonding and van der Waals interactions and increases suspension stability through negative electrostatic repulsive interactions. It is also possible that anionic PAA

is adsorbed predominantly into the positively charged tube's lumen, neutralizing positive inner charge, and increases the magnitude of the overall negative particle zeta potential.[189] Polyurethane foam was first primed for LbL deposition through exposure to a PAA/HNO_3 solution. The primed foam was then immersed in the BPEI-HNT (cationic) suspension followed by the PAA-HNT suspension. This procedure was repeated until the desired number of bilayers was deposited. Thickness as a function of bilayers was measured using profilometry and is shown in **Figure 3.1**b. A 5 BL coating of BPEI and PAA without HNT was also applied to PUF in the same fashion to act as a control.

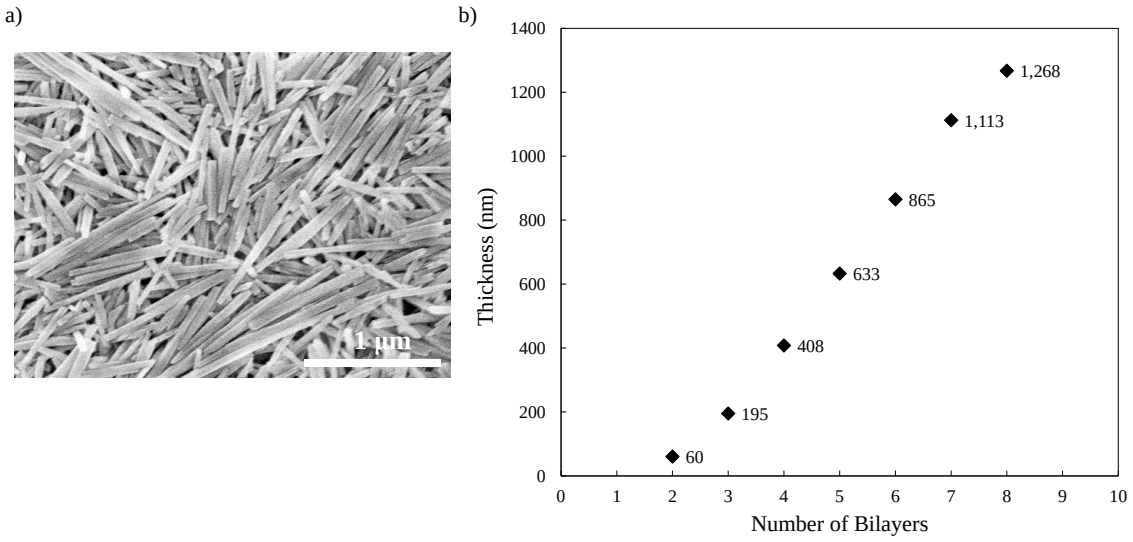

Figure 3.1. SEM micrograph of halloysite powder (a). Layer-by-layer film thickness as a function of BPEI-HNT/PAA-HNT bilayers deposited on a silicon wafer.

SEM micrographs of 3 and 5 BL HNT-based coatings, shown in **Figure 3.2**, reveal complete conformal coverage of the three-dimensional foam surface. Large aggregates (highlighted in the green and red boxes) of halloysite tube bundles are visible on the surface of the coated foam, but individual tube-like structures are also present throughout the entire film, suggesting that HNT is well dispersed/exfoliated. AFM micrographs of these same films deposited on Si wafers reveal significant uniformity of the tubular structures. Micrographs of the 5 BL BPEI/PAA control coating show a smooth conformal film, indicating that the texture observed in the HNT-containing films is from halloysite. Also evident from the micrographs is the conservation of the open porous structure of the PUF. This is an important advantage of LbL-assembly, as it is able to uniformly coat complex structures with little change to the porosity.

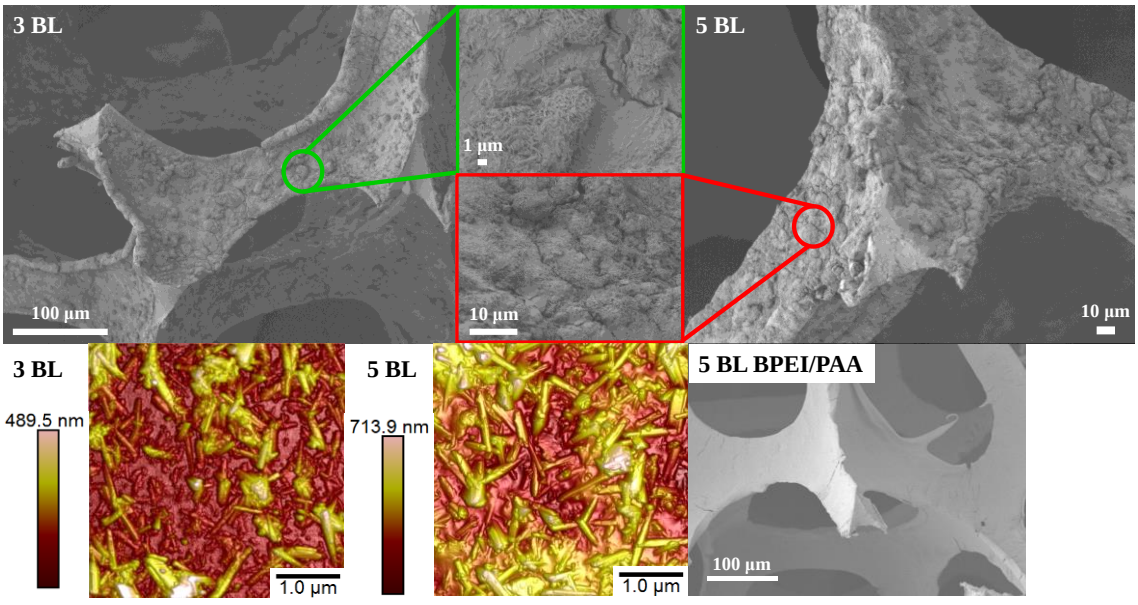

Figure 3.2. SEM micrographs of 3 and 5-bilayer HNT-containing flame retardant coatings and 5 BL BPEI/PAA on polyurethane foam. AFM micrographs of 3 and 5-bilayer HNT-containing flame retardant coatings on silicon wafers are also shown.

3.3.2 Thermal Analysis of Halloysite Multilayers

Halloysite-containing multilayer coatings are effective flame retardants because they form a ceramic insulating barrier similar to those seen in other clay-based nanocoatings.[51-52] Thermogravimetric analysis (TGA) was used to assess the thermo-oxidative stability of uncoated and coated PUF. Weight percent and derivative weight loss as a function of temperature are shown in **Figure 3.3**, with insets displaying plots for unaltered HNT. Uncoated PUF shows an initial onset at ~260 °C (**Figure 3.3b**). Polyurethanes typically degrade in two or three primary steps.[190-192] This peak at ~260 °C corresponds to the first step, which is the degradation of hard segments in PU and the formation of isocyanates and alcohols, primary or secondary amines, olefins, and carbon dioxide. The second degradation step is associated with soft segment degradation, represented by two additional peaks at ~310 and ~348 °C (associated with the remaining polyol thermal decomposition). There is no residue remaining beyond 600 °C.

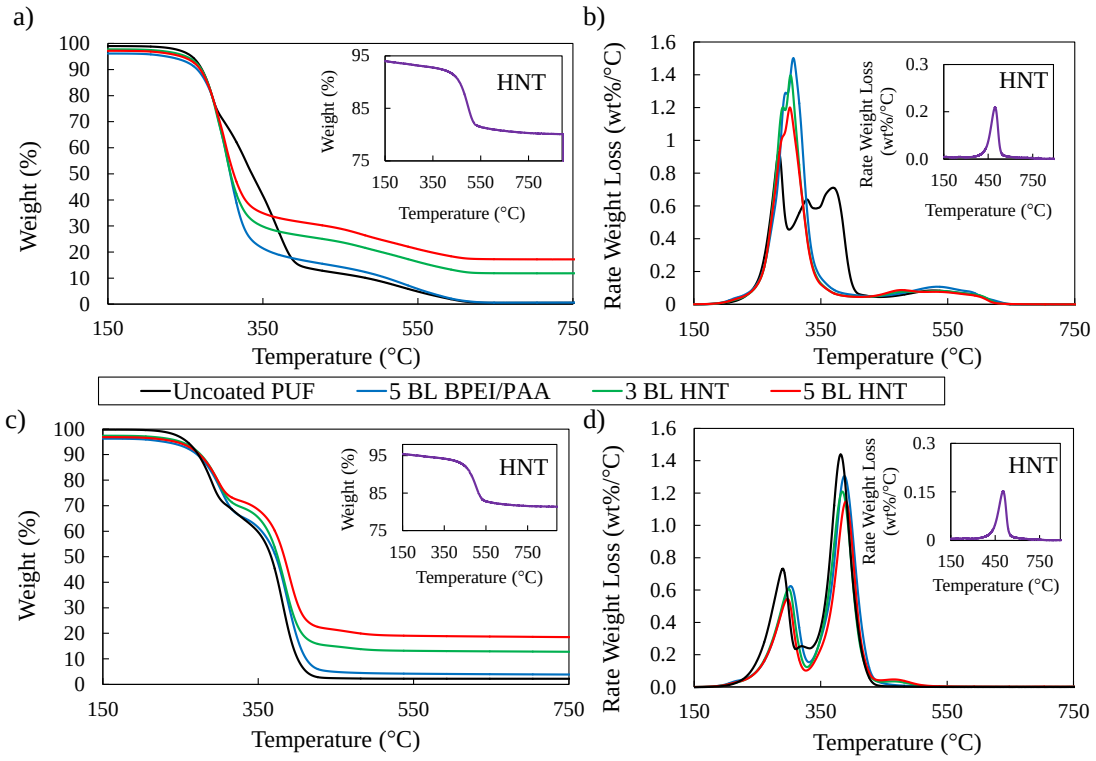

Figure 3.3. Weight loss and derivative weight loss as a function of temperature for uncoated and coated PUF under air (a,b), and under nitrogen (c,d).

A 5 BL of BPEI/PAA coating does not significantly alter the initial depolymerization of the underlying polyurethane foam. The degradation of polyols happens simultaneously in coated foam (single sharp peak), while two broad degradation peaks are observed with uncoated foam, due to the lack of melt pool formation. Foam collapse and pool formation reduces the total surface area, slowing the rate of oxidative degradation. This behavior does not occur with the coated foam, and high surface area is maintained throughout combustion. Thermo-oxidative degradation happens more rapidly with more surface area, which results in the single sharp peak observed in Figure 3.3b.

Similar to uncoated PUF, there is no char residue beyond 600 °C. Three and five-bilayer HNT coated foam exhibits similar behavior to 5 BL BPEI/PAA. Initial onset of depolymerization is not significantly affected by the coating. It is believed that HNT-containing coatings form ceramic barriers, preventing mass/energy transfer, and confine the melt within the ceramic exo-skeleton, accelerating the decomposition of the polyol segments. Unlike uncoated PUF and 5 BL BPEI/PAA, a significant amount of residue remained in the sample crucible (11.9% for 3 BL HNT and 17.2% for 5 BL HNT). This residue is believed to be predominately halloysite. The estimated HNT content in the 3 and 5 BL coatings is 91 and 86 wt%, respectively.

TGA was also carried out under inert an atmosphere (N2). Figures 3c and 3d show weight loss as a function of temperature. Uncoated PUF undergoes two stages of non-oxidative thermal degradation. The initial stage, with an onset of ~250 °C (from the peak in the derivative plot), is the depolymerization of polyurethane hard segments into isocyanate units. Polyol degradation follows, with an onset at ~355 °C, and is characterized by formation of a melt pool and rapid mass loss. The accelerated mass loss observed under oxygen is not observed here, suggesting that non-oxidative thermal degradation occurs independently of surface area. All coatings slightly delay the onset of degradation by no more than 5 °C and have even less of an influence on polyol decomposition (≤ 3 °C). Under inert conditions, 5 BL BPEI/PAA coated (and uncoated) PUF exhibit little char residue (3.8% and 2.2% respectively) due to lack of oxygen for formation of combustion products. Neat HNT (insets) shows a single decomposition event at 500 °C, observed in both oxidative and inert atmospheres, which is associated

with thermal dihydroxylation (an endothermic event).[183, 193] The water generated is also believed to help dilute the gas phase in a fire scenario.

3.3.3 Cone Calorimetry

Cone calorimetry is a standard bench-scale technique to measure the flammability of a material. Heat release rate is measured based on oxygen consumption during combustion and used to determine material behavior during a fire.[194-195] Cone calorimetry was conducted on uncoated and coated foam samples at a constant heat flux (35 kWm-2) following ASTM E-1354 (**Figure 3.4**). Uncoated PUF (black line) displays two distinct heat release peaks. The first is the result of hard segment degradation into isocyanates, alcohols, amines, and olefins, which all contribute to the toxicity and quantity of smoke generated during combustion. The second larger peak is a result of polyol degradation, which forms a large melt pool (in the absence of structural support of the hard segments) that rapidly combusts, releasing a large amount of energy.[34] During a structural, fire melt dripping can aid fire spread. Applying a 5 BL BPEI/PAA coating does little to reduce the flammability of PUF since both polymers are inherently flammable. A slight 2.1% decrease in the peak HRR was observed, but there was an increase in the initial HRR, and an increased total heat release (THR) and total smoke release of 9.9% and 22%, respectively. It is evident from cone calorimetry that BPEI/PAA multilayers, in the absence of halloysite clay, increase the flammability of polyurethane foam.

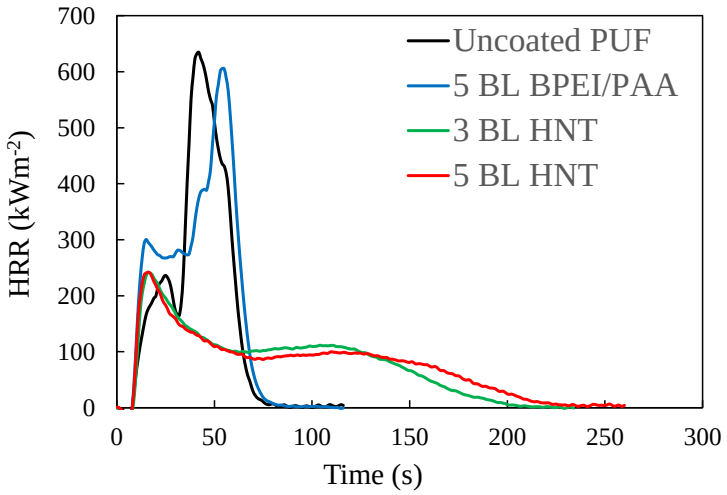

Figure 3.4. Heat release rate, as a function of time in the cone calorimeter, for coated and uncoated polyurethane foam.

Applying 3 BL of BPEI-HNT/PAA-HNT (~200 nm thick) to PUF has a dramatic impact on flammability. During combustion, a halloysite-rich barrier is formed, delaying mass loss/transfer (i.e. less fuel available at the flame zone) and resulting in a reduced HRR. This barrier can be seen in SEM images of foam taken after open flame testing (**Figure 3.5**). Because mass transfer is limited, the large melt pool observed with uncoated foam is prevented from forming, which forces degradation to occur within the confined space of the shell formed by the coating. This reduction in HRR is the largest contributor to increasing the safety of synthetic polymer materials in a structure fire.[196] The coated foam maintains its original shape and porosity, where uncoated PUF leaves only residue in the sample holder. Even though there is a large reduction in HRR, this coating acts passively (i.e. does not prevent total degradation). SEM micrographs of

post-burn samples show hollow struts (**Figure 3.5**), indicating that the underlying PUF is completely consumed in the fire (also evidenced by the HNT-based films having the same THR as uncoated foam (**Table 3.1**).

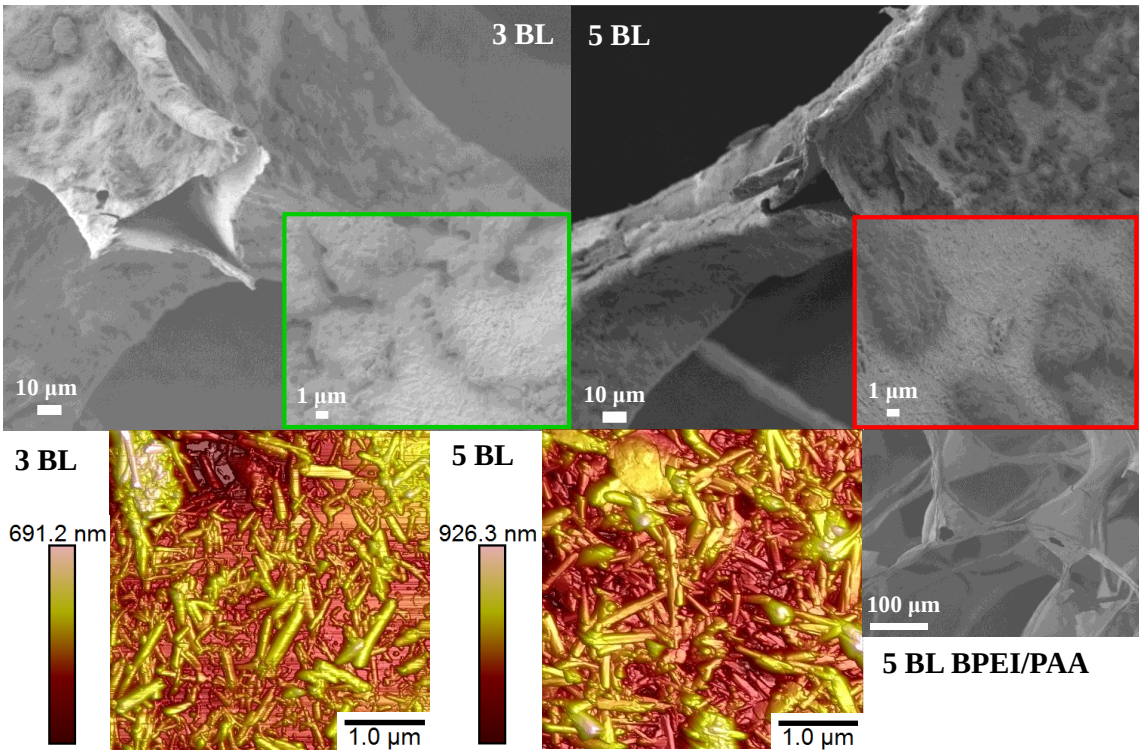

Figure 3.5. SEM micrographs of polyurethane foam, with 3 and 5 bilayer HNT coatings or 5 BL BPEI/PAA, after torch testing. Insets (green and red) highlight tube morphology of the HNT coatings. AFM micrographs of 3 and 5 BL HNT coatings after exposure to 800 °C for two hours in air.

Table 3.1. Cone calorimeter data for coated polyurethane foam.

Coating	Weight Gain [%]	HNT [%]	pkHRR [kWm^{-2}]	THR [MJm^{-2}]	TSR [m^2m^{-2}]
Uncoated	N/A	N/A	634 ± 31	18.4 ± 0.1	178 ± 7
5 BL PEI/PAA	10.6 ± 0.5	N/A	621 ± 11	20.2 ± 0.3	217 ± 4
3 BL HNT	26.2 ± 0.6	91	244 ± 2	18.1 ± 0.2	93 ± 8
5 BL HNT	34.2 ± 0.5	86	243 ± 2	18.8 ± 0.2	71 ± 7

Five bilayers of BPEI-HNT/PAA-HNT provides a significant reduction in HRR, but there is no significant difference with a 3 BL nanocoating. Peak heat release rates of HNT-containing coatings were reduced by 61.5% and 61.7% for 3 and 5 BL coatings, respectively. Increasing bilayers beyond three primarily reduces smoke release. 3 and 5 BL coatings reduce TSR by 47.8 and 60.1%, respectively. Reduction in TSR scales with increased halloysite mass, which increases the capacity for volatile compound adsorption. Reduction in smoke release has been observed previously in other clay-containing multilayer films, (and films with nanotube fillers).[52, 55-56]

3.3.4 Fourier Transform Infared Spectroscopy

Fourier transform infrared (FTIR) spectroscopy was used to analyze these HNT-containing multilayer composites deposited on silicon wafers. Error! Reference source ot found. shows the FTIR spectra of the individual components (i.e. BPEI, PAA, and HNT), and 20 bilayers of BPEI-HNT/PAA-HNT, before and after exposure to 800 °C. Before thermal treatment, the characteristic stretching peak from carbonyl groups (1690 cm^{-1}) is observed in the 20 BL film. There is also a peak at 1535 cm^{-1} for N-H stretching, associated with BPEI, along with stretching peaks of the interior hydroxides (3691 cm^{-1} and 3618 cm^{-1}) from HNT.[197] There is no evidence of BPEI or PAA remaining in the film after exposure to 800 °C, confirming complete degradation of the polymers. The hydroxide shifts associated with HNT also disappear due to the thermal dehydroxylation observed at ~500 °C in TGA (**Figure 3.3**)The tube-like surface morphology observed in both AFM and SEM micrographs (**Figure 3.5**), and the presence of the Si-O stretching

peak at 1034 cm^{-1}, suggest that the remaining coating is predominantly halloysite. It is believed that the formation of this clay barrier causes these HNT-containing coatings to be effective by forming a physical, clay-rich barrier that significantly reduces both heat and mass transfer.

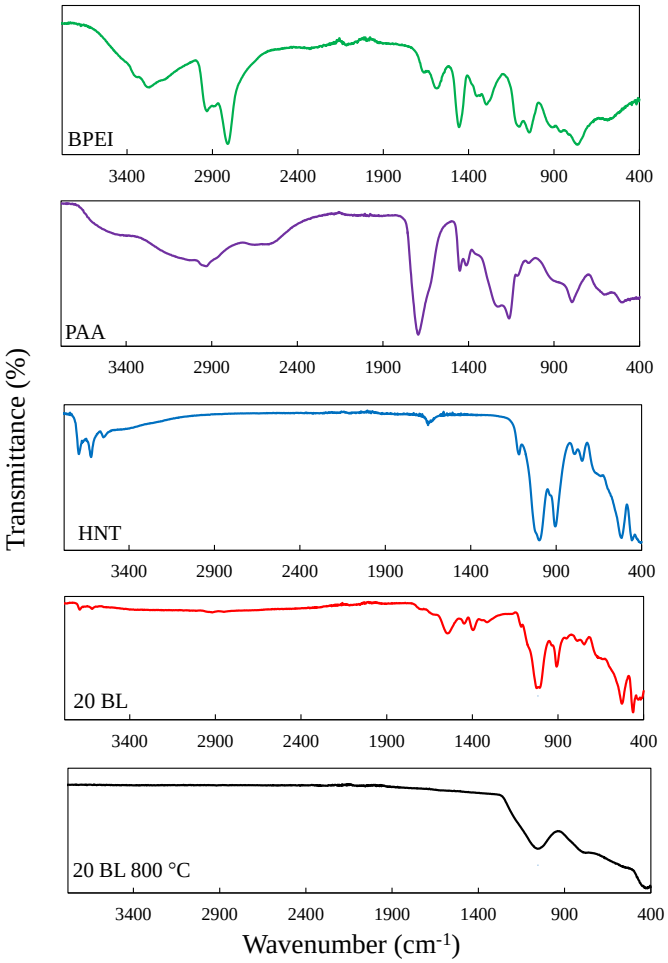

Figure 3.6. FTIR spectra of 20 BL BPEI-HNT/PAA-HNT and the individual ingredients before and after two hours in a 800 °C oven.

3.3.5 Direct Flame Testing of Coated Foam

Open flame testing was conducted on foam samples to assess coating performance as a flame retardant. 5 cm^2 PUF samples were exposed to a butane torch for 10 seconds and then monitored until the flame extinguished. Uncoated PUF ignites quickly upon exposure to the torch, generating dense smoke and flaming melt drips that could ignite underlying flammable materials (e.g., carpet and textiles). This test simulates how PUF in a piece of furniture would behave during a house fire. The foam continues to burn upon torch removal, until only residue remains. With the addition of 5 BL BPEI/PAA, foam burns vigorously when the torch is applied. The fire continues upon torch removal until only a very thin char mass remains (**Figure 3.7a**). Surprisingly, this polymer coating prevents melt dripping. A 3BL BPEI-HNT/PAA-HNT coating allows the flame to travel over the entire surface of the foam after removal of the torch, but a cross section (**Figure 3.7b**) shows that much of the internal foam remains unharmed, covered by a layer of fluffy, insulating char. A 5 BL HNT coating ignites upon application of the torch, and burns after torch removal, but the foam self-extinguishes before the flame spreads over the entire surface, preserving a large portion of the sample. The halloysite within the films acts as a barrier preventing mass transfer and as a thermal barrier that prevents the flame from spreading over the entire sample. The HNT-containing films also prevent melt dripping, without collapsing the foam structure like the BPEI/PAA coated foam. Post burn SEM of BPEI/PAA-coated foam reveals destruction of the network with a very thin layer of hollow char remaining (**Figure 3.5**). Images of HNT-coated foam reveal the porous network remains as hollow shells. The tube-like texture observed with AFM and SEM

pre-burn is clearly visible qualitatively in these post-burn images. The self-extinguishing behavior and melt drip prevention impart fire safety with relatively benign chemistries.

Figure 3.7 Cross sectional images of 5 BL BPEI/PAA (a), 3 BL HNT (b), and 5 BL HNT (c) coated PUF after 10 second exposure to a butane torch.

3.4 Conclusions

The incorporation of halloysite nanotubes into an effective and safe flame retardant multilayer nanocoating for polyurethane foam was demonstrated for the first time. Using benign polymers and clay to create aqueous suspensions, layer-by-layer assembly was used to make conformal composite coatings on the three-dimensional foam structure, while maintaining the porosity and reducing flammability. Only five bilayers of BPEI-HNT/PAA-HNT (~633 nm thick) is needed to self-extinguish foam in an open flame test and cone calorimetry reveals a peak heat release rate reduction of 61.7% (and a 60.1% reduction in total smoke release.) The large reduction in overall foam flammability suggests these halloysite-based composites could reduce fire related injuries and deaths by increasing the time to escape a burning home (or office building). This protective composite coating is scalable and low cost, making it attractive for possible commercialization and widespread implementation.

CHAPTER IV

POLYELECTROLYTE MULTIALYER NANOCOATING DRAMATICALLY* REDUCES BACTERIAL ADHESION TO POLYESTER FABRIC

4.1 Introduction

Bacterial adhesion is a significant problem in medical devices which can lead to systemic infections and device failure.[58-59] Textiles, especially in clothing, linens, and wound dressings should be resistant to bacterial adhesion to reduce the spread of harmful bacterial strains in medical centers.[198] According to the United States Center for Disease Control (CDC), methicillin resistant *Staphylococcus aureus* (MRSA) infections were reduced by 54% between 2005 and 2011, due to improved hygienic practices and better antibiotic stewardship, that resulted in 9,000 fewer deaths.[199] Due to the prolific use of polyester (PET) fabric in modern textiles, and its propensity to undergo MRSA adhesion,[200] it is a good candidate for modification to reduce adhesion and possibly reduce the number of dangerous infections in medical centers. Polyelectrolyte complexes deposited using layer-by-layer assembly have been developed as a possible solution to reduce bacterial adhesion to various surfaces, or kill the bacteria on contact.[31-32] These coatings typically reduce the ability for bacteria to adhere to a surface by changing surface properties (e.g. negative surface charge or increased hydrophilicity).[63-74] They can also kill bacteria by exposing bacteria to bactericidal agents.[75-88]

* Reproduced with permission from Smith R. J.; Moule, M. G.; Sule, P.; Smith, T.; Cirillo, J. D.; Grunlan, J. C. Polyelectrolyte multilayer nanocoating dramatically reduces bacterial adhesion to polyester fabric. *ACS Biomater. Sci*. **2017**, *3*(8), 1845-1852. Copyright 2017 American Chemical Society

This chapter focuses on the development of a poly(diallyldimethylammonium chloride) (PDDA) and poly(acrylic acid) (PAA) polyelectrolyte complex deposited to the surface of polyester fabric using layer-by-layer assembly. The efficacy of this coating was found to increase with the number of bilayers added. At 10 BL, >99% of deposited bacteria was removed after simple rinsing with deionized water. The efficacy of this coating is attributed to electrostatic repulsion between the PAA in the film and the negatively charged bacterial surface, and the increase in surface roughness observed with increasing bilayers. In order to evaluate the efficacy of these coatings, an assay using bioluminescent bacteria, often used with living laboratory animals in vivo,[201-203] was developed to easily measure the amount of viable bacteria on the fabric surface.

4.2 Experimental Section

4.2.1 Materials

Poly(diallyldimethylammonium chloride) (M_W = 100,000 g/mol, 20 wt% aqueous solution) and poly(acrylic acid) (M_W = 100,000 g/mol, 35 wt% aqueous solution) were purchased from Sigma-Aldrich (Milwaukee, WI). All chemicals were used as received. Deionized water with a specific resistance greater than 18 MΩ was used in all aqueous solutions and rinses. Single-side-polished, 500-μm-thick silicon wafers (University Wafer, South Boston, MA) were used as deposition substrates for ellipsometry, and atomic force microscopy (AFM). Silicon-wafers were rinsed with deionized water and methanol and then plasma treated for 10 minutes using a plasma

cleaner model PDC-32G (Harrick Plasma Inc. Ithaca NY). Contact angle experiments were conducted on 179 μm thick poly(ethylene terephthalate) (PET) (Tekra, New Berlin, WI) that was rinsed with deionized water and methanol before use. The PET surface was imparted a negative charge using a BD-20 corona treater (Electro-Teching, Inc. Chicago IL). Polyester 720H fabric, supplied by Test Fabrics Inc. (West Pittston, PA), was washed thoroughly with deionized water thoroughly and dried at 70 °C prior to use.

4.2.2 Layer-by-Layer Assembly

LbL deposition on two-dimensional substrates (Si, PET) was carried out using a robotic coater.[204] The substrate was first immersed in 0.2 wt% PDDA with an unaltered pH (~6.5) for 5 min, rinsed with DI water, then blown dry with compressed air. This procedure was followed by an identical dipping, rinsing, and drying procedure with the 0.2 wt% PAA solution at an unaltered pH of ~3.0, resulting in one PDDA/PAA bilayer. Following the deposition of the initial bilayer, immersion times were reduced to 1 minute. The longer initial immersion times (5 min.) were employed to ensure the best possible surface coverage. For fabric samples, 5 minute immersion in 0.2 wt% PDDA at unaltered pH, followed by rinsing in DI water and wringing out, was followed by an identical procedure for 0.2 wt% PAA at unaltered pH, resulting in one PDDA/PAA bilayer on fabric. The dip times were reduced to 1 minute and repeated until the desired number of bilayers were deposited, as shown in **Figure 4.1**.

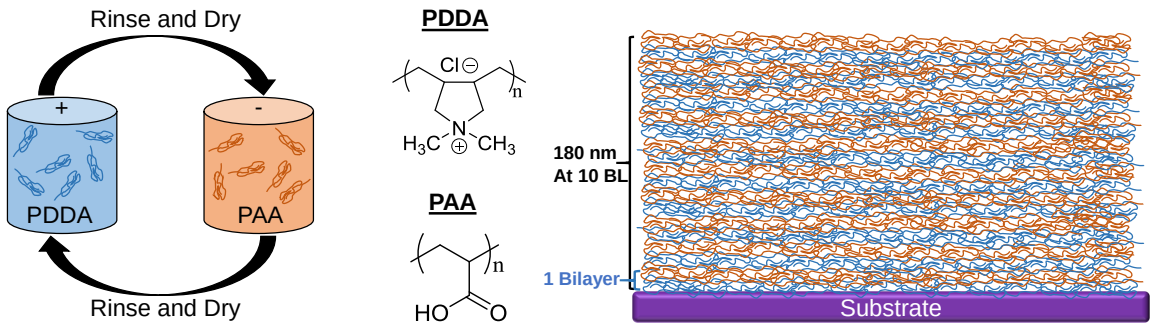

Figure 4.1. Schematic of layer by layer deposition of PDDA and PAA onto a substrate.

4.2.3 Bacterial Adhesion Assay

Bioluminescent Staphylococcus aureus Xen36 (Caliper LifeSciences) was used for bacterial adhesion testing. Overnight cultures were grown in Luria-Burtani (LB) media containing 200 ug/mL of kanamycin. Cultures were then centrifuged at 8000 rpm and re-suspended in phosphate buffered saline (PBS) and diluted to a concentration of 5x108 CFU/mL. Two-fold dilutions were prepared in PBS to test a range of bacterial concentrations for bacterial adherence. Circular swatches of 8.5 cm diameter polyester fabric, coated with the 2, 4, 6, 8 and 10 PDDA/PAA bilayers (and an uncoated control), were sterilized with 70% ethanol for 15 minutes. The fabric was then rinsed with sterile water and allowed to dry for approximately 30 minutes in a biological safety cabinet. The fabric swatches were then spotted with 10 µL of each bacterial dilution in triplicate. After spotting, fabric samples were imaged using an IVIS Lumina II imaging system (PerkinElmer, Waltham, MA) with one minute exposure time on luminescence imaging setting f-stop 2, field of view 12.8, and binning factor 8. Following imaging, the samples

were rinsed together in a 1 L beaker, using 125 mL per fabric sample, for 15 minutes in sterilized water. The rinse water was decanted off and fabric samples were rinsed in 100 mL sterilized water. This rinse procedure was then repeated one additional time. Rinsed fabric was placed on an LB agar plate containing 200 μg/mL kanamycin. The plated samples were imaged again to determine the amount of bacteria lost following rinsing. To determine the ability of the bacteria to regrow on each fabric, the swatches were then incubated at 37 °C and reimaged hourly for 3 hours. To assess whether the coating was bactericidal or anti-adhesive, samples were spotted with 10 μl of 5 x 10^8 colony forming unit per ml (CFU/ml) of *S. aureus* and imaged to quantify radiance. The samples were rinsed individually in 125 ml PBS for 15 minutes with a magnetic stir plate and then imaged to determine amount of bacteria removed using bioluminescence. Rinse water for each sample underwent three 10-fold dilutions, which were all spotted on an LB agar plate coating 200 μg/ml kanamycin. Bacterial colonies were counted to determine the amount of viable bacteria in the rinse water.

4.2.4 Multilayer Film Characterization

Thickness was evaluated using an α-SE ellipsometer (J.A. Woolam Co. Lincoln, NE). Film surfaces were characterized using a Dimension Icon atomic force microscope (Bruker, Billerica, MA) in tapping mode. Surface wettability was evaluated using a CAM 200 goniometer optical contact angle and surface tension meter (KSV Instruments, Ltd. Monroe, CT). Weight gain on polyester fabric was measured on 33 by 33 cm2

sheets, which were weighed dry before and after coating to measure the change in mass due to the coating.

4.3 Results and Discussion

4.3.1 Multilayer Film Growth and Morphology

Thickness of poly(diallyldimethylammonium chloride)/poly(acrylic acid) assemblies, measured at two bilayer increments, is shown in **Figure 4.2**. Growth is linear, even beyond 10 bilayers, suggesting uniform growth per bilayer and minimal interdiffusion between PDDA and PAA.[205] Studies reporting exponential growth for this system were carried out under similar conditions (i.e. pH and solution concentration),[206] but deviation from a linear fit was only observed at bilayers beyond the scope of this study. Deposition of the two polyelectrolytes was performed at differing pH (PAA ~3.0 and PDDA ~6.5). During PAA deposition, the polymer is in a very weakly- charged globular conformation. It is believed that during deposition, a large amount of poly(acrylic acid) is adsorbed onto the PDDA to achieve charge balance and increases the observed texture of the coating (**Figure 4.3**). During PDDA deposition, the solution pH causes the previously deposited poly(acrylic acid) to be highly charged. It is believed that a small amount of PDDA is adsorbed based on the results of other studies involving deposition of highly charged polyelectrolytes.[205, 207] Weight gain on fabric exhibited two different linear growth regimes. Beyond four bilayers there was heavier deposition, which is attributed to formation of a coherent coating. The initial layer deposition relies

on van der Waals interactions between PDDA and the PET substrate, which can result in island-like deposition that can persist for a few bilayers (sometimes known as the induction period).[208-209] Once the polyelectrolytes achieve complete coverage, a greater growth rate occurs due to more surface area with ionic bonding sites.

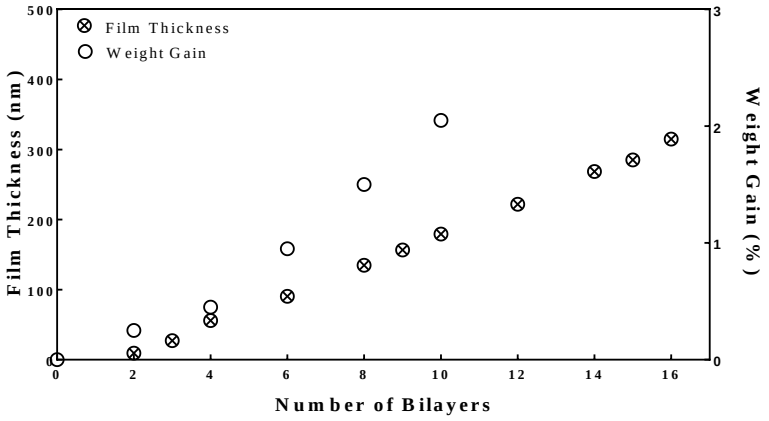

Figure 4.2. Film thickness on a silicon wafer and weight gain on PET fabric as a function of PDDA/PAA bilayers deposited.

The surface of PDDA/PAA films deposited on a silicon wafer were imaged using atomic force microscopy (AFM), as shown in Figure 2. Uncoated silicon has no remarkable surface features and an average surface roughness of 1 nm. Two bilayers (BL) of PDDA/PAA display island-like domains scattered across the surface of the silicon wafer. Bare silicon is observed and the surface roughness increased to approximately 4 nm (measured using a 20 x 20 μm2 micrograph). At 4 BL of deposition, improved yet incomplete coverage can be seen in the form of porosity. One such pore is highlighted with an arrow in the micrograph. The depth of this pore is 40-50 nm, which correlates

with the film thickness of 56 nm (Figure 1). The surface roughness of four bilayers is ~11 nm. This agrees with prior studies, where the charge state of the polymer during deposition played an important role in the surface topology.[210] Significant texture can be seen at the surface of the 10 BL film, with a surface roughness of 16 nm, but the pores seen at 4 BL are not observed. This increase in surface roughness is believed to cause the observed decrease in contact angle (see insets in micrographs of **Figure 4.3**) by increasing surface area of the film.

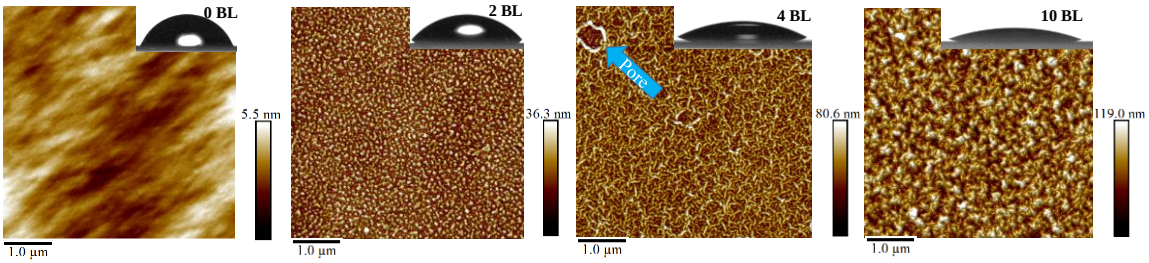

Figure 4.3. Atomic force microscope tapping mode surface images of a bare silicon wafer and coated with 2, 4 and 10 PDDA/PAA bilayers (from left to right). The inset images are contact angle images of these surfaces on a 179 µm PET substrate.

The contact angle of uncoated PET film is 71±2°, while two bilayers of PDDA/PAA reduced this value to 46±3°. At 4 BL, the contact angle was further reduced to 28±1° (and 20±1° with 10 BL). This increase in hydrophilicity with PDDA/PAA bilayers can be explained by the degree of protonation of PAA. During deposition, the pH of the PAA solution was ~3. The pKa of PAA is reported to be 4.5,[211] so the vast majority of the carboxylic acid groups are protonated (a ratio of approximately 100:1) at pH 3. These protonated acid species can participate in hydrogen bonding (also known as polar

interactions) with water to form a hydration layer at the film surface,[212] which leads to the spreading of the water and a decrease in the contact angle. It is believed that the increased surface roughness across the 10 BL coating results in more PAA available to participate in lowering the contact angle. Contact angle roughness values are summarized in **Table 4.1**.

Table 4.1. Thickness and surface properties of PDDA/PAA deposited on silicon wafers.

Bilayers	Thickness [nm]	Roughness [nm]	Contact Angle [°]
0	N/A	1.24	71 ± 2
2	9.4 ± 0.3	3.98	46 ± 3
4	56.0 ± 0.7	10.5	28 ± 1
10	179.3 ± 0.5	16.1	20 ± 1

*Contact angle measured on PET film**.**

4.3.2 Bacterial Adhesion

In an effort to quantify bacterial adhesion to the surface of polyester fabric, Staphylococcus aureus was selected due to its natural abundance on human skin.[213] This abundance contributes to infections around surgical sites and other opportunistic wound infections. Polyester was chosen as a model substrate because of its prolific use as a fabric for apparel. When the PDDA/PAA nanocoating was applied, a reduction in the amount of adhered bacteria after a simple rinse with sterilized water was observed, as shown in **Figure 4.4**. A bioluminescent strain of *S. aureus* containing an integrated copy of the luxABCDE operon from Photorhabdus luminescens was used to visualize and quantitatively measure bacterial populations on fabric. The colorful spots indicate

luminescence from viable bacteria, with brighter/warmer colors and larger spots representing more bacteria present on the fabric. When the fabric is rinsed with sterilized water the intensity is reduced, demonstrating the removal of viable bacteria.

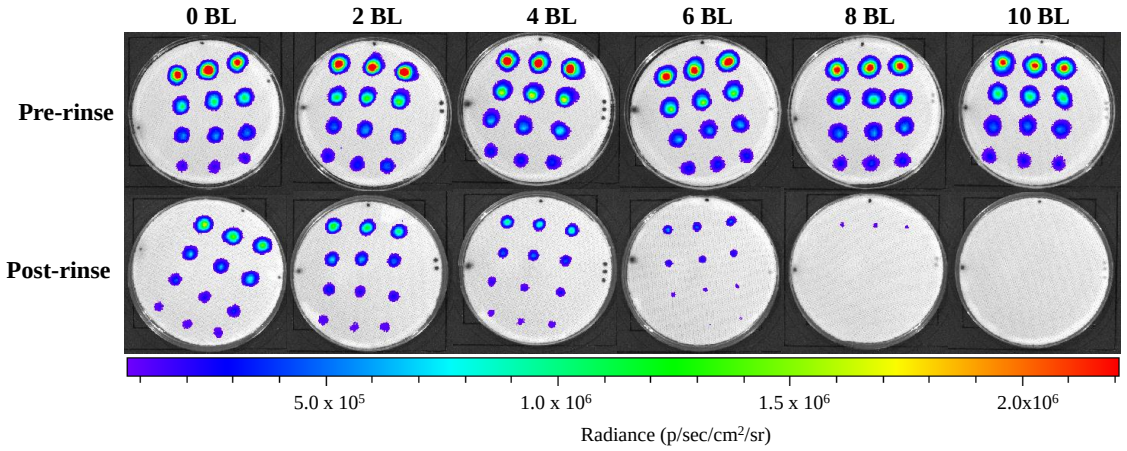

Figure 4.4. Representative fabric samples before and after rinsing with sterilized water. Higher radiance indicates more viable bacteria present on fabric. Rows consist of spots with the same bacterial concentration. Columns consist of spots with bacterial concentration decreasing by 50% per row, starting with 5 x 108 CFU/mL. Extraneous dots on the edge of each sample are lab marker spots for identification and positioning purposes.

Increasing the bilayers of PDDA/PAA deposited onto the fabric decreases bacterial adhesion, with 10 BL releasing bacteria below the limit of detection after rinsing. This data was quantified using Living Image software (Perkin Elmer) and correlated to bacterial colony forming units (CFU) using a standard curve generated from 10 fold dilutions of bioluminescent S. aureus Xen36. CFU were calculated for the most concentrated spots on the fabric (top row of each sample). The data are summarized in **Table 4.2**, showing a steady decrease in the amount of S. aureus detected before and after rinsing. At 6 BL, there is an order of magnitude reduction in detected

bacteria. At 10 BL, the amount of bacteria detected is two orders of magnitude less than uncoated fabric. The percent removal of bacteria was calculated for all trials by calculating the difference in luminescence measured before and after rinsing the fabric and dividing by the total luminescence measured for each dilution (**Figure 4.5**). As bilayers of PDDA/PAA increase, the percent removal of bacteria detected increased. With no coating, rinsing removes ~50% of S. aureus from the polyester fabric surface, while ~99% is removed with a 10 BL PDDA/PAA coating that adds only 2.5% to the weight.

Table 4.2. Colony forming units (CFU) detected before and after water rinse of polyester fabric.

Bilayers	**Before Wash [CFU]**	**After Rinse [CFU]**
Uncoated	$1.50 \times 10^7 \pm 2 \times 10^6$	$7.02 \times 10^6 \pm 5 \times 10^5$
2	$1.51 \times 10^7 \pm 2 \times 10^5$	$4.98 \times 10^6 \pm 5 \times 10^5$
4	$1.71 \times 10^7 \pm 7 \times 10^5$	$2.89 \times 10^6 \pm 1 \times 10^5$
6	$1.59 \times 10^7 \pm 1 \times 10^6$	$1.08 \times 10^6 \pm 5 \times 10^4$
8	$1.48 \times 10^7 \pm 4 \times 10^5$	$2.97 \times 10^5 \pm 1 \times 10^4$
10	$1.41 \times 10^7 \pm 3 \times 10^5$	$1.72 \times 10^5 \pm 8 \times 10^3$

Figure 4.5 shows the slight decrease in anti-adhesive activity seen between different dilutions of bacteria spotted onto the fabric. A two-way ANOVA test shows statistical significance between bilayers up to 8. Tukey's multiple comparison posttest was used to compare column means and $P<0.001$ for all conditions except for the comparison between 6 and 8 BL and the comparison between 6 and 10 BL where $P<0.01$. The PDDA/PAA nanocoating clearly diminishes the ability of the bacteria to

adhere to the fabric. This antifouling performance of coated fabric is remarkable, especially considering that 10 BL is only 180 nm thick and has no adverse influence on the hand (i.e. feel) of the fabric. There are several factors that contribute to the decreased adhesion of S. aureus. Derjaguin–Landau–Verwey–Overbeek (DLVO) theory describes the interaction of colloids with surfaces. Due to bacteria's negative surface charge, it can be treated as a colloid when examining bacterial adhesion.[142] According to DLVO theory, bacterial interactions with a smooth surface can be attributed to two types of interactions. Van der Waals interactions are always attractive forces, while electrostatic interactions can be either attractive or repulsive depending on the charge conditions of the surface. Other conditions that were explored in this study, but are not taken into account in the DLVO theory, are hydrophobic/hydrophilic interactions and contributions of surface roughness.

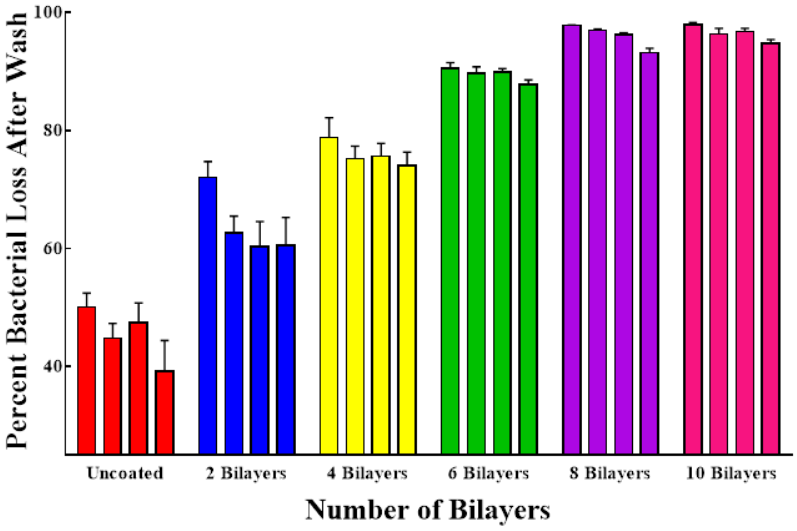

Figure 4.5. Percent loss of bacteria after rinsing as a function of PDDA/PAA bilayers deposited. Each bar within a color set represents a 2-fold dilution of bacteria initially deposited, starting with a concentration of 5 x10^8 CFU/mL, moving left to right within each set.

Polyester fabric is inherently nonpolar (i.e. no formal surface charge), making van der Waals interactions the primary means of bacterial adhesion on uncoated fabric. Bacteria removed from uncoated fabric is simply due to rinsing eliminating the most weakly bound individual *S. aureus* cells. Upon applying the PDDA/PAA multilayer coating, bacterial adhesion is more dramatically diminished. Contact angle measurements indicate an increase in hydrophilicity that creates a hydration layer through hydrogen bonding between the carboxylic acid repeat units in PAA and water molecules. The LbL deposited coatings increase the surface roughness, so this may contribute to the observed reduction in bacterial adhesion. During adhesion testing, bacteria are suspended in pH 7 PBS. At this pH, surface PAA exposed to the bacterial

suspension will be highly ionized due to the interaction between phosphate and carboxylic acid. Previous studies suggest electrostatic repulsion between a negatively-charged surface and the negatively-charged bacterial wall is the predominate factor in limiting bacterial adhesion.[66-68] Studies have also shown that nanoscale surface roughness can reduce or slow the adhesion of *S. aureu*s to a surface[214-215] It is believed that, due to the observed surface roughness, there is less surface area for the bacteria to adhere to, which reduces the magnitude of attractive van der Waals forces. Under the conditions of the bacterial adhesion assay, the PAA on the surface is highly ionized, providing repulsive electrostatic forces from the negatively charged bacterial cell wall that likely further diminishes adhesion.

In an effort to confirm that the PDDA/PAA nanocoating is truly antifouling (i.e., releasing bacteria) rather than bactericidal, the same fabric samples shown in Figure 3 were put onto a nutrient rich agar plate and placed in a 37 °C incubator. These samples were then imaged hourly, as shown in **Figure 4.6**. Over three hours luminescence increased, radiating out from the spotting location, which was especially evident in the samples with fewer bilayers (**Figure 4.6a**). It is believed that increased bacterial growth is not the result of random adherence of viable bacteria during rinsing, but rather regrowth of viable *S. aureus* that remained adhered after rinsing. In examining the raw pictures of the regrowth and plotting bacterial population as a function of time after rinsing (**Figure 4.6b**), it is clear that fabric with more PDDA/PAA bilayers created an environment that resulted in slower bacterial regrowth because fewer colonies remained attached to the fabric. Rather than the film acting as a bactericidal agent, it is believed

that the bacteria that remained after rinsing were too poorly adherent for effective biofilm formation, which requires stable adherence as its first step.[145] The rate of regrowth observed for the 10 BL coated fabric, relative to uncoated PET (**Table 4.3**), can be explained by poor adherence rather than contact killing. To reinforce this hypothesis, aliquots of rinse buffer were spotted onto nutrient rich agar plates. Viable colonies were counted after 24 hours at 37 °C and plotted in **Figure 4.7**. As the number of bilayers increases and the quantity of bacteria adhered to the fabric decreases, the amount of viable bacteria in the rinse water increases by an order of magnitude. If the coating was only killing on contact, and not affecting adherence, there would be no relationship between viable bacteria in the rinse water and bilayer count.

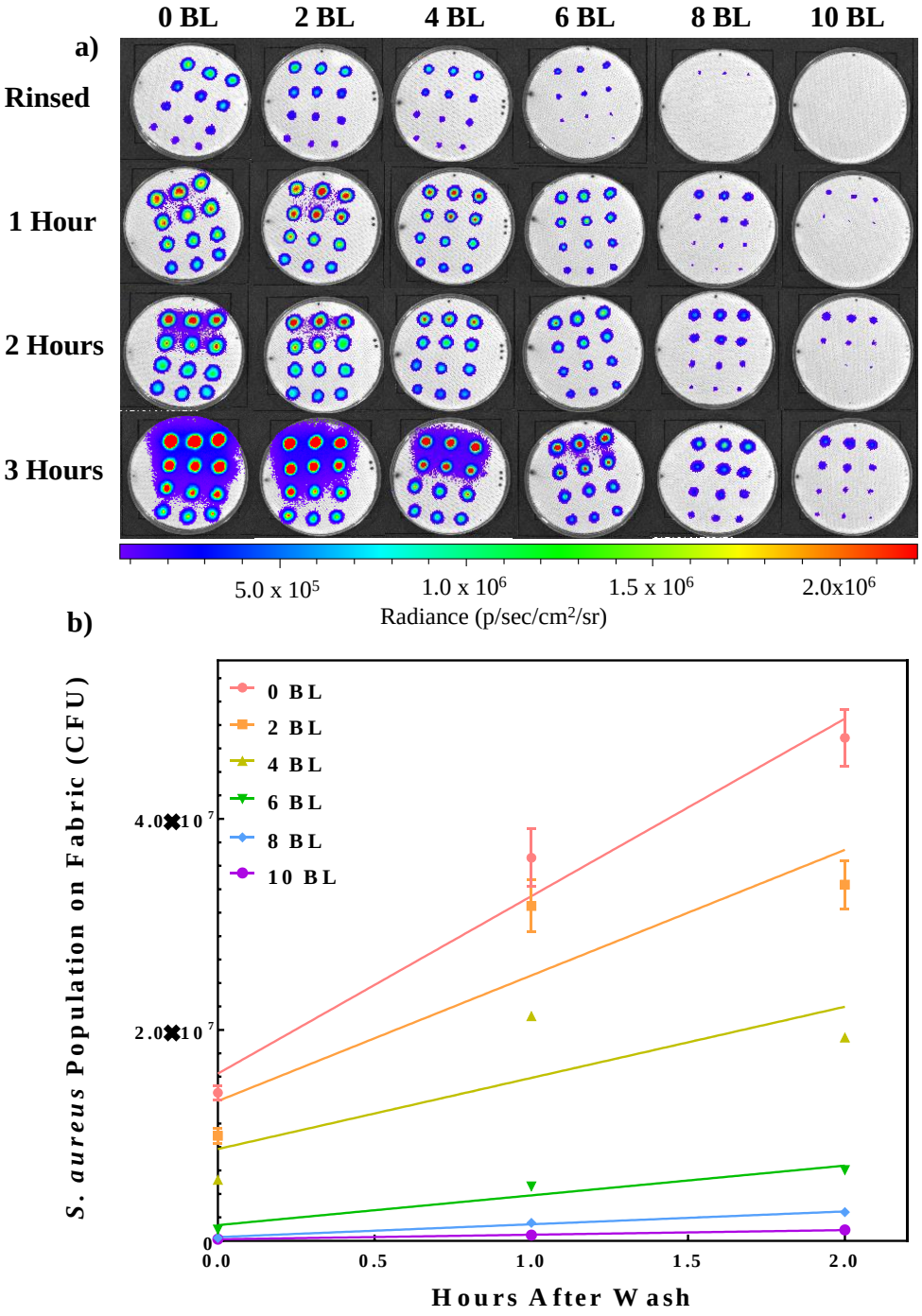

Figure 4.6. Representative experiment monitoring regrowth of *S. aureus* on PET fabric after rinsing. Smaller spots with cooler colors indicate lower bacterial concentration (a). Regrowth of *S. aureus* as a function of hours incubated after rinse for PET fabric coated with varying bilayers of PDDA/PAA (b).

Table 4.3. Rates of bacterial regrowth as a function of bilayers deposited on PET.

Bilayers	Regrowth Rate (CFU/ hour)
Uncoated	1.68×10^7
2	1.19×10^7
4	6.74×10^6
6	5.64×10^6
8	2.43×10^6
10	8.71×10^5

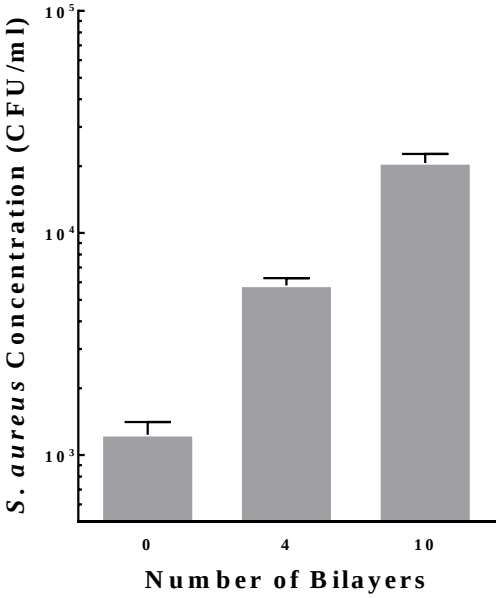

Figure 4.7. Concentration of *S. aureus* in rinse water as a function of bilayers deposited on PET fabric. Taller bars indicate a higher population of viable bacteria. Statistical variance assessed using a one-way ANOVA test ($P<0.001$).

4.4 Conclusion

A layer-by-layer deposited nanocoating was shown reduce the adhesion of *S. aureus* on a model polyester fabric. Just ten bilayers of poly(diallyldimethylammonium chloride) and poly(acrylic acid) caused 99% of bacteria to be released from the fabric surface with simple water rinsing. The efficacy of the coating was evaluated using a bioluminescence technique. A commercially available bioluminescent strain of *S. aureus* was deposited on coated and uncoated fabric and imaged to quantify its radiance, which correlates to viable CFUs, resulting in a quick and quantitative assessment of bacterial concentration on the fabric. With a 10-bilayer coating of PDDA/PAA (180 nm thick and adding only 2.5 wt% to the fabric), a two orders of magnitude reduction in detected bacteria was observed before and after rinsing relative to uncoated polyester. This performance can be attributed to a combination of hydrophilicity, increased surface roughness, and charge repulsion between bacteria and the surface, which is likely the largest contributing factor. It was determined that this nanocoating is truly antifouling, rather than bactericidal, by measuring regrowth of plates spotted with rinse water. Because of its prolific use in apparel, including medical garments, modifying polyester fabric to inhibit bacterial adhesion could be very useful for reducing the transmission and spread of MRSA infections. Additionally this technology could be easily scaled up using a conventional pad dry process,[216] making it commercially viable.

CHAPTER V

FUNCTIONAL POLYLECTROLYTE COMPLEX THIN FILMS DEPOSITED IN A SINGLE STEP

5.1 Introduction

Due to the difficulty of processing polyelectrolyte complexes in aqueous media, LbL has proven to be a valuable technique to conveniently deposit PEC thin films sequentially on a wide variety of surfaces and with a wide variety of properties.[1-3] Even so, the process of building PEC films sequentially (nanometers at a time) often requires tens to hundreds of processing steps to deposit enough material to meet performance goals. This drawback has limited the commercial viability of these films, despite their variety of commercially attractive properties. As highlighted in Chapter II, other methods to develop coatings using PEC have been investigated (e.g. pH control,[161-163, 166] coacervates,[108-109] sedimentation, [174-175] etc.) but their properties has been limited in scope.

In this chapter, polyelectrolyte complexes containing poly(diallydimethylammonium chloride) and poly(acrylic acid), deposited in a single-step, were investigated to effectively reduce the adhesion of *S. aureus* to polyester fabric and reduce the oxygen transmission rate of polyester (PET) thick films. Film properties were found to be dependent on the curing method (i.e. formation of ionic crosslinks). When these films were cured while the deposited polyelectrolyte mixture was still wet, the coating was found to be effective at removing > 95% of deposited bacteria to

polyester fabric. It is believed that the PEC thin films increase surface charge, causing electrostatic repulsion between the surface and bacteria. If the polyelectrolyte mixture was dried before curing, the resulting film was less effective at removing bacteria from fabric, but is effective at reducing the oxygen transmission rate (OTR) of a thick PET film by two orders of magnitude. Increased cohesive energy and decreased free volume are the factors believed to influence the barrier properties. This discovery dramatically reduces the processing steps and time needed to prepare similar LbL assemblies, while also maintaining the desirable properties of the underlying substrates (e.g. flexibility of fabric or optical clarity for PET film).

5.2 Experimental

5.2.1 Materials for Antifouling Coatings

Poly(diallydimethylammonium chloride) (PDDA; 100 kg/mol; 20 wt% aqueous solution), poly(acrylic acid) (PAA; 100 kg/mol; 35 wt% aqueous solution), and citric acid monohydrate (CA; 99%), were purchased from Sigma Aldrich (St. Louis, MO) and used as recieved. 18 MΩ Deionized water was used for all aqueous solutions and rinsing procedures. 200 mM CA solutions were prepared at pH 3 and pH 5. Single-side-polished, 500 μm-thick silicon wafers (University Wafer, South Boston, MA) were rinsed with a sequence of deionized water, methonal, and deionized water. Si-wafers were dryed with filtered compressed air prior to a five minute plasma cleaning using a PDC-32G plasma cleaner (Harrick Plasma Inc. Ithica NY). Polyester 720H purchased from Test Fabrics Inc. (West Pittston, PA) was cut into 20x20 cm^2 squares and soaked

in 100% ethanol for 20 minutes, washed with deionized water, and dried at 70 ˚C, prior to polyelectrolyte complex deposition. Bioluminexcent *Staphylococus aureus* Xen36 (Caliper Life Sciences, Waltham, MA) was used for bacterial adhesion assays.

5.2.2 Materials for Oxygen Barrier Coatings

PDDA (400-500 kg/mol; 20 wt% aqueous solution), PAA (250 kg/mol; 35 wt% aqueous solution), citric acid monohydrate (CA; 99%), were purchased from Sigma Aldrich and used as recieved. 18 MΩ Deionized water was used for all aqueous solutions and rinsing procedures. CA was prepared in 25, 100, 200, and 300 mM solutions. Solutions at the same concentrations were also prepared at constant ionic strength (~150 mM) by adding the appropiate amount of sodium chloride. All CA solutions were adjusted to pH 3. Poly(ethylene terephthalate) film (PET, 178 μm thick, ST505, Dupont-Teijin) was purchased from Tekra (New Berlin, WI). The PET was rinsed with a sequence of DI water, methanol, and DI water and dried with filtered compressed air. Clean PET was exposed to plasma cleaning for five minutes using a PDC-32G plasma cleaner (Harrick Plasma Inc. Ithica, NY). Glass slides for atomic force microsopy, UV-Vis light transmission, nanoindentation, and aluminum foil for FTIR, were prepared the same way.

5.2.3 Deposition of Polyelectrolyte Complex Thin Films

Deposition of PEC thin films for the reduction of bacterial adhesion was done as described here. PDDA (100 kg/mol) and PAA (100 kg/mol) were diluted with DI water (5 wt% and 8.75wt% respectively). PAA was slowly added to PDDA until a 1:3 molar ratio (based on repeat units) is reached. The polyelectrolyte mixture (PM) is then diluted to either 1.5 or 3 wt% dissolved solids with DI water. The pH was adjusted to 2 using 5 M HCl. The solution is allowed to stir (magnetic) overnight to dissolve any complex formed during intial mixing. The final solution was non-turbid and homogeneous. For dry cured (DPEC) coatings, washed and dried fabric was immersed in the PM for 5 minutes. Fabric was then squeezed several times to remove exess polyelectrolyte solution, and dried for 3 hours at 70 °C. Dried fabric was then immeresed in 200 mM citric acid at pH 3 or 5 for 20 minutes. The fabric was then rinsed with deionized water and dried at 70 °C overnight. For wet cured (WPEC) coatings, washed and dried fabric was immersed in the PM mixture for 5 minutes. Fabric was then squeezed several times to remove exess polyelectrolyte solution, and then placed into 200 mM citric acid at pH 3 or 5 for 20 minutes. The fabric is then rinsed with deionized water and dried at 70 °C overnight. Two-dimensional substrates (e.g. PET and Si-wafers) were coated in a similar manner. The only difference being that excess polyelectrolyte mixture was wicked away with a paper towel three times before drying (for DPEC) and immersion in buffer (for WPEC). This process is shown schematically in **Figure 5.1b**.

Gas barrier coatings were deposited on 178 µm thick PET film as described here. PDDA (400-500 kg/mol) and PAA (250 kg/mol) were diluted with DI water (5 wt% and 8.75wt% respectively). PAA was slowly added to PDDA until a 1:3 molar ratio (based

on repeat units) was reached. The polyelectrolyte mixture was then diluted to 1.5, 3, 4.5 or 6 wt% dissolved solids with DI water. The pH was adjusted to 2 using 5 M HCl. The solution is allowed to stir (magnetic) overnight to dissolve any complex formed during intial mixing. The final solution was non-turbid and homogeneous. Cleaned PET film was immersed in the polyelectroltye solution for five minutes, after which the excess polymer solution was wicked away, and the sample was placed in the oven at 150 °C for 20 minutes. The sample was then placed in a dry box (~ 11% RH) for 3 hours. It was then immersed in citric acid buffer at pH 3 for 20 minutes to cure the coating (i.e. form ionic crosslinks). The sample was dip rinsed in DI water for 20 seconds three times, and placed in the oven for 20 minutes at 150 °C. The finished samples were stored in a dry box (~11% RH) prior to testing. This process was carried out in an identical fashion on glass slides and Al foil.

5.2.4 Evaluation of Bacterial Adhesion

Adhesion of *Staphylococcus aureus* to circular swatches of 8.5 cm diameter polyester fabric, coated with the dry and wet cured PEC coatings at pH 3 and 5 (and an uncoated control), were evaluated in an identical manner to that reported previously (and outlined in Chapter IV).[217]

5.2.5 Film Characterization

Thickness of PEC films deposited on glass slides was measured using a DektakXT Surface Profiler (Bruker, Billerica, MA), with a stylus force of 2 mg and stylus radius of 12.5 μm. Static contact angles were measured on PEC coatings deposited on 178 μm PET film using a CAM 200 goniometer optical contact angle and surface tension meter (KSV Instruments, Ltd. Monroe, CT). Coated PET fabric samples were imaged using a field-emission scanning electron microscope (SEM) (Model JSM-7500, JEOL; Tokyo, Japan). Samples were mounted on an aluminum block with carbon tape and sputter coated with 5 nm of platinum/palladium alloy prior to imaging. Surface morphology was evaluated using a Dimension Icon atomic force microscope (Bruker, Billerica, MA) in tapping mode. Probes (HQ:NSC35/Al BS, Micromasch USA Watsonville, CA) had a force constant of 5.5-16 N/m and a tip radius of ~8 nm. Reduced modulus (E_r) of PEC barrier coatings was evaluated using a TI 950 Triboindenter (Hysitron, Inc, Minneapolis, MN). A Berkovich tip with a radius of curvature of ~150 nm was used with a loading force of 200 μN (to keep indentation depth ~10% of coating thickness) and was calibrated against a fused quartz standard to generate the area function. A loading profile of 10 s of loading, followed by 5 seconds at a stationary position and 2 seconds of unloading was used. Infrared spectra were taken on PEC coatings deposited on aluminum foil,[218] using an Alpha Platinum-ATR FTIR spectrometer (Bruker, Billerica, MA), taking 30 scans from a range of 400-4000 cm^{-1} range with a resolution of 4 cm^{-1}. Light transmission through gas barrier coatings deposited on glass slides was measured using a USB2000 UV-Vis spectrometer (Ocean Optics Inc., Largo, FL) at 550 nm. Data was normalized so uncoated glass slides

measured ~100 % transmission. Oxygen transmission rate measurements were performed by Ametek-Mocon (Minneapolis, MN) using an Oxtran 2/21 ML oxygen permeability instrument (in accordance with ASTM Standard D-3985) at 23 °C and at 0% RH.

5.3 Results and Discussion

5.3.1 Polyelectrolyte Complex Deposition

In order to simultaneously deposit oppositely charged polyelectrolytes as a uniform thin film, the electrostatic interactions must be inhibited to prevent complexation. This can typically be achieved through the introduction of salt and/or pH adjustments, depending on the polyelectrolytes involved.[103, 107, 109] This leads to a homogeneous solution of oppositely charged polyelectrolytes suitable for deposition. PDDA and PAA can be mixed at pH ~2 to form a homogeneous mixture. PDDA is a strong polyelectrolyte and the charge density is independent of pH. PAA on the other hand, has a pKa of ~4.5[211] and charge density can be reduced by reducing pH though protonation of the carboxylic acid. Increasing the pH of the PM initially causes small insoluble PEC aggregates to form, which are easily suspended in the mixture. By increasing the pH further, the charge density of the PAA increases sufficiently to promote the formation of an interpolymer composite between PDDA and PAA (coalescence) and macroscopic precipitation is observed (**Figure 5.1a**). The PM at pH 2 is suitable for coating a wide variety of substrates (e.g. glass, silicon wafer, PET film,

and PET fabric). Deposition of the polyelectrolyte mixture onto a substrate was carried out through immersion of the substrate into the polymer solution. The polyelectrolytes likely adsorb through a combination of van der Waals and dipole interactions. After initial deposition of the PM, the coating can either be dried, thereby immobilizing the polymers onto the substrate surface, or the PM can be directly cured, while still dissolved in water on the substrate (**Figure 5.1b**). Curing is done by exposing the PM to citric acid buffer, which causes deprotonation of PAA and subsequent formation of ionic crosslinks with PDDA. This forms the functional and insoluble polyelectrolyte complex film (coating) on the substrate.

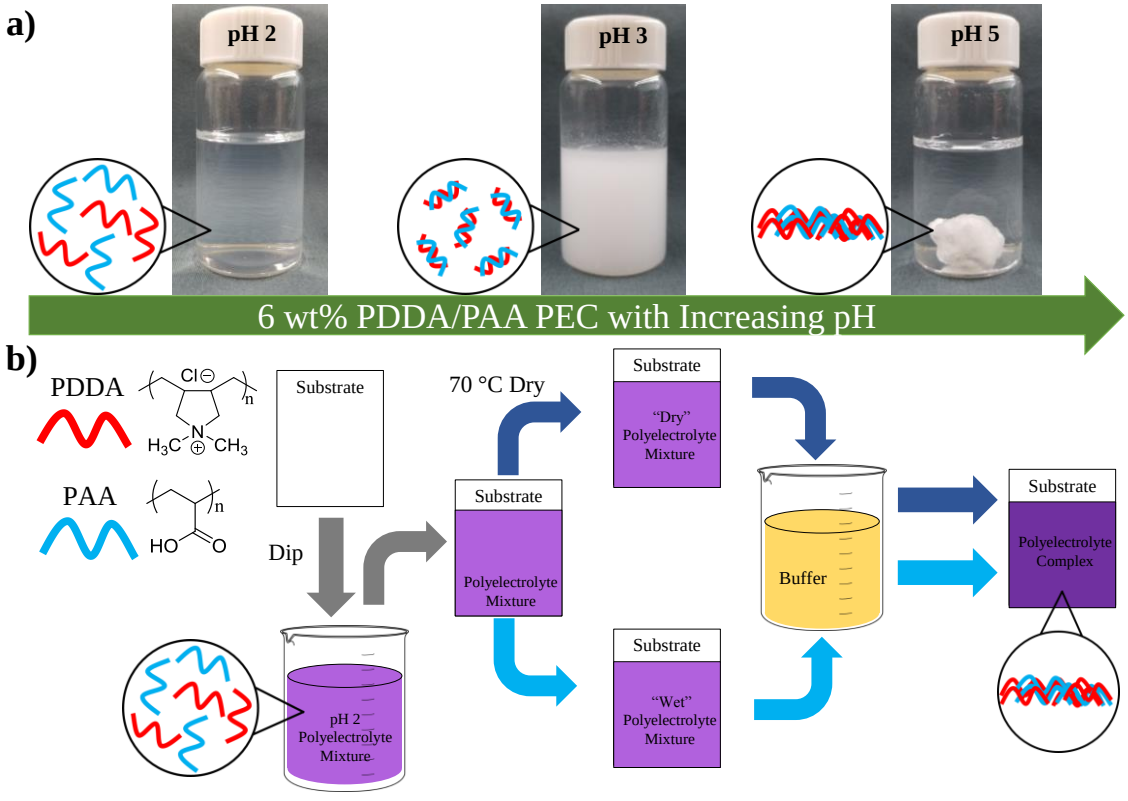

Figure 5.1. Photographs and schematic representation of 6 wt% PDDA/PAA PEC at various pH values (a). Schematic of PEC deposition (b).

The effect of curing the polyelectrolyte mixture after drying, or while still wet on the substrate, and curing pH was compared using 200 mM citric acid buffer at pH 3 and 5. ATR-FTIR spectroscopy was conducted on both wet and dry cured coatings deposited on aluminum foil (**Figure 5.2**). Al foil has very minimal background signal and makes for a good substrate to examine polyelectrolyte complex coatings without the need for freestanding films.[218] By increasing pH, PAA charge density increases through deprotonation and electrostatic complexes form on the substrate. Before complexation, the deposited polyelectrolyte mixture has a large asymmetric carbonyl stretch at 1700 cm^{-1} from PAA, indicating that the PAA is completely protonated. Upon exposure to pH 3 buffer, the intensity of the protonated peak decreases and a new assymetric carbonyl stretch at 1550 cm^{-1} from the carboxylate formed during curing. The intensity of the carboxylate peak increases upon exposure to pH 5 buffer, while the intensity of the protonated acid decreases, suggesting an increase in the charge density of PAA at this pH. At a higher charge density (i.e. higher pH) more interpolymer networking between PDDA and PAA takes place,[93] leading to the increased coalescence observed in **Figure 5.1a**.

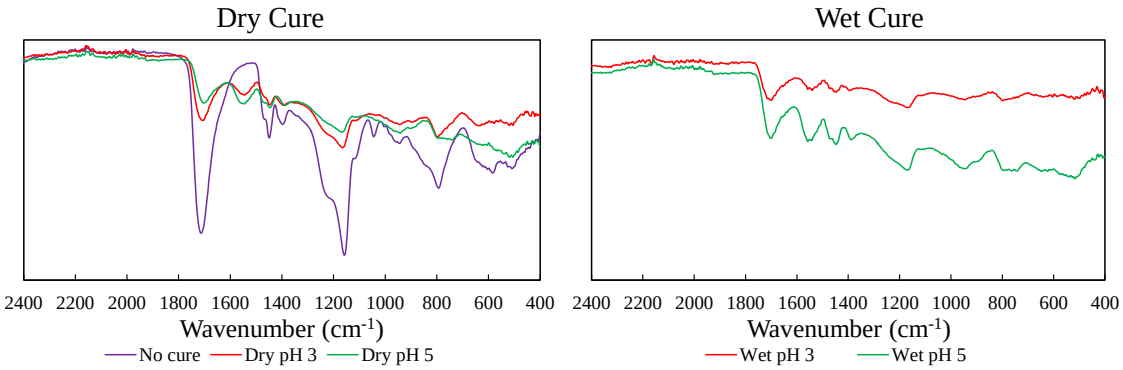

Figure 5.2. FTIR spectra of dry and wet cured PDDA/PAA polyelectrolyte complex coatings deposited on Al foil.

The thickness of coatings is influenced by the concentration of dissolved polyelectrolytes in the PM solution used for deposition. Thickness of dry cured coatings deposited on Si wafers were measured using profilometry at different pH and PM concentrations. The thickness of the DPEC coatings without curing increases as the concentration of the solution increases (**Figure 5.3**). As this process utilizes solvent evaporation to deposit the initial coating, having more dissolved polyelectrolyte in solution leads to more polymer deposited.[219] There isn't a significant difference between films thicknesses cured at different pH values. This is likely due to the fact that the PM is immobilized through drying, and stays deposited on the substrate surface during PEC formation. This suggests that the thickness of the cured coatings are dependent only on the amount of material initially deposited. Because of the lack of uniform coverage observed in AFM (**Figure 5.4**) and SEM (**Figure 5.5**), the thickness of WPEC coatings could not be reliably measured, but increasing the concentration of the deposition solution does lead to increased coverage and coalescence in both pH 3 and pH 5

coatings, along with increased weight gain when deposited on PET fabric (**Table 5.1**), suggesting that more PEC is deposited.

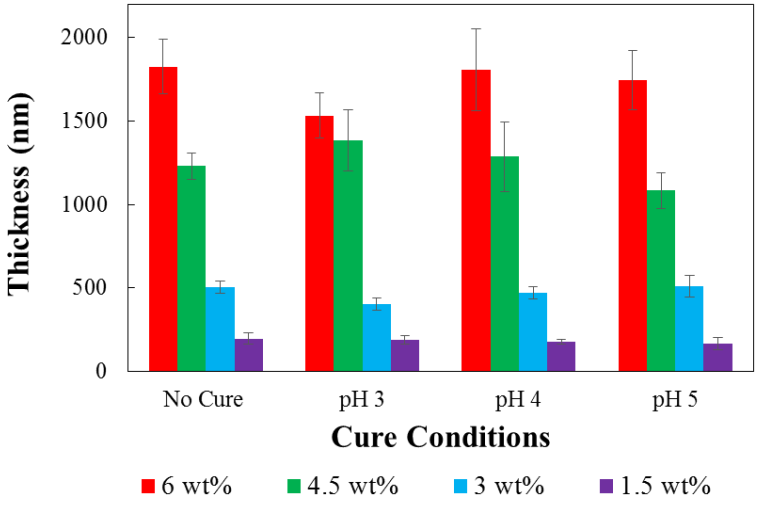

Figure 5.3. Thickness of dry cured PDDA/PAA coatings using different dissolved polyelectrolyte concentrations and cured with 200 mM citric acid at different pH values.

Coating morphology was observed using atomic force microscopy, as shown in **Figure 5.4**. DPEC coatings show relatively uniform surface coverage. These coatings do not possess any distinct features, apart from the porosity observed in pH 5 films. This is likely from the increased PEC mobility during cure due to the higher ionic strength of the buffer at pH 5 that allows for pore formation. Changes in PEC film morphology due to exposure to salt solutions (i.e. increased ionic strength) have been reported previously.[220-221] Since the coatings are immobilized through drying before curing, formed complex stays adhered to the surface rather than becoming suspended in the curing solution, leading to the observed uniform coverage. Relative to dry cured

polyelectrolyte complex, WPEC coatings have significantly different structure. pH 3 cured coatings appear to consist of aggregates of small polyelectrolyte complex particles. Increasing polymer concentration leads to increased aggregation of the complexes. pH 5 cured coatings still show aggregation, however the films have a signicant increase in coalescence. This is likely occuring due to two factors. By increasing the PAA charge density, each PAA chain has more carboxylate groups available for complexation. Each chain can form ionic crosslinks with more sites on an individual PDDA chain, or can complex with sites on other PDDA chains. This leads to the significantly more coalesced films (compared to pH 3 cured coatings) through interpolymer ionic bonding. It is also believed that the electrostatic interactions that do form during curing are likely more shielded (i.e. weaker) than those in the pH 3 coating due the increased ionic strength of the buffer.[221] This leads to the polymer chains being more mobile within the formed PEC and aiding in the coelescence of the film. Increasing the concentration of dissolved polylectrolytes from 1.5 to 3 wt% increases the aggregation and coalecence observed in both pH 3 and pH 5 wet cure coatings. This is likely due to there simply being more polyelectrolytes available to form PEC.

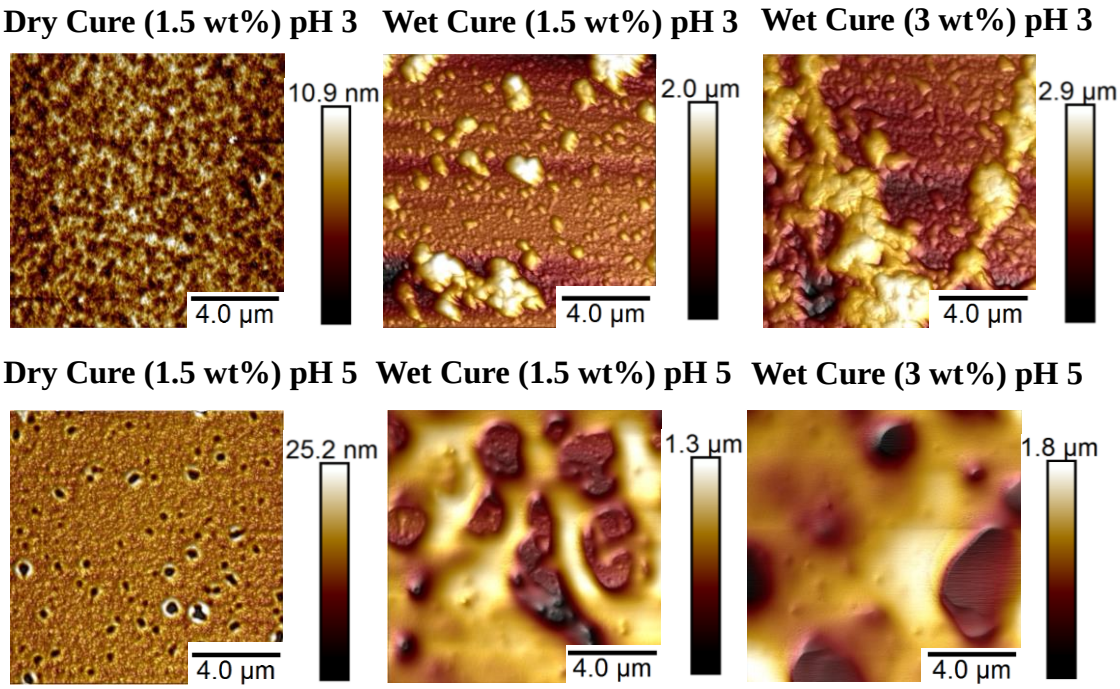

Figure 5.4. AFM images of wet and dry cured coatings deposited at pH 3 and 5 on a Si wafer at different deposition concentrations.

5.3.2 Reduction of Bacterial Adhesion to Polyester Fabric

The amount of coating deposited on the surface of fabric was monitored by evaluating the weight gain (**Table 5.1**). 1.5 wt% polymer mixture was used for DPEC coatings and the weight gain was 2.1 wt% and 2.3 wt% for pH 3 and 5, respectively. When WPEC coatings are made at the same polymer concentrations, the weight gain is lower (1.3 and 2.1 wt% at pH 3 and 5, respectively), especially at pH 3. During dry curing, the coating is already immobilized onto the substrate surface and complexation occurs with little PEC loss in the curing solution. This is not the case with the wet cured coatings. Significant amounts of flocculants (i.e. non-adheard PEC) are visible through

the increased turbidity in the curing solution. This in turn leads to the lower weight gain observed. Increasing polymer solution concentration from 1.5 to 3 wt% increased the wet cure weight gains to 3.2 and 4 wt% for pH 3 and 5, respectively, simply due to more polymer being available to complex and deposit. The morphology observed in AFM is also observed with PEC deposited on fabric in SEM. (**Figure 5.5**). The difference in weight gain as a function of pH can be explained by two factors. The increase in ionic strength of the buffer solution at pH 5 allows the polymer chains more mobility at higher ionic strength due to electrostatic charge shielding, allowing PEC aggregates to coalesce more readily and resulting in higher weight gain. Similar results have been observed with PEC deposited on paper pulp.[175] Increasing pH also allows for a greater charge density on PAA (through deprotonation) and as a result there is a greater amount of interpolymer networking between PDDA and PAA that leads to more coalescence.[222]

Table 5.1. Weight gain of PEC deposited on polyester fabric and contact angle of PEC deposited on PET film.

Coating Cure Conditions	Weight Gain [%]	Contact Angle [°]
Uncoated	N/A	77.01 ± 2.82
Dry Cure pH 3	2.08 ± 0.12	51.46 ± 4.33
Dry Cure pH 5	2.31 ± 0.15	31.14 ± 4.11
Wet Cure 1.5% pH 3	1.22 ± 0.14	N/A
Wet Cure 3% pH 3	3.22 ± 0.08	15.77 ± 1.73
Wet Cure 1.5% pH 5	2.09 ± 0.18	N/A
Wet Cure 3% pH 5	3.95 ± 0.14	23.38 ± 3.09

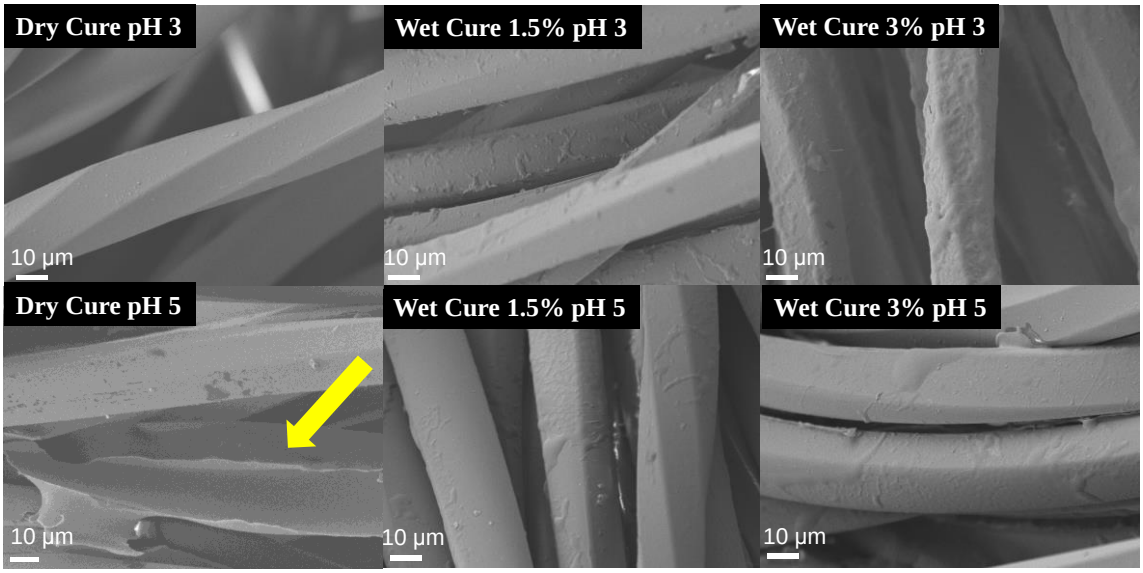

Figure 5.5. SEM micrographs of PET fabric with PEC deposited using wet and dry cure methods.

The difference in observed morphology indicates that the curing conditions should be tailored to the substrate and application. This was investigated by depositing PDDA/PAA polyelectrolyte complexes on the surface of polyester fabric. Micrographs obtained using SEM show that DPEC coatings are uniform and don't change the underlying morphology of the fabric fibers. However, extensive bridging of PEC between multiple fibers occurs. Broken bridges can be observed in the micrographs, leaving the underlying substrate with no coating (**Figure 5.5** yellow arrow and **5.6**) and are especially evident in pH 5 coatings. This is not suitable for applications were complete surface coverage is needed (e.g. reduction of bacterial adhesion). Not only is there incomplete surface coverage due to bridging, but the intact bridges lead to significantly stiffer fabric compared to uncoated fabric, which adversely impacts the hand. PET fabric with WPEC has similar aggregate morphology as observed in AFM, and even though the topology is not uniform (there are some areas with significant aggregation), complete surface coverage is achieved. Bridging is significantly reduced as well. Drying the PM to the fabric before PEC formation immobilizes the PM bridges, which during curing are not removed. Curing while the PM is still dissolved leads to deposition only on fibers because the material that would cause bridging is loosely adhered. During curing, the PEC formed is suspended into the curing solution rather than bridging fibers together. The stiffness of WPEC coated fabric is significantly lower (and close to uncoated fabric) relative to DPEC coatings, in part due to higher fiber mobility. More PEC is deposited by increasing the dissolved polymer concertation from 1.5 to 3 wt%. More bridging is observed, but there is significantly less than the DPEC coatings at

pH 3 and 5. The bridging that is present seems to be from the coating settling on the areas of the fabric with higher fiber density rather than fibers being "glued" together with PEC.

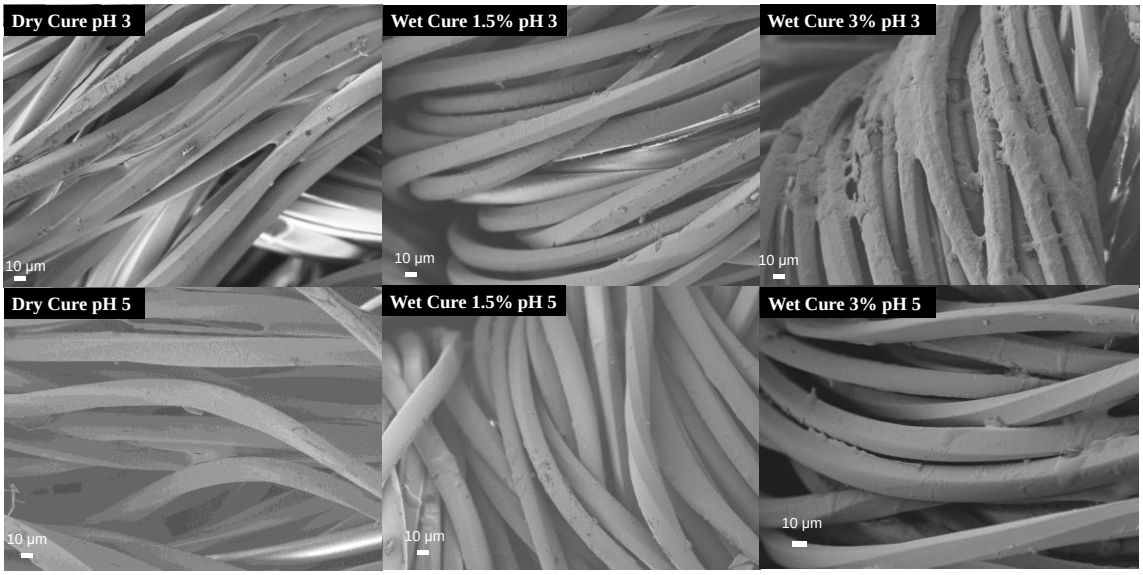

Figure 5.6. SEM micrographs showing bridging of dry and wet cured PDDA/PAA PEC on polyester fabric.

Differences in the adhesion of *Staphylococcus aureus* to coated fabric was evaluated using the same technique outlined in Chapter IV. Briefly, the amount of photons detected from bioluminescent *S. aureus* was compared after depositing (10 µL spots at 9.5 x 10^8 CFU/mL) and rinsing uncoated and PEC-coated PET fabrics. This generates a "heat" map showing where viable bacteria are on the fabric. Larger spots with warmer colors (red and yellow) indicated more photons detected (i.e. more viable

bacteria). It should be noted that initial bacterial populations on uncoated fabric are higher due growth between the time of deposition and initial measurement (**Figure 5.7a**). Using a standard curve, radiance was converted to colony forming units (CFU) quantitatively evaluate bacterial adhesion before and after rinsing (**Table 5.2**). When rinsed, ~42% of deposited bacteria remains on uncoated fabric. This was similar to the value shown in Chapter IV. The best coating (wet cured 3 wt% pH 3) only allows ~3% of the initially deposited bacteria to remain after rinsing. One-way Anova analysis, followed by Tukey's comparison test (calculated using GraphPad Prism software) showed that all coated fabric reduced the adhesion of deposited bacteria significantly compared to uncoated fabric ($p < 0.001$), as shown in **Figure 5.7b**. Dry cured pH 5 coatings show a significant deficit in antifouling ability relative to all other coatings ($p < 0.001$). Dry cured coatings at pH 3, also show a diminished ability to reduce bacterial adhesion relative to wet cured coatings 3 wt% pH 3 ($p < 0.05$). Beyond that the difference observed between coated fabrics were not statistically significant. It should be noted that there is slightly better anti-adhesion (i.e. more bacteria removed) in the wet cured coatings when increasing the polymer concentration from 1.5 wt% to 3 wt%. This is likely due to the increased surface coverage observed in both AFM and SEM (**Figure 5.5**). Overall, there is an order of magnitude reduction in the amount of detected bacteria in wet cured 3wt% coatings at both pH 3 and 5, relative to the uncoated control.

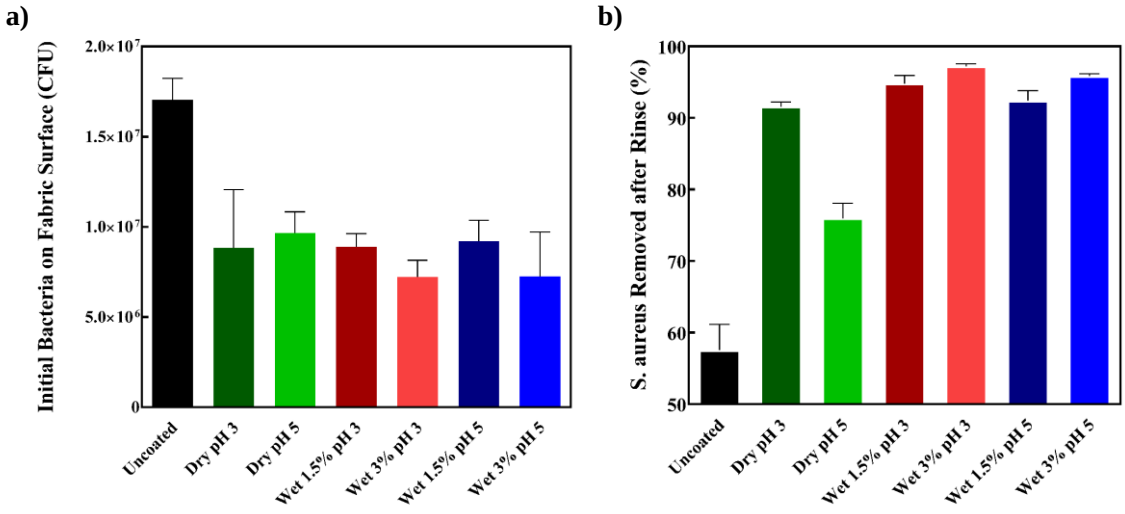

Figure 5.7. Differences in initial adhesion of *S. aureus* to coated and uncoated polyester fabric deposited at 9.5 x 10^8 CFU/mL (a). Amount of bacteria removed after rinsing (b).

Table 5.2. Measured CFU of *S. aureus* before and after DI water rinse.

Cure Conditions*	***S. aureus* Before Rinse [CFU]**	***S. aureus* After Rinse [CFU]**	**Bacteria Remaining [%]**
Uncoated	$1.71 \times 10^7 \pm 0.1 \times 10^7$	$7.38 \times 10^6 \pm 1.4 \times 10^6$	43
DPEC pH 3	$8.83 \times 10^6 \pm 0.21 \times 10^6$	$7.40 \times 10^5 \pm 0.26 \times 10^5$	8
DPEC pH 5	$9.67 \times 10^6 \pm 0.17 \times 10^6$	$2.33 \times 10^6 \pm 0.02 \times 10^6$	24
WPEC 1.5% pH 3	$8.89 \times 10^6 \pm 0.31 \times 10^6$	$4.60 \times 10^5 \pm 1.20 \times 10^5$	5
WPEC 3% pH 3	$7.23 \times 10^6 \pm 0.04 \times 10^6$	$2.04 \times 10^6 \pm 0.14 \times 10^5$	3
WPEC 1.5% pH 5	$9.21 \times 10^6 \pm 0.09 \times 10^6$	$7.06 \times 10^5 \pm 0.42 \times 10^5$	8
WPEC 3% pH 5	$7.25 \times 10^6 \pm 0.37 \times 10^6$	$3.05 \times 10^5 \pm 0.06 \times 10^5$	4

* Percent value in the Cure Conditions column refer to the percent of dissolved solids in the deposition solution.

The diminished ability of bacteria to adhere to coated fabric is a result of the changes in surface properties imparted by the coating. The interaction between a surface

and bacteria can be described using modified Derjaguin–Landau–Verwey–Overbeek (DLVO) theory.[142] This theory describes the interactions between a colloid and a surface by describing van der Waals (always attractive) and electrostatic interactions (attractive or repulsive depending on surface charge). Bacteria is usually negatively charged in aqueous media, so these interactions can be described using DLVO theory, but other interaction also need to be taken into account, including Lewis acid and base interactions (usually in the form of a hydrogen-bonded hydration layer).[143-144] The decrease in contact angle (**Table 5.1**) suggests the formation of a hydration layer, which may reduce the bacteria's ability to adhere to coated fabric. Repulsion from electrostatic interactions can also explain the observed behavior. PEC is formed with an excess of PAA present, is only 3% ionized (i.e. deprotonated) at pH 3, so there is still an excess of protonated PAA in the final PEC evidenced by the carbonyl stretch at 1700 cm^1 in FTIR (**Figure 5.2**). At high pH, PAA will ionize and can repel negatively-charged bacteria.

Dry cured coatings were exposed to pH 7 buffer and dried to simulate similar conditions to those in the antifouling assay. The films were compared to ambient films to estimate the differences in carboxylate within the films at higher pH using FTIR (**Figure 5.8**). It was observed that the films at pH 7 have predominately carboxylate functionality because of the strong absorbance at ~1550 cm^{-1}. The carboxylic acid stretch (1600 cm^{-1}) is also significantly reduced. This suggests that there is very high negative charge density of the coating at the pH of the assay for bacterial adhesion, which would lead to significant electrostatic repulsion between the film and *S. aureus*. This test was conducted on both DPEC films at pH 3 and 5 (**Figures 5.8a** and **5.8b**, respectively) and

the same trend is observed in both films. Because the stretching peak at 1550 cm^{-1} is very strong in both pH 3 and 5 dry cured coatings, it is believed that the major difference observed in the antifouling behavior between these films is due to the extensive amount of broken bridges seen in SEM mages of the dry cured pH 5 fabric, which is highlighted in **Figure 5.5** with a yellow arrow. This is mainly due to the fact that broken bridging appears to delaminate the coating from the fabric, potentially leaving large areas of uncoated fabric that bacteria can adhere to.

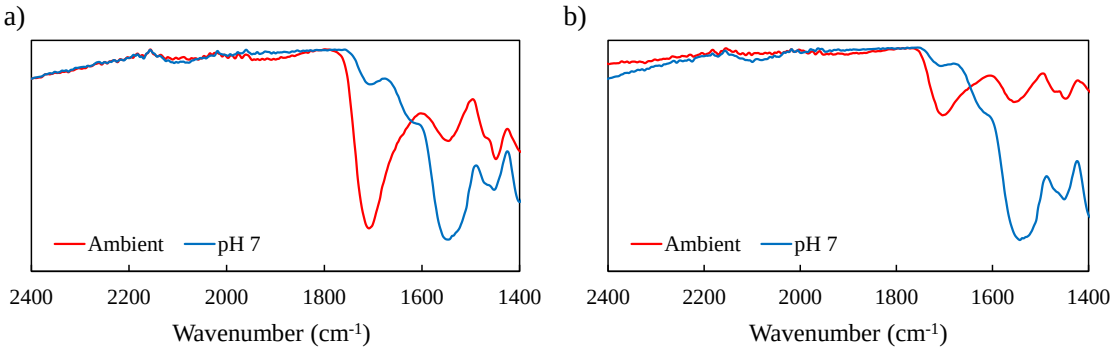

Figure 5.8. FTIR spectra of PEC coatings dry cured at pH 3 (a) or 5 (b), under ambient conditions and after exposure to pH 7 Tris buffer.

5.3.3 Oxygen Transmission Rate Reduction

Thin, transparent, and flexible films are required for food packaging to improve shelf-life and minimize food waste.[223-224] These properties often achieved through constructing multilayered plastic films or with metalized plastics.[225] Both of these processes are energy intensive and lead to a product with low recyclability. As an alternative, polyelectrolyte complex thin films have been applied using layer-by-layer

assembly to reduce transmission rates of various substrates.[23] Clay-platelet containing composites have been deposited using LbL, creating significant tortuosity and slowing the transport of small molecules through a film.[226-228] Transparent polymer-only thin films have also been prepared via layer-by-layer deposition that have high barrier and selectivity towards small molecules due to increased cohesive energy and reduced free volume within the PEC.[210, 229] These coatings are very efficient, but the number of processing steps inherently required to construct these barrier coatings diminishes commercial feasibility. Recently a BPEI/PAA coacervate was deposited in a single step and significantly reduced the oxygen transmission rate of PET film.[109] This coating exhibited remarkable barrier while significantly reducing the number of processing steps, but has significant room for improvement due to poor wettability of the coacervate and the post-cure "healing" needed to fill in pinholes.

Transparent coatings that impart low gas transmission must be dense and uniform with complete surface coverage (i.e. no pores and low roughness). WPEC coatings generate non-uniform surfaces either in the form of large aggregates (pH 3) or insufficient surface coverage (pH 5) (**Figure 5.4**). This leads to non-transparent films that have poor barrier due to inconsistent surface coverage. DPEC coatings on the other hand, show complete surface coverage and are much more conformal (i.e. smooth) by comparison. This makes them an ideal candidate for gas barrier coatings. 6 wt% mixtures of PDDA/PAA at a 1:3 molar ratio (based on repeat unit molar mass) were deposited onto 178 μm thick PET. The effect of citric acid concentration and ionic strength during the curing step was evaluated. Increasing buffer concentration increases

the ionic strength of the curing solution, and ionic strength is well known to influence the formation of polyelectrolyte complexes.[115-117] In order to account for this, samples were also cured in CA buffer solutions that were at a constant ionic strength (~150 mM) by adding NaCl. **Figure 5.9** shows the coating thickness as a function of curing conditions at pH 3. Increasing buffer concentration, with and without added salt, does not appear to influence the final thickness of the coatings. On average, these coatings are ~ 1900 μm thick. The uncured coatings are also ~1900 μm thick, suggesting that the thickness is determined by the initial amount of polymer mixture deposited rather than curing conditions. This was also observed when comparing the thickness of the same PEC coatings as a function of curing pH of 200 mM citric acid buffer (**Figure 5.3**).

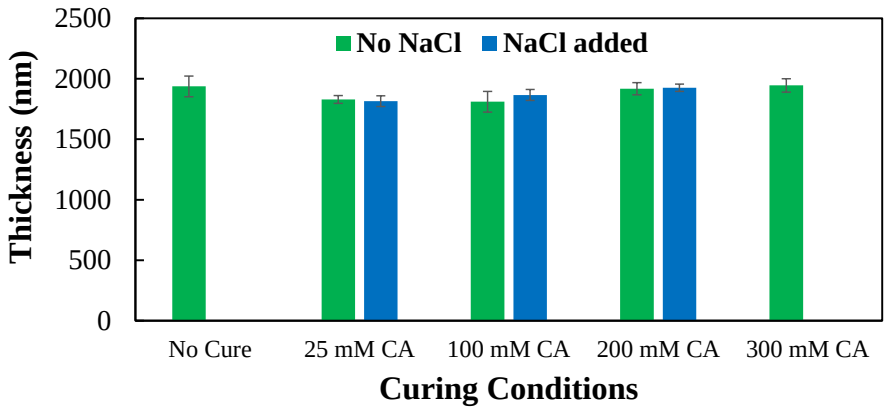

Figure 5.9. Thickness of PDDA/PAA PEC films as a function of citric acid buffer concentration at constant ionic strength (~150 mM adjusted with NaCl) (blue), and buffer concentration with naturally increasing ionic strength (green).

PDDA/PAA PEC was deposited and cured on glass slides to observe any difference in film transparency due to buffer concentration and ionic strength. Data was

normalized so that uncoated glass slides showed ~ 99.2 ± 0.6 percent light transmitted. The uncured polyelectrolyte mixture has a percent transmittance of ~ 99.3 ± 1.0. Formation of PEC through curing causes some rearrangement of the polymers, as evidenced by the reduction of light transmission. **Figure 5.10** shows light transmission as a function of curing conditions. Increasing the buffer concentration appears to increase light transmission through the film. Performing curing at the same ionic strength (i.e. adding NaCl) showed an increase in the light transmission at 25 mM and 100 mM CA relative to curing without added salt. Coating uniformity is also much better when NaCl is included in the curing solutions at 25 mM and 100 mM CA. This can be seen by the considerably smaller standard deviation in transparency for these films with added NaCl. At 200 mM CA (with and without NaCl) and 300 mM CA, almost all light is transmitted (> 95%). Salt is known to plasticize PEC through electrostatic charge shielding,[230-232] and adding salt to the curing solutions likely gives the polymers increased mobility and a more coalesced structure results (rather than an aggregated rough structure). When the ionic strength is held constant with NaCl an increase in transparency is observed, indicating that ionic strength is not the only determining factor. It is believed that increasing buffer concentration increases the citrate concentration, allowing for increased deprotonation (up to ~3 %) and leading to more interpolymer ionic crosslinks and a more uniform coalesced coating. These findings are reinforced by measurement of surface topography.

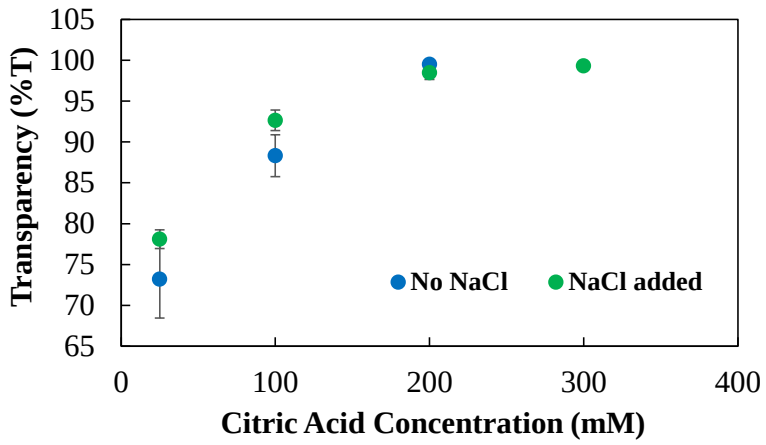

Figure 5.10. Percent light transmission (%T) of PDDA/PAA PEC deposited on glass slides as a function of citric acid buffer concentration and ionic strength.

The morphology and surface roughness of PDDA/PAA PEC films was measured using AFM. The roughness and surface topology was measured as a function increasing buffer concentration, with and without a constant ionic strength of ~150 mM. **Figure 5.11** shows the topography of these coatings deposited on glass slides. The polyelectrolyte mixture was imaged before curing, and a very smooth (R_q < 1 nm) featureless surface is observed Exposing the PM to citric acid forms a PEC through deprotonation of PAA due to increased negative charge density. This causes significant morphological changes in the coating as the polymers rearrange to form ionic crosslinks. Curing the coatings in buffer with increasing concentration leads to coatings with lower surface roughness as summarized in **Table 5.4**. This increase in surface roughness scatters more light and explains the reduced transparency.[233] By increasing ionic strength, either through the addition of NaCl or by increasing the buffer concentration,

the polymer chains in the PEC have more mobility and can form a more uniform coalesced structure with lower roughness and higher transparency.

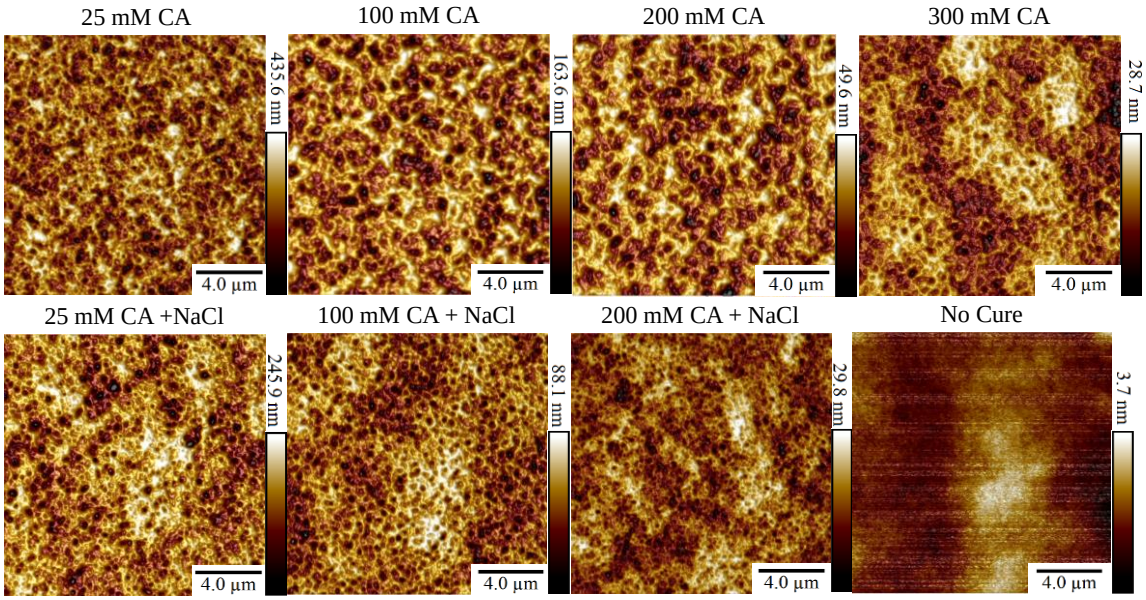

Figure 5.11. AFM height images of PDDA/PAA PEC thin film surfaces deposited on glass slides formed with varying curing conditions.

Table 5.3. Surface roughness of PDDA/PAA PEC films.

Roughness* [nm]	**25 mM CA**	**100 mM CA**	**200 mM CA**	**300 mM CA**
No NaCl	55.7 ± 3.0	23.9 ± 1.3	7.4 ± 0.7	3.3 ± 1.4
With NaCl	29.0 ± 5.2	11.5 ± 0.4	4.5 ± 0.2	N/A

*Roughness measurements taken on PEC films deposited on glass slides.

The oxygen transmission rate (OTR) for PEC coatings deposited on both sides of a 178 μm PET film (~1.9 μm/side) was evaluated under different curing conditions (**Figure 5.12**). Surprisingly, depositing a PDDA/PAA polymer mixture without curing reduces the OTR by a factor of 36. This is significant considering that there is minimal barrier improvements between 127 μm thick PET and 178 μm PET (OTR is 9.5 and 8.6 $cm^3m^{-2}day^{-1}$, respectively).[109, 229] It is believed that dipole interactions between PDDA and PAA, observed at low pH,[234] leads to higher cohesive energy in the film, reducing oxygen's ability to move through the coating. Exposing the deposited polyelectrolyte mixture to buffer further reduces the barrier by a factor of 8.7-18, depending on the buffer and NaCl concentration (**Figure 5.12**). The large increase in the cohesive forces during complexation can explain the differences in barrier observed. Complexation increases cohesive forces within the PEC due to the formation of ionic crosslinks.[115] Higher cohesion energy in general leads to better small molecule barrier in polymeric materials.[235] Greater cohesive energy increases oxygen barrier by an order of magnitude after the PEC films are cured. This increase in cohesive energy is evidenced by the increase in reduced elastic modulus (E_r) of the films during curing (**Table 5.5**). Nanoidentation of the cured coatings reveals an average reduced modulus of 12.3 GPa irrespective of buffer concentration or ionic strength. Even though there is no correlation between salt concentration and modulus, adding NaCl to the curing solutions increases the oxygen barrier (i.e. reduces OTR) in both 25 and 200 mM CA cured coatings by a factor of 2. It is believed that the salt increases the free volume of the coating during the curing process,[236] allowing any PEC aggregates to coalesce (through increased free

motion of polyelectrolyte chains), leading to a less aggregated structure with reduced free volume (once the film is rinsed and dried).[237]

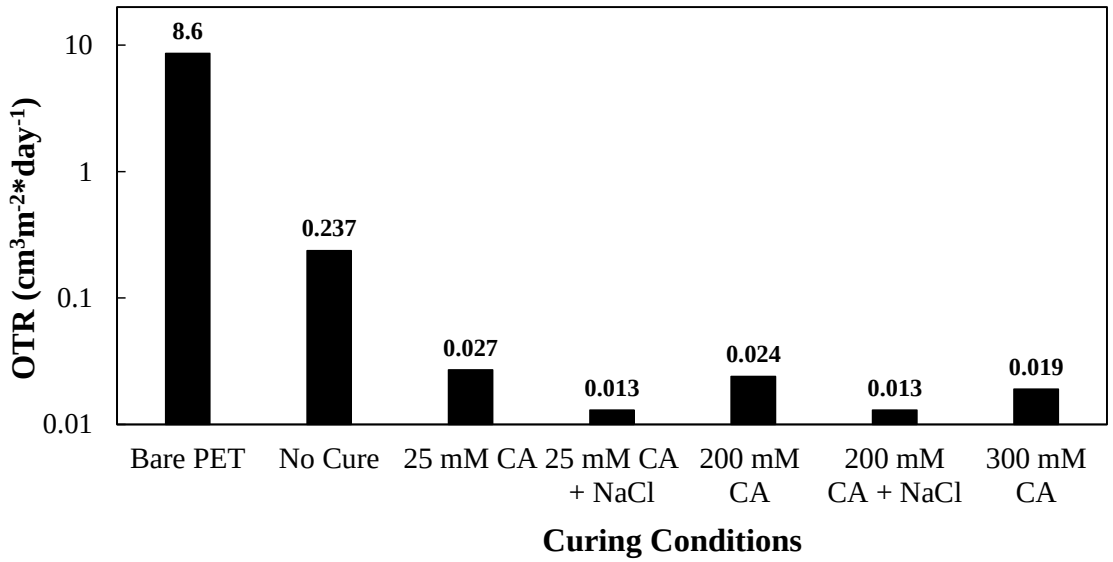

Figure 5.12. Oxygen transmission rates of uncoated 178 μm PET film (Ref. 230) and PDDA/PAA PEC films deposited on PET.

Table 5.4. Reduced modulus of PDDA/PAA PEC films.

Reduced Modulus*	No Cure [GPa]	25 mM CA [GPa]	100 mM CA [GPa]	200 mM CA [GPa]	300 mM CA [GPa]
No NaCl	6.95 ± 0.11	12.53 ± 3.69	13.01 ± 1.55	12.43 ± 0.96	11.37 ± 0.35
With NaCl	N/A	12.00 ± 2.11	12.86 ± 1.21	11.98 ± 0.61	N/A

*Nanoindentation measurements taken on PEC films deposited on glass slides. Reduced modulus is very nearly the elastic modulus (to a first approximation).

5.4 Conclusions

Polyelectrolyte complexes of PDDA and PAA were deposited as functional thin films in a single step, significantly reducing the number of processing steps that would be required for similar layer-by-layer assembled thin films. Homogenously mixed polyelectrolyte solutions were prepared at pH 2, eliminating electrostatic interactions between PDDA and PAA and allowing both polymers to be deposited simultaneously. Film morphology can be tailored based on curing method. If the coatings are cured without drying, a highly aggregated film is formed, which significantly reduces the adhesion of bacteria to polyester fabric. These coatings were found to have a high degree of negative charge density at pH 7, leading to electrostatic repulsion between bacteria and the coating. PEC thin films where the polyelectrolyte mixture dried prior to curing made smooth, uniform coatings that provided a two orders of magnitude reduction in oxygen transmission rate through a polyester thick film. The optical transparency of these films can be improved by increasing buffer concentration or by adding salt to the curing solution, which reduces the surface roughness and generates a more coalesced network. These coatings, when cured, significantly increase the cohesive energy of the film and reduce free volume because of the ionic network formed, leading to high oxygen barrier. This process significantly reduces processing steps to deposit a polyelectrolyte complex thin film (relative to layer-by-layer assembly). This study highlights the tailorability of these coating through simple changes in the curing process, which could potentially lead to more opportunities to use functional PEC thin films.

CHAPTER VI

CONCLUSIONS AND FUTURE WORK

6.1 Functionalization of Polymer Substrates Using Polyelectrolyte Complexes

This dissertation describes the deposition of polyelectrolyte complexes on polyurethane foam, as a flame retardant treatment, and on polyester fabric to reduce bacterial adhesion. These coatings were deposited using the layer-by-layer assembly technique. Reducing the number of processing steps often required with layer-by-layer assembly is of significant interest. The final topic of this dissertation focused on the parameters that influence the formation and film properties of poly(diallydimethylammonium chloride) and poly(acrylic acid) polyelectrolyte complexes deposited in a single step. Depending on the conditions under which these complexes are formed, coatings were found to effectively reduce bacterial adhesion to polyester fabric and reduce oxygen transmission rate of poly(ethylene terephthalate) film. The significant reduction in processing steps associated with this process could lead to commercial use of functional PEC thin films.

6.1.1 Environmentally-Benign Halloysite Nanotube Multilayer Assembly Significantly Reduces Polyurethane Flammability

Chapter III highlights the development of a polyelectrolyte complex nanocomposite thin film utilizing halloysite clay to reduce the flammability of polyurethane foam. By stabilizing halloysite with branched polyethylenimine and

poly(acrylic acid), cationic and anionic-halloysite suspensions could be used to form a PEC-clay nanocomposite thin film via layer-by-layer assembly. At 5 BL, ~36 wt% was deposited on the surface of PUF, leading to a 60% reduction in peak heat release rate and a 60% reduction in total smoke release. This coating was also found to exhibit self-extinguishing behavior during direct flame testing. It is believed that this halloysite nanocomposite coating forms a physical barrier during combustion, which prevents heat and mass transfer, reducing fire's ability to spread. Because of the efficacy at low bilayers and the environmentally-friendly nature of the ingredients, this coating has the potential for wide-spread use as a safe flame retardant treatment to increase fire-safety in homes.

6.1.2 Polyelectrolyte Multilayer Nanocoatings Dramatically Reduce Bacterial Adhesion to Polyester Fabric

Chapter IV discusses the development of a polyelectrolyte complex made of PDDA and PAA that, when deposited to the surface of polyester fabric, reduces bacterial adhesion. An assay using bioluminescent *Staphylococcus aureus* was used to detect photons emitted from viable bacteria on the fabric surface. A 10 BL coating only adds 2.5 wt% to the fabric and reduces the amount of detectable bacteria by two orders of magnitude (>99%) after simple rinsing with deionized water. It was observed that the efficacy of the coating increased as a function of BL deposited. Since PAA is the terminal layer, the surface is negatively charged, which repels the negatively-charged bacteria through electrostatic repulsion. It is also believed that the surface roughness and

the formation of a hydration layer contribute to the reduction of bacterial adhesion. The bacteria were shown to regrow on the surface of coated fabric, suggesting that the coating is truly antifouling and not bactericidal. This process could easily be scaled up using a pad dry process, or applied to other substrates, providing a possible solution to reducing the spread of antibiotic resistant infections in medical centers.

6.1.3 Functional Polyelectrolyte Complex Thin Films Deposited in a Single Step

PDDA/PAA PEC formation and film characteristics were evaluated under a number of different curing conditions. It was observed that curing the polyelectrolyte complex (i.e. forming ionic crosslinks) when the PM was dried (immobilized) on the substrate, rather than solubilized (wet and highly mobile), lead to films with significantly different properties. AFM surface images revealed that WPEC films have a more aggregated structure (less conformal). DPEC films have conformal, smooth morphologies due to the decreased mobility of the dried polyelectrolytes on the substrate surface. Because of these different film morphologies, different applications of these PEC thin films were studied.

Dry and wet-cured coatings were compared in the reduction of bacterial adhesion to polyester fabric. A 3 wt% WPEC at pH 3 was found to remove > 95% of deposited bacteria, while only adding ~2 wt% to the fabric surface with (minimal impact to fabric hand). DPEC coatings significantly increased the stiffness of coated fabric, and in general were less effective at reducing bacterial adhesion, mainly due to the extensive bridging of fibers by the PEC. These bridges can easily break (observed in SEM),

delaminating the coating from the fabric and leaving exposed areas of fabric. It is believed that these PEC coatings are effective due to electrostatic repulsion between negatively-charged bacteria and the negatively-charged surface.

Dry cured PDDA/PAA PEC coatings have very uniform surface coverage and were also explored as a thin film oxygen barrier. A 6wt% PDDA/PAA solution was cast on 178 μm PET. Films were cured at different concentrations of citric acid buffer at pH 3, with and without keeping the ionic strength constant. It was observed that the transparency of these films increased with increasing buffer concentration due to the reduction of surface roughness. When the buffer ionic strength was kept constant by adding NaCl, the light transmittance increased relative to the cured films with no added salt. This was due to the increased polyelectrolyte mobility from charge shielding, leading to smoother, more coalesced coatings. Coatings cured at 200 mM citric acid, with salt added to obtain ~150 mM ionic strength, exhibited an oxygen transmission reduction of two orders of magnitude (a factor of 660) mainly due to the increase of cohesive energy in the cured coatings.

6.2 Future Research Directions

6.2.1 Polyelectrolyte Complex Thin Film Properties Impact on Barrier Properties

Chapter V examined polyelectrolyte complexes formed between PDDA and PAA deposited in a single step, which exhibited a significant reduction in oxygen transmission rate. PEC deposited via layer-by-layer assembly have produced transparent thin films

that reduce the OTR below the limit of detection of standard testing equipment.[23, 210, 229] There is still opportunity for improvement with these "one-pot" PEC thin films to achieve the LbL level of effectiveness. It has been observed that the strength of the ionic crosslinks within a PEC vary depending on polymer chemistry,[102] which may also impact barrier properties (e.g. films with stronger ionic bonds may increase barrier). Intrinsic versus extrinsic compensation within the PEC could also play a role in improving barrier properties. This could be altered by studying PEC formation at different molar ratios of polyelectrolytes,[117] or by treating PEC films after curing with salt and subsequent exposure to low concentrations of polycations or polyanions.[238] Variation in film compensation could be measured using radiolabeled small counter ions.[239-240] Films with different compensation could be tested for their barrier properties. A better understanding of film properties could lead to films with much better barrier.

6.2.2 Improvement of Flame Retarndant PEC

Polyelectrolyte complexes deposited using layer-by-layer assembly have been significantly developed and have proven to be a versatile method for rendering numerous substrates flame retardant.[29-30] Intumescent PEC thin film coatings have been deposited in a single step onto cotton,[164] polyester-cotton,[165] and nylon-cotton blended fabric.[166] Fabric consisting of blends of cotton and synthetic fibers, such as polyester and nylon, are more difficult to flame retard due to different burning characteristics of the synthetic fibers, which tend to melt and release more heat during combustion. One strategy to combat this is to improve the intumescent coatings, producing greater

insulating char formation to help reduce heat transfer during combustion. PEC coatings incorporating melamine have been shown to be more effective due to the formation of melamine polyphosphate (MPP), which significantly increases char formation.[241] MPP is insoluble in water and melamine needs to be incorporated in a separate step to include it in the final PEC. Melamine could be grafted to a polyelectrolyte such as BPEI and could be complexed with a polyphosphate to produce a more effective intumescent PEC. Increased char formation could be measured using Raman spectroscopy. Films using unmodified BPEI could be compared to films using melamine-modified BPEI. The MPP formed in the PEC could lead to better charring with cotton in the fabric blend, shielding the increased heat release from the synthetic fibers.

6.2.3 Improvements of Antifouling PEC Coatings

The PEC coating highlighted in Chapter V to reduce bacterial adhesion has significant room for improvement. These coatings have been shown to be antifouling, but cannot kill bacteria that do manage to adhere, which still leads to fouling over time. This aspect could be improved by making the coatings bactericidal as well. Multifunctional PEC coatings deposited using layer-by-layer assembly have been shown recently to reduce bacterial adhesion and also kill surrounding bacteria.[74, 98-100] It is possible that similar coatings could be developed and deposited in a single-step. Gentamicin or ionic antibiotics could be incorporated into the polyelectrolyte mixtures. Upon deposition and curing, the antibiotic could be electrostatically bound in the PEC and could slowly be released under various stimuli (i.e. salinity, pH, or temperature),

similar to layer-by-layer films.[84-88] If these coatings were formulated with a large excess of one polymer (like those developed in Chapter V) the ratio of the two polyelectrolytes could be altered to evaluate the influence of excess polyelectrolyte and antibiotic loading. This could then be tuned to increase the time that the coating remains effective. If the coatings have excess polyanion, they may also exhibit antifouling characteristics (due to electrostatic repulsion). The polyelectrolyte ratio could be tuned to find the best balance between antibiotic loading and ideal surface charge density for efficient reduction in adhesion.

REFERENCES

1. Jaber, J. A.; Schlenoff, J. B., Recent developments in the properties and applications of polyelectrolyte multilayers. *Current Opinion in Colloid & Interface Science* **2006,** *11* (6), 324.

2. *Mulitlayer thin films*. 2 ed.; Wiely-VCH Verlag & Co.: Weinheim, Germany, 2012.

3. Richardson, J. J.; Björnmalm, M.; Caruso, F., Technology-driven layer-by-layer assembly of nanofilms. *Science* **2015,** *348* (6233).

4. Trigueiro, J. P. C.; Silva, G. G.; Pereira, F. V.; Lavall, R. L., Layer-by-layer assembled films of multi-walled carbon nanotubes with chitosan and cellulose nanocrystals. *J Colloid Interf Sci* **2014,** *432*, 214.

5. Decher, G., Fuzzy nanoassemblies: Toward layered polymeric multicomposites. *Science* **1997,** *277* (5330), 1232.

6. Dierendonck, M.; De Koker, S.; De Rycke, R.; De Geest, B. G., Just spray it - lbl assembly enters a new age. *Soft Matter* **2014,** *10* (6), 804.

7. Hu, H.; Pauly, M.; Felix, O.; Decher, G., Spray-assisted alignment of layer-by-layer assembled silver nanowires: A general approach for the preparation of highly anisotropic nano-composite films. *Nanoscale* **2017,** *9* (3), 1307.

8. Saetia, K.; Schnorr, J. M.; Mannarino, M. M.; Kim, S. Y.; Rutledge, G. C.; Swager, T. M.; Hammond, P. T., Spray-layer-by-layer carbon nanotube/electrospun fiber electrodes for flexible chemiresistive sensor applications. *Adv Funct Mater* **2014,** *24* (4), 492.

9. Suarez-Martinez, P. C.; Robinson, J.; An, H.; Nahas, R. C.; Cinoman, D.; Lutkenhaus, J. L., Spray-on polymer–clay multilayers as a superior anticorrosion metal pretreatment. *Macromolecular Materials and Engineering* **2017,** *302* (6), 1600552.

10. Lee, S.-S.; Hong, J.-D.; Kim, C. H.; Kim, K.; Koo, J. P.; Lee, K.-B., Layer-by-layer deposited multilayer assemblies of ionene-type polyelectrolytes based on the spin-coating method. *Macromolecules* **2001,** *34* (16), 5358.

11. Karahan, H. E.; Eyüboğlu, L.; Kıyılar, D.; Demirel, A. L., Ph-stability and ph-annealing of h-bonded multilayer films prepared by layer-by-layer spin-assembly. *Eur Polym J* **2014,** *56*, 159.

12. Zhao, Y.-B.; Liu, H.-P.; Li, C.-Y.; Chen, Y.; Li, S.-Q.; Zeng, R.-C.; Wang, Z.-L., Corrosion resistance and adhesion strength of a spin-assisted layer-by-layer assembled coating on az31 magnesium alloy. *Appl Surf Sci* **2018,** *434*, 787.

13. Chang, L.; Kong, X. X.; Wang, F.; Wang, L. Y.; Shen, J. C., Layer-by-layer assembly of poly (n-acryloyl-n '-propylpiperazine) and poly (acrylic acid): Effect of ph and temperature. *Thin Solid Films* **2008,** *516* (8), 2125.

14. Humood, M.; Chowdhury, S.; Song, Y.; Tzeng, P.; Grunlan, J. C.; Polycarpou, A. A., Nanomechanical behavior of high gas barrier multilayer thin films. *Acs Appl Mater Inter* **2016,** *8* (17), 11128.

15. Findenig, G.; Kargl, R.; Stana-Kleinschek, K.; Ribitsch, V., Interaction and structure in polyelectrolyte/clay multilayers: A qcm-d study. *Langmuir* **2013,** *29* (27), 8544.

16. Zhai, L.; Cebeci, F. Ç.; Cohen, R. E.; Rubner, M. F., Stable superhydrophobic coatings from polyelectrolyte multilayers. *Nano Lett* **2004,** *4* (7), 1349.

17. Bravo, J.; Zhai, L.; Wu, Z. Z.; Cohen, R. E.; Rubner, M. F., Transparent superhydrophobic films based on silica nanoparticles. *Langmuir* **2007,** *23* (13), 7293.

18. Fukumoto, H.; Yonezawa, Y., Layer-by-layer self-assembly of polyelectrolyte and water soluble cyanine dye. *Thin Solid Films* **1998,** *327-329*, 748.

19. Anwar, N.; Vagin, M.; Naseer, R.; Imar, S.; Ibrahim, M.; Mal, S. S.; Kortz, U.; Laffir, F.; McCormac, T., Redox switching of polyoxometalate–methylene blue-based layer-by-layer films. *Langmuir* **2012,** *28* (12), 5480.

20. Wang, D.; Wang, X., Self-assembled graphene/azo polyelectrolyte multilayer film and its application in electrochemical energy storage device. *Langmuir* **2011,** *27* (5), 2007.

21. Fan, F.; Zhou, C.; Wang, X.; Szpunar, J., Layer-by-layer assembly of a self-healing anticorrosion coating on magnesium alloys. *Acs Appl Mater Inter* **2015,** *7* (49), 27271.

22. Rouse, J. H.; Lillehei, P. T., Electrostatic assembly of polymer/single walled carbon nanotube multilayer films. *Nano Lett* **2003,** *3* (1), 59.

23. Priolo, M. A.; Holder, K. M.; Guin, T.; Grunlan, J. C., Recent advances in gas barrier thin films via layer-by-layer assembly of polymers and platelets. *Macromolecular Rapid Communications* **2015,** *36* (10), 866.

24. Rajasekar, R.; Kim, N. H.; Jung, D.; Kuila, T.; Lim, J. K.; Park, M. J.; Lee, J. H., Electrostatically assembled layer-by-layer composites containing graphene oxide for enhanced hydrogen gas barrier application. *Compos Sci Technol* **2013,** *89*, 167.

25. Wang, L.; Dou, Y.; Wang, J.; Han, J.; Liu, L.; Wei, M., Layer-by-layer assembly of layered double hydroxide/rubber multilayer films with excellent gas barrier property. *Composites Part A: Applied Science and Manufacturing* **2017,** *102*, 314.

26. Wu, Z.; Walish, J.; Nolte, A.; Zhai, L.; Cohen, R. E.; Rubner, M. F., Deformable antireflection coatings from polymer and nanoparticle multilayers. *Adv Mater* **2006,** *18* (20), 2699.

27. Shimomura, H.; Gemici, Z.; Cohen, R. E.; Rubner, M. F., Layer-by-layer-assembled high-performance broadband antireflection coatings. *Acs Appl Mater Inter* **2010,** *2* (3), 813.

28. Eshaghi, A.; Mojab, M., Fabrication of antireflective antifogging nano-porous silica thin film on glass substrate by layer-by-layer assembly method. *Journal of Non-Crystalline Solids* **2014,** *405*, 148.

29. Holder, K. M.; Smith, R. J.; Grunlan, J. C., A review of flame retardant nanocoatings prepared using layer-by-layer assembly of polyelectrolytes. *J Mater Sci* **2017,** *52* (22), 12923.

30. Qiu, X.; Li, Z.; Li, X.; Zhang, Z., Flame retardant coatings prepared using layer by layer assembly: A review. *Chemical Engineering Journal* **2018,** *334* (Supplement C), 108.

31. Zhu, X. Y.; Loh, X. J., Layer-by-layer assemblies for antibacterial applications. *Biomater Sci-Uk* **2015,** *3* (12), 1505.

32. Séon, L.; Lavalle, P.; Schaaf, P.; Boulmedais, F., Polyelectrolyte multilayers: A versatile tool for preparing antimicrobial coatings. *Langmuir* **2015,** *31* (47), 12856.

33. McKenna, S. T.; Hull, T. R., The fire toxicity of polyurethane foams. *Fire Science Reviews* **2016,** *5* (1), 1.

34. Lefebvre, J.; Bastin, B.; Le Bras, M.; Duquesne, S.; Ritter, C.; Paleja, R.; Poutch, F., Flame spread of flexible polyurethane foam: Comprehensive study. *Polymer Testing* **2004,** *23* (3), 281.

35. Agency, N. F. P. White paper on upholstered furniture flammability. http://www.nfpa.org/Assets/files/AboutTheCodes/277/2156%20-%20UpholsteredFurnWhitePaper.pdf (accessed 03/05/2017).

36. Rahman, F.; Langford, K. H.; Scrimshaw, M. D.; Lester, J. N., Polybrominated diphenyl ether (pbde) flame retardants. *Science of The Total Environment* **2001,** *275* (1–3), 1.

37. Stapleton, H. M.; Klosterhaus, S.; Eagle, S.; Fuh, J.; Meeker, J. D.; Blum, A.; Webster, T. F., Detection of organophosphate flame retardants in furniture foam and u.S. House dust. *Environmental Science & Technology* **2009,** *43* (19), 7490.

38. Chain, E. P. o. C. i. t. F., Scientific opinion on emerging and novel brominated flame retardants (bfrs) in food. *EFSA Journal* **2012,** *10* (10), 2908.

39. Covaci, A.; Voorspoels, S.; Abdallah, M. A.-E.; Geens, T.; Harrad, S.; Law, R. J., Analytical and environmental aspects of the flame retardant tetrabromobisphenol-a and its derivatives. *J Chromatogr A* **2009,** *1216* (3), 346.

40. Durso, F. Hot seat: A new look at the problem of furniture flammability and home fire losses. http://www.nfpa.org/news-and-research/publications/nfpa-journal/2013/september-october-2013/features/old-problem-fresh-look (accessed 9/15/2016).

41. Westervelt, A. California's fire code update: The end of toxic flame retardants? http://www.forbes.com/sites/amywestervelt/2013/02/08/californias-fire-code-update-the-end-of-toxic-flame-retardants/#29f4c7d3aa02 (accessed 9/15/2016).

42. Laufer, G.; Kirkland, C.; Morgan, A. B.; Grunlan, J. C., Exceptionally flame retardant sulfur-based multilayer nanocoating for polyurethane prepared from aqueous polyelectrolyte solutions. *Acs Macro Lett* **2013,** *2* (5), 361.

43. Wang, X.; Pan, Y. T.; Wan, J. T.; Wang, D. Y., An eco-friendly way to fire retardant flexible polyurethane foam: Layer-by-layer assembly of fully bio-based substances. *Rsc Advances* **2014,** *4* (86), 46164.

44. Carosio, F.; Negrell-Guirao, C.; Alongi, J.; David, G.; Camino, G., All-polymer layer by layer coating as efficient solution to polyurethane foam flame retardancy. *Eur Polym J* **2015,** *70*, 94.

45. Carosio, F.; Di Blasio, A.; Cuttica, F.; Alongi, J.; Malucelli, G., Self-assembled hybrid nanoarchitectures deposited on poly(urethane) foams capable of chemically adapting to extreme heat. *Rsc Advances* **2014,** *4* (32), 16674.

46. Carosio, F.; Alongi, J., Ultra-fast layer-by-layer approach for depositing flame retardant coatings on flexible pu foams within seconds. *Acs Appl Mater Inter* **2016,** *8* (10), 6315.

47. Laufer, G.; Kirkland, C.; Cain, A. A.; Grunlan, J. C., Clay-chitosan nanobrick walls: Completely renewable gas barrier and flame-retardant nanocoatings. *Acs Appl Mater Inter* **2012,** *4* (3), 1643.

48. Li, Y. C.; Kim, Y. S.; Shields, J.; Davis, R., Controlling polyurethane foam flammability and mechanical behaviour by tailoring the composition of clay-based multilayer nanocoatings. *J Mater Chem A* **2013,** *1* (41), 12987.

49. Cain, A. A.; Nolen, C. R.; Li, Y. C.; Davis, R.; Grunlan, J. C., Phosphorous-filled nanobrick wall multilayer thin film eliminates polyurethane melt dripping and reduces heat release associated with fire. *Polymer Degradation and Stability* **2013,** *98* (12), 2645.

50. Holder, K. M.; Huff, M. E.; Cosio, M. N.; Grunlan, J. C., Intumescing multilayer thin film deposited on clay-based nanobrick wall to produce self-extinguishing flame retardant polyurethane. *J Mater Sci* **2015,** *50* (6), 2451.

51. Kim, Y. S.; Li, Y. C.; Pitts, W. M.; Werrel, M.; Davis, R. D., Rapid growing clay coatings to reduce the fire threat of furniture. *Acs Appl Mater Inter* **2014,** *6* (3), 2146.

52. Cain, A. A.; Plummer, M. G. B.; Murray, S. E.; Bolling, L.; Regev, O.; Grunlan, J. C., Iron-containing, high aspect ratio clay as nanoarmor that imparts substantial thermal/flame protection to polyurethane with a single electrostatically-deposited bilayer. *J Mater Chem A* **2014,** *2* (41), 17609.

53. Patra, D.; Vangal, P.; Cain, A. A.; Cho, C.; Regev, O.; Grunlan, J. C., Inorganic nanoparticle thin film that suppresses flammability of polyurethane with only a single electrostatically-assembled bilayer. *Acs Appl Mater Inter* **2014,** *6* (19), 16903.

54. Yang, Y. H.; Li, Y. C.; Shields, J.; Davis, R. D., Layer double hydroxide and sodium montmorillonite multilayer coatings for the flammability reduction of flexible polyurethane foams. *J Appl Polym Sci* **2015,** *132* (14).

55. Pan, H. F.; Wang, W.; Pan, Y.; Song, L.; Hu, Y.; Liew, K. M., Formation of layer-by-layer assembled titanate nanotubes filled coating on flexible polyurethane foam with improved flame retardant and smoke suppression properties. *Acs Appl Mater Inter* **2015,** *7* (1), 101.

56. Holder, K. M.; Cain, A. A.; Plummer, M. G.; Stevens, B. E.; Odenborg, P. K.; Morgan, A. B.; Grunlan, J. C., Carbon nanotube multilayer nanocoatings prevent

flame spread on flexible polyurethane foam. *Macromolecular Materials and Engineering* **2016,** *301* (6), 665.

57. Kraigsley, A. M.; Finkel, S. E., Adaptive evolution in single species bacterial biofilms. *FEMS Microbiology Letters* **2009,** *293* (1), 135.

58. Arciola, C. R.; Campoccia, D.; Speziale, P.; Montanaro, L.; Costerton, J. W., Biofilm formation in staphylococcus implant infections. A review of molecular mechanisms and implications for biofilm-resistant materials. *Biomaterials* **2012,** *33* (26), 5967.

59. Bazaka, K.; Jacob, M. V.; Crawford, R. J.; Ivanova, E. P., Efficient surface modification of biomaterial to prevent biofilm formation and the attachment of microorganisms. *Applied Microbiology and Biotechnology* **2012,** *95* (2), 299.

60. Hanssen, A. D., Managing the infected knee: As good as it gets. *The Journal of Arthroplasty* **2002,** *17* (4, Supplement 1), 98.

61. Liu, L.; Ercan, B.; Sun, L.; Ziemer, K. S.; Webster, T. J., Understanding the role of polymer surface nanoscale topography on inhibiting bacteria adhesion and growth. *ACS Biomaterials Science & Engineering* **2016,** *2* (1), 122.

62. von Eiff, C.; Jansen, B.; Kohnen, W.; Becker, K., Infections associated with medical devices. *Drugs* **2005,** *65* (2), 179.

63. Shan, W.; Bacchin, P.; Aimar, P.; Bruening, M. L.; Tarabara, V. V., Polyelectrolyte multilayer films as backflushable nanofiltration membranes with tunable hydrophilicity and surface charge. *Journal of Membrane Science* **2010,** *349* (1), 268.

64. Tang, L.; Gu, W.; Yi, P.; Bitter, J. L.; Hong, J. Y.; Fairbrother, D. H.; Chen, K. L., Bacterial anti-adhesive properties of polysulfone membranes modified with polyelectrolyte multilayers. *Journal of Membrane Science* **2013,** *446* (Supplement C), 201.

65. Diagne, F.; Malaisamy, R.; Boddie, V.; Holbrook, R. D.; Eribo, B.; Jones, K. L., Polyelectrolyte and silver nanoparticle modification of microfiltration

membranes to mitigate organic and bacterial fouling. *Environmental Science & Technology* **2012,** *46* (7), 4025.

66. Zhu, X.; Guo, S.; He, T.; Jiang, S.; Jańczewski, D.; Vancso, G. J., Engineered, robust polyelectrolyte multilayers by precise control of surface potential for designer protein, cell, and bacteria adsorption. *Langmuir* **2016,** *32* (5), 1338.

67. Kovačević, D.; Pratnekar, R.; Godič Torkar, K.; Salopek, J.; Dražić, G.; Abram, A.; Bohinc, K., Influence of polyelectrolyte multilayer properties on bacterial adhesion capacity. *Polymers* **2016,** *8* (10), 345.

68. Zhu, X.; Janczewski, D.; Guo, S.; Lee, S. S.; Parra Velandia, F. J.; Teo, S. L.; He, T.; Puniredd, S. R.; Vancso, G. J., Polyion multilayers with precise surface charge control for antifouling. *ACS Appl Mater Interfaces* **2015,** *7* (1), 852.

69. Jisr, R. M.; Rmaile, H. H.; Schlenoff, J. B., Hydrophobic and ultrahydrophobic multilayer thin films from perfluorinated polyelectrolytes. *Angewandte Chemie International Edition* **2005,** *44* (5), 782.

70. Illergård, J.; Wågberg, L.; Ek, M., Bacterial-growth inhibiting properties of multilayers formed with modified polyvinylamine. *Colloids and Surfaces B: Biointerfaces* **2011,** *88* (1), 115.

71. Lu, Y.; Wu, Y.; Liang, J.; Libera, M. R.; Sukhishvili, S. A., Self-defensive antibacterial layer-by-layer hydrogel coatings with ph-triggered hydrophobicity. *Biomaterials* **2015,** *45*, 64.

72. Ji, J.; Fu, J.; Shen, J., Fabrication of a superhydrophobic surface from the amplified exponential growth of a multilayer. *Adv Mater* **2006,** *18* (11), 1441.

73. Yang, H.; Deng, Y., Preparation and physical properties of superhydrophobic papers. *J Colloid Interf Sci* **2008,** *325* (2), 588.

74. Shen, L.; Wang, B.; Wang, J.; Fu, J.; Picart, C.; Ji, J., Asymmetric free-standing film with multifunctional anti-bacterial and self-cleaning properties. *Acs Appl Mater Inter* **2012,** *4* (9), 4476.

75. Malcher, M.; Volodkin, D.; Heurtault, B.; André, P.; Schaaf, P.; Möhwald, H.; Voegel, J.-C.; Sokolowski, A.; Ball, V.; Boulmedais, F.; Frisch, B., Embedded silver ions-containing liposomes in polyelectrolyte multilayers: Cargos films for antibacterial agents. *Langmuir* **2008,** *24* (18), 10209.

76. Song, R.; Yan, J.; Xu, S.; Wang, Y.; Ye, T.; Chang, J.; Deng, H.; Li, B., Silver ions/ovalbumin films layer-by-layer self-assembled polyacrylonitrile nanofibrous mats and their antibacterial activity. *Colloids and Surfaces B: Biointerfaces* **2013,** *108*, 322.

77. Meng, M.; He, H.; Xiao, J.; Zhao, P.; Xie, J.; Lu, Z., Controllable in situ synthesis of silver nanoparticles on multilayered film-coated silk fibers for antibacterial application. *J Colloid Interf Sci* **2016,** *461*, 369.

78. Kruk, T.; Szczepanowicz, K.; Kręgiel, D.; Szyk-Warszyńska, L.; Warszyński, P., Nanostructured multilayer polyelectrolyte films with silver nanoparticles as antibacterial coatings. *Colloids and Surfaces B: Biointerfaces* **2016,** *137*, 158.

79. Detsri, E.; Kamhom, K.; Ruen-ngam, D., Layer-by-layer deposition of green synthesised silver nanoparticles on polyester air filters and its antimicrobial activity. *Journal of Experimental Nanoscience* **2016,** *11* (12), 930.

80. Yuan, W.; Fu, J.; Su, K.; Ji, J., Self-assembled chitosan/heparin multilayer film as a novel template for in situ synthesis of silver nanoparticles. *Colloids and Surfaces B: Biointerfaces* **2010,** *76* (2), 549.

81. Cady, N. C.; Behnke, J. L.; Strickland, A. D., Copper-based nanostructured coatings on natural cellulose: Nanocomposites exhibiting rapid and efficient inhibition of a multi-drug resistant wound pathogen, a. Baumannii, and mammalian cell biocompatibility in vitro. *Adv Funct Mater* **2011,** *21* (13), 2506.

82. Liu, P.; Zhao, Y.; Yuan, Z.; Ding, H.; Hu, Y.; Yang, W.; Cai, K., Construction of zn-incorporated multilayer films to promote osteoblasts growth and reduce bacterial adhesion. *Materials Science and Engineering: C* **2017,** *75*, 998.

83. Uğur, Ş. S.; Sarıışık, M.; Aktaş, A. H.; Uçar, M. Ç.; Erden, E., Modifying of cotton fabric surface with nano-zno multilayer films by layer-by-layer deposition method. *Nanoscale Research Letters* **2010,** *5* (7), 1204.

84. Schmidt, D. J.; Moskowitz, J. S.; Hammond, P. T., Electrically triggered release of a small molecule drug from a polyelectrolyte multilayer coating. *Chemistry of Materials* **2010,** *22* (23), 6416.

85. Pavlukhina, S.; Zhuk, I.; Mentbayeva, A.; Rautenberg, E.; Chang, W.; Yu, X.; van de Belt-Gritter, B.; Busscher, H. J.; van der Mei, H. C.; Sukhishvili, S. A., Small-molecule-hosting nanocomposite films with multiple bacteria-triggered responses. *Npg Asia Materials* **2014,** *6*, e121.

86. Zhuk, I.; Jariwala, F.; Attygalle, A. B.; Wu, Y.; Libera, M. R.; Sukhishvili, S. A., Self-defensive layer-by-layer films with bacteria-triggered antibiotic release. *Acs Nano* **2014,** *8* (8), 7733.

87. Wang, B.; Jin, T.; Xu, Q.; Liu, H.; Ye, Z.; Chen, H., Direct loading and tunable release of antibiotics from polyelectrolyte multilayers to reduce bacterial adhesion and biofilm formation. *Bioconjugate Chemistry* **2016,** *27* (5), 1305.

88. Albright, V.; Zhuk, I.; Wang, Y.; Selin, V.; van de Belt-Gritter, B.; Busscher, H. J.; van der Mei, H. C.; Sukhishvili, S. A., Self-defensive antibiotic-loaded layer-by-layer coatings: Imaging of localized bacterial acidification and ph-triggering of antibiotic release. *Acta Biomaterialia* **2017,** *61*, 66.

89. Bratskaya, S.; Marinin, D.; Simon, F.; Synytska, A.; Zschoche, S.; Busscher, H. J.; Jager, D.; van der Mei, H. C., Adhesion and viability of two enterococcal strains on covalently grafted chitosan and chitosan/κ-carrageenan multilayers. *Biomacromolecules* **2007,** *8* (9), 2960.

90. Elsabee, M. Z.; Abdou, E. S.; Nagy, K. S. A.; Eweis, M., Surface modification of polypropylene films by chitosan and chitosan/pectin multilayer. *Carbohyd Polym* **2008,** *71* (2), 187.

91. Lichter, J. A.; Rubner, M. F., Polyelectrolyte multilayers with intrinsic antimicrobial functionality: The importance of mobile polycations. *Langmuir* **2009,** *25* (13), 7686.

92. Cui, D.; Szarpak, A.; Pignot-Paintrand, I.; Varrot, A.; Boudou, T.; Detrembleur, C.; Jérôme, C.; Picart, C.; Auzély-Velty, R., Contact-killing polyelectrolyte

microcapsules based on chitosan derivatives. *Adv Funct Mater* **2010,** *20* (19), 3303.

93. Wong, S. Y.; Li, Q.; Veselinovic, J.; Kim, B.-S.; Klibanov, A. M.; Hammond, P. T., Bactericidal and virucidal ultrathin films assembled layer by layer from polycationic n-alkylated polyethylenimines and polyanions. *Biomaterials* **2010,** *31* (14), 4079.

94. Deng, H.; Wang, X.; Liu, P.; Ding, B.; Du, Y.; Li, G.; Hu, X.; Yang, J., Enhanced bacterial inhibition activity of layer-by-layer structured polysaccharide film-coated cellulose nanofibrous mats via addition of layered silicate. *Carbohyd Polym* **2011,** *83* (1), 239.

95. Pinto, M. S.; McGahan, M. E.; Steiner, W. W.; Priefer, R., The use of the pseudo-polyelectrolyte, poly(4-vinylphenol), in multilayered films as an antimicrobial surface coating. *Colloids and Surfaces A: Physicochemical and Engineering Aspects* **2011,** *377* (1), 182.

96. Illergård, J.; Römling, U.; Wågberg, L.; Ek, M., Biointeractive antibacterial fibres using polyelectrolyte multilayer modification. *Cellulose* **2012,** *19* (5), 1731.

97. Xin, S.; Li, X.; Ma, Z.; Lei, Z.; Zhao, J.; Pan, S.; Zhou, X.; Deng, H., Cytotoxicity and antibacterial ability of scaffolds immobilized by polysaccharide/layered silicate composites. *Carbohyd Polym* **2013,** *92* (2), 1880.

98. Wei, T.; Zhan, W.; Cao, L.; Hu, C.; Qu, Y.; Yu, Q.; Chen, H., Multifunctional and regenerable antibacterial surfaces fabricated by a universal strategy. *Acs Appl Mater Inter* **2016,** *8* (44), 30048.

99. Wei, T.; Tang, Z.; Yu, Q.; Chen, H., Smart antibacterial surfaces with switchable bacteria-killing and bacteria-releasing capabilities. *Acs Appl Mater Inter* **2017,** *9* (43), 37511.

100. Fu, J.; Ji, J.; Yuan, W.; Shen, J., Construction of anti-adhesive and antibacterial multilayer films via layer-by-layer assembly of heparin and chitosan. *Biomaterials* **2005,** *26* (33), 6684.

101. Bertrand, P.; Jonas, A.; Laschewsky, A.; Legras, R., Ultrathin polymer coatings by complexation of polyelectrolytes at interfaces: Suitable materials, structure and properties. *Macromolecular Rapid Communications* **2000,** *21* (7), 319.

102. Fu, J.; Fares, H. M.; Schlenoff, J. B., Ion-pairing strength in polyelectrolyte complexes. *Macromolecules* **2017,** *50* (3), 1066.

103. Wang, Q.; Schlenoff, J. B., The polyelectrolyte complex/coacervate continuum. *Macromolecules* **2014,** *47* (9), 3108.

104. de Jong, H. G. B.; Kruyt, H. R., Koazervation. *Kolloid-Zeitschrift* **1930,** *50* (1), 39.

105. Fuoss, R. M.; Sadek, H., Mutual interaction of polyelectrolytes. *Science* **1949,** *110* (2865), 552.

106. Michaels, A. S., Polyelectrolyte complexes. *Industrial & Engineering Chemistry* **1965,** *57* (10), 32.

107. Perry, S.; Li, Y.; Priftis, D.; Leon, L.; Tirrell, M., The effect of salt on the complex coacervation of vinyl polyelectrolytes. *Polymers* **2014,** *6* (6), 1756.

108. Kelly, K. D.; Schlenoff, J. B., Spin-coated polyelectrolyte coacervate films. *Acs Appl Mater Inter* **2015,** *7* (25), 13980.

109. Haile, M.; Sarwar, O.; Henderson, R.; Smith, R.; Grunlan, J. C., Polyelectrolyte coacervates deposited as high gas barrier thin films. *Macromolecular Rapid Communications* **2017,** *38* (1), 1600594.

110. Priftis, D.; Megley, K.; Laugel, N.; Tirrell, M., Complex coacervation of poly(ethylene-imine)/polypeptide aqueous solutions: Thermodynamic and rheological characterization. *J Colloid Interf Sci* **2013,** *398*, 39.

111. Chollakup, R.; Smitthipong, W.; Eisenbach, C. D.; Tirrell, M., Phase behavior and coacervation of aqueous poly(acrylic acid)−poly(allylamine) solutions. *Macromolecules* **2010,** *43* (5), 2518.

112. Zhang, Y.; Yildirim, E.; Antila, H. S.; Valenzuela, L. D.; Sammalkorpi, M.; Lutkenhaus, J. L., The influence of ionic strength and mixing ratio on the colloidal stability of pdac/pss polyelectrolyte complexes. *Soft Matter* **2015,** *11* (37), 7392.

113. Michaels, A. S.; Mir, L.; Schneider, N. S., A conductometric study of polycation—polyanion reactions in dilute aqueous solution. *The Journal of Physical Chemistry* **1965,** *69* (5), 1447.

114. Alonso, T.; Irigoyen, J.; Iturri, J. J.; larena, I. L.; Moya, S. E., Study of the multilayer assembly and complex formation of poly(diallyldimethylammonium chloride) (pdadmac) and poly(acrylic acid) (paa) as a function of ph. *Soft Matter* **2013,** *9* (6), 1920.

115. Gucht, J. v. d.; Spruijt, E.; Lemmers, M.; Cohen Stuart, M. A., Polyelectrolyte complexes: Bulk phases and colloidal systems. *J Colloid Interf Sci* **2011,** *361* (2), 407.

116. Karibyants, N.; Dautzenberg, H.; Cölfen, H., Characterization of pss/pdadmac-co-aa polyelectrolyte complexes and their stoichiometry using analytical ultracentrifugation. *Macromolecules* **1997,** *30* (25), 7803.

117. Chen, J.; Heitmann, J. A.; Hubbe, M. A., Dependency of polyelectrolyte complex stoichiometry on the order of addition. 1. Effect of salt concentration during streaming current titrations with strong poly-acid and poly-base. *Colloids and Surfaces A: Physicochemical and Engineering Aspects* **2003,** *223* (1), 215.

118. A., K. V.; B., Z. A., Soluble interpolymeric complexes as a new class of synthetic polyelectrolytes. *Pure and Applied Chemistry* **1984,** *56* (3), 343.

119. Iler, R. K., Multilayers of colloidal particles. *J Colloid Interf Sci* **1966,** *21* (6), 569.

120. Decher, G.; Hong, J. D.; Schmitt, J., Buildup of ultrathin multilayer films by a self-assembly process: Iii. Consecutively alternating adsorption of anionic and cationic polyelectrolytes on charged surfaces. *Thin Solid Films* **1992,** *210-211* (Part 2), 831.

121. Kharlampieva, E.; Sukhishvili, S. A., Hydrogen-bonded layer-by-layer polymer films. *Polym Rev* **2006,** *46* (4), 377.

122. Wang, L.; Wang, Z.; Zhang, X.; Shen, J.; Chi, L.; Fuchs, H., A new approach for the fabrication of an alternating multilayer film of poly(4-vinylpyridine) and poly(acrylic acid) based on hydrogen bonding. *Macromolecular Rapid Communications* **1997,** *18* (6), 509.

123. Nestler, P.; Block, S.; Helm, C. A., Temperature-induced transition from odd–even to even–odd effect in polyelectrolyte multilayers due to interpolyelectrolyte interactions. *The Journal of Physical Chemistry B* **2012,** *116* (4), 1234.

124. Tan, H. L.; McMurdo, M. J.; Pan, G. Q.; Van Patten, P. G., Temperature dependence of polyelectrolyte multilayer assembly. *Langmuir* **2003,** *19* (22), 9311.

125. Shiratori, S. S.; Rubner, M. F., Ph-dependent thickness behavior of sequentially adsorbed layers of weak polyelectrolytes. *Macromolecules* **2000,** *33* (11), 4213.

126. Izumrudov, V.; Sukhishvili, S. A., Ionization-controlled stability of polyelectrolyte multilayers in salt solutions. *Langmuir* **2003,** *19* (13), 5188.

127. Dubas, S. T.; Schlenoff, J. B., Swelling and smoothing of polyelectrolyte multilayers by salt. *Langmuir* **2001,** *17* (25), 7725.

128. Gong, X.; Gao, C., Influence of salt on assembly and compression of pdadmac/pssma polyelectrolyte multilayers. *Physical Chemistry Chemical Physics* **2009,** *11* (48), 11577.

129. Apaydin, K.; Laachachi, A.; Ball, V.; Jimenez, M.; Bourbigot, S.; Toniazzo, V.; Ruch, D., Polyallylamine-montmorillonite as super flame retardant coating assemblies by layer-by layer deposition on polyamide. *Polymer Degradation and Stability* **2013,** *98* (2), 627.

130. Guin, T.; Krecker, M.; Hagen, D. A.; Grunlan, J. C., Thick growing multi layer nanobrick wall thin films: Super gas barrier with very few layers. *Langmuir* **2014,** *30* (24), 7057.

131. Hagen, D. A.; Box, C.; Greenlee, S.; Xiang, F.; Regev, O.; Grunlan, J. C., High gas barrier imparted by similarly charged multilayers in nanobrick wall thin films. *RSC Advances* **2014,** *4* (35), 18354.

132. Kim, Y. S.; Davis, R., Multi-walled carbon nanotube layer-by-layer coatings with a trilayer structure to reduce foam flammability. *Thin Solid Films* **2014,** *550*, 184.

133. Podsiadlo, P.; Michel, M.; Lee, J.; Verploegen, E.; Wong Shi Kam, N.; Ball, V.; Lee, J.; Qi, Y.; Hart, A. J.; Hammond, P. T.; Kotov, N. A., Exponential growth of lbl films with incorporated inorganic sheets. *Nano Lett* **2008,** *8* (6), 1762.

134. Green, J., Mechanisms for flame retardancy and smoke suppression - a review. *J Fire Sci* **1996,** *14* (6), 426.

135. Morgan, A. B.; Wilkie, C. A., *Flame retardant polymer nanocomposites*. John Wiley & Sons: 2007.

136. Haile, M.; Fomete, S.; Lopez, I. D.; Grunlan, J. C., Aluminum hydroxide multilayer assembly capable of extinguishing flame on polyurethane foam. *J Mater Sci* **2016,** *51* (1), 375.

137. Zhang, X.; Shen, Q.; Zhang, X.; Pan, H.; Lu, Y., Graphene oxide-filled multilayer coating to improve flame-retardant and smoke suppression properties of flexible polyurethane foam. *J Mater Sci* **2016,** *51* (23), 10361.

138. Hori, K.; Matsumoto, S., Bacterial adhesion: From mechanism to control. *Biochemical Engineering Journal* **2010,** *48* (3), 424.

139. Marjaka, I. W.; Miyanaga, K.; Hori, K.; Tanji, Y.; Unno, H., Augmentation of self-purification capacity of sewer pipe by immobilizing microbes on the pipe surface. *Biochemical Engineering Journal* **2003,** *15* (1), 69.

140. Wang, Z.-W.; Chen, S., Potential of biofilm-based biofuel production. *Applied Microbiology and Biotechnology* **2009,** *83* (1), 1.

141. Marshall, K. C.; Stout, R.; Mitchell, R., Mechanism of the initial events in the sorption of marine bacteria to surfaces. *Microbiology* **1971,** *68* (3), 337.

142. Hermansson, M., The dlvo theory in microbial adhesion. *Colloids and Surfaces B: Biointerfaces* **1999,** *14* (1–4), 105.

143. Van Oss, C. J., The forces involved in bioadhesion to flat surfaces and particles — their determination and relative roles. *Biofouling* **1991,** *4* (1-3), 25.

144. Chen, S.; Li, L.; Zhao, C.; Zheng, J., Surface hydration: Principles and applications toward low-fouling/nonfouling biomaterials. *Polymer* **2010,** *51* (23), 5283.

145. Garrett, T. R.; Bhakoo, M.; Zhang, Z., Bacterial adhesion and biofilms on surfaces. *Progress in Natural Science* **2008,** *18* (9), 1049.

146. Riga, E. K.; Vöhringer, M.; Widyaya, V. T.; Lienkamp, K., Polymer-based surfaces designed to reduce biofilm formation: From antimicrobial polymers to strategies for long-term applications. *Macromolecular Rapid Communications* **2017,** *38* (20), 1700216.

147. Soto, G. E.; Hultgren, S. J., Bacterial adhesins: Common themes and variations in architecture and assembly. *Journal of Bacteriology* **1999,** *181* (4), 1059.

148. Klemm, P.; Schembri, M. A., Bacterial adhesins: Function and structure. *International Journal of Medical Microbiology* **2000,** *290* (1), 27.

149. Pratt, L. A.; Kolter, R., Genetic analysis of escherichia coli biofilm formation: Roles of flagella, motility, chemotaxis and type i pili. *Molecular Microbiology* **1998,** *30* (2), 285.

150. Berne, C.; Ducret, A.; Hardy, G. G.; Brun, Y. V., Adhesins involved in attachment to abiotic surfaces by gram-negative bacteria. *Microbiology spectrum* **2015,** *3* (4), 10.1128/microbiolspec.MB.

151. Scott, J. R.; Zähner, D., Pili with strong attachments: Gram-positive bacteria do it differently. *Molecular Microbiology* **2006,** *62* (2), 320.

152. Nielsen, P. H.; Jahn, A.; Palmgren, R., Conceptual model for production and composition of exopolymers in biofilms. *Water Science and Technology* **1997,** *36* (1), 11.

153. Whitney, J. C.; Howell, P. L., Synthase-dependent exopolysaccharide secretion in gram-negative bacteria. *Trends in microbiology* **2013,** *21* (2), 63.

154. Peng George, W.; Hongjie, G.; Wen, Y.; Jing, K. S., Current understanding on biosynthesis of microbial polysaccharides. *Current Topics in Medicinal Chemistry* **2008,** *8* (2), 141.

155. Feng, Q. L.; Wu, J.; Chen, G. Q.; Cui, F. Z.; Kim, T. N.; Kim, J. O., A mechanistic study of the antibacterial effect of silver ions on escherichia coli and staphylococcus aureus. *Journal of Biomedical Materials Research* **2000,** *52* (4), 662.

156. Lee, S. B.; Koepsel, R. R.; Morley, S. W.; Matyjaszewski, K.; Sun, Y.; Russell, A. J., Permanent, nonleaching antibacterial surfaces. 1. Synthesis by atom transfer radical polymerization. *Biomacromolecules* **2004,** *5* (3), 877.

157. Kügler, R.; Bouloussa, O.; Rondelez, F., Evidence of a charge-density threshold for optimum efficiency of biocidal cationic surfaces. *Microbiology* **2005,** *151* (5), 1341.

158. Yu, Q.; Cho, J.; Shivapooja, P.; Ista, L. K.; López, G. P., Nanopatterned smart polymer surfaces for controlled attachment, killing, and release of bacteria. *Acs Appl Mater Inter* **2013,** *5* (19), 9295.

159. Yu, Q.; Ge, W.; Atewologun, A.; Lopez, G. P.; Stiff-Roberts, A. D., Rir-maple deposition of multifunctional films combining biocidal and fouling release properties. *Journal of Materials Chemistry B* **2014,** *2* (27), 4371.

160. Katsuhiko, A.; Yusuke, Y.; Gaulthier, R.; Qingmin, J.; Yusuke, Y.; C.-W., W. K.; P., H. J., Layer-by-layer nanoarchitectonics: Invention, innovation, and evolution. *Chemistry Letters* **2014,** *43* (1), 36.

161. Zhao, Q.; An, Q. F.; Ji, Y.; Qian, J.; Gao, C., Polyelectrolyte complex membranes for pervaporation, nanofiltration and fuel cell applications. *Journal of Membrane Science* **2011,** *379* (1), 19.

162. Zhumadilova, G. T.; Gazizov, A. D.; Bimendina, L. A.; Kudaibergenov, S. E., Properties of polyelectrolyte complex membranes based on some weak polyelectrolytes. *Polymer* **2001,** *42* (7), 2985.

163. Smitha, B.; Sridhar, S.; Khan, A. A., Polyelectrolyte complexes of chitosan and poly(acrylic acid) as proton exchange membranes for fuel cells. *Macromolecules* **2004,** *37* (6), 2233.

164. Haile, M.; Fincher, C.; Fomete, S.; Grunlan, J. C., Water-soluble polyelectrolyte complexes that extinguish fire on cotton fabric when deposited as ph-cured nanocoating. *Polymer Degradation and Stability* **2015,** *114* (Supplement C), 60.

165. Haile, M.; Leistner, M.; Sarwar, O.; Toler, C. M.; Henderson, R.; Grunlan, J. C., A wash-durable polyelectrolyte complex that extinguishes flames on polyester-cotton fabric. *RSC Advances* **2016,** *6* (40), 33998.

166. Leistner, M.; Haile, M.; Rohmer, S.; Abu-Odeh, A.; Grunlan, J. C., Water-soluble polyelectrolyte complex nanocoating for flame retardant nylon-cotton fabric. *Polymer Degradation and Stability* **2015,** *122*, 1.

167. Porcel, C. H.; Izquierdo, A.; Ball, V.; Decher, G.; Voegel, J. C.; Schaaf, P., Ultrathin coatings and (poly(glutamic acid)/polyallylamine) films deposited by continuous and simultaneous spraying. *Langmuir* **2005,** *21* (2), 800.

168. Lefort, M.; Popa, G.; Seyrek, E.; Szamocki, R.; Felix, O.; Hemmerlé, J.; Vidal, L.; Voegel, J.-C.; Boulmedais, F.; Decher, G.; Schaaf, P., Spray-on organic/inorganic films: A general method for the formation of functional nano- to microscale coatings. *Angewandte Chemie International Edition* **2010,** *49* (52), 10110.

169. Kim, M.; Yeo, S. J.; Highley, C. B.; Burdick, J. A.; Yoo, P. J.; Doh, J.; Lee, D., One-step generation of multifunctional polyelectrolyte microcapsules via nanoscale interfacial complexation in emulsion (nice). *Acs Nano* **2015,** *9* (8), 8269.

170. Wang, Q.; Schlenoff, J. B., Single- and multicompartment hollow polyelectrolyte complex microcapsules by one-step spraying. *Adv Mater* **2015,** *27* (12), 2077.

171. Zhang, L.; Cai, L.-H.; Lienemann, P. S.; Rossow, T.; Polenz, I.; Vallmajo-Martin, Q.; Ehrbar, M.; Na, H.; Mooney, D. J.; Weitz, D. A., One-step microfluidic fabrication of polyelectrolyte microcapsules in aqueous conditions for protein release. *Angewandte Chemie* **2016,** *128* (43), 13668.

172. Hann, S. D.; Niepa, T. H. R.; Stebe, K. J.; Lee, D., One-step generation of cell-encapsulating compartments via polyelectrolyte complexation in an aqueous two phase system. *Acs Appl Mater Inter* **2016,** *8* (38), 25603.

173. Duan, G.; Haase, M. F.; Stebe, K. J.; Lee, D., One-step generation of salt-responsive polyelectrolyte microcapsules via surfactant-organized nanoscale interfacial complexation in emulsions (so nice). *Langmuir* **2017**.

174. Ball, V.; Michel, M.; Toniazzo, V.; Ruch, D., The possibility of obtaining films by single sedimentation of polyelectrolyte complexes. *Industrial & Engineering Chemistry Research* **2013,** *52* (16), 5691.

175. Mocchiutti, P.; Galván, M. V.; Peresin, M. S.; Schnell, C. N.; Zanuttini, M. A., Complexes of xylan and synthetic polyelectrolytes. Characterization and adsorption onto high quality unbleached fibres. *Carbohyd Polym* **2015,** *116*, 131.

176. Cain, A. A.; Murray, S.; Holder, K. M.; Nolen, C. R.; Grunlan, J. C., Intumescent nanocoating extinguishes flame on fabric using aqueous polyelectrolyte complex deposited in single step. *Macromolecular Materials and Engineering* **2014,** *299* (10), 1180.

177. Lvov, Y.; Abdullayev, E., Functional polymer–clay nanotube composites with sustained release of chemical agents. *Progress in Polymer Science* **2013,** *38* (10–11), 1690.

178. Liu, M.; Jia, Z.; Jia, D.; Zhou, C., Recent advance in research on halloysite nanotubes-polymer nanocomposite. *Progress in Polymer Science* **2014,** *39* (8), 1498.

179. Lvov, Y.; Wang, W.; Zhang, L.; Fakhrullin, R., Halloysite clay nanotubes for loading and sustained release of functional compounds. *Adv Mater* **2016,** *28* (6), 1227.

180. Kim, J.; Park, N.-h.; Na, J. H.; Han, J., Development of natural insect-repellent loaded halloysite nanotubes and their application to food packaging to prevent plodia interpunctella infestation. *Journal of Food Science* **2016,** *81* (8), E1956.

181. Jin, Y.; Yendluri, R.; Chen, B.; Wang, J.; Lvov, Y., Composite microparticles of halloysite clay nanotubes bound by calcium carbonate. *J Colloid Interf Sci* **2016,** *466*, 254.

182. Zheng, T.; Ni, X., Loading an organophosphorous flame retardant into halloysite nanotubes for modifying uv-curable epoxy resin. *RSC Advances* **2016,** *6* (62), 57122.

183. Joshi, A. R.; Null, R.; Graham, S.; Abdullayev, E.; Mazurenko, V.; Lvov, Y., Enhanced flame retardancy of latex coating doped with clay nanotubes. *Journal of Coatings Technology and Research* **2016,** *13* (3), 535.

184. Olugebefola, S. C.; Hamilton, A. R.; Fairfield, D. J.; Sottos, N. R.; White, S. R., Structural reinforcement of microvascular networks using electrostatic layer-by-layer assembly with halloysite nanotubes. *Soft Matter* **2014,** *10* (4), 544.

185. Cavallaro, G.; Lazzara, G.; Konnova, S.; Fakhrullin, R.; Lvov, Y., Composite films of natural clay nanotubes with cellulose and chitosan. *Green Materials* **2014,** *2* (4), 232.

186. Lvov, Y.; Price, R.; Gaber, B.; Ichinose, I., Thin film nanofabrication via layer-by-layer adsorption of tubule halloysite, spherical silica, proteins and polycations. *Colloids and Surfaces A: Physicochemical and Engineering Aspects* **2002,** *198–200*, 375.

187. Lu, Z.; Eadula, S.; Zheng, Z.; Xu, K.; Grozdits, G.; Lvov, Y., Layer-by-layer nanoparticle coatings on lignocellulose wood microfibers. *Colloids and Surfaces A: Physicochemical and Engineering Aspects* **2007,** *292* (1), 56.

188. Gamboa, D.; Priolo, M. A.; Ham, A.; Grunlan, J. C., Note: Influence of rinsing and drying routines on growth of multilayer thin films using automated deposition system. *Rev Sci Instrum* **2010,** *81* (3), 036103.

189. Zhao, Y.; Cavallaro, G.; Lvov, Y., Orientation of charged clay nanotubes in evaporating droplet meniscus. *J Colloid Interf Sci* **2015,** *440*, 68.

190. Bilbao, R.; Mastral, J. F.; Ceamanos, J.; Aldea, M. E., Kinetics of the thermal decomposition of polyurethane foams in nitrogen and air atmospheres. *Journal of Analytical and Applied Pyrolysis* **1996,** *37* (1), 69.

191. Wang, T.-L.; Hsieh, T.-H., Effect of polyol structure and molecular weight on the thermal stability of segmented poly(urethaneureas). *Polymer Degradation and Stability* **1997,** *55* (1), 95.

192. Benbow, A. W.; Cullis, C. F., The combustion of flexible polyurethane foams: Mechanisms and evaluation of flame retardance. *Combustion and Flame* **1975,** *24*, 217.

193. Zatta, L.; Gardolinski, J. E. F. d. C.; Wypych, F., Raw halloysite as reusable heterogeneous catalyst for esterification of lauric acid. *Applied Clay Science* **2011,** *51* (1–2), 165.

194. Huggett, C., Estimation of rate of heat release by means of oxygen consumption measurements. *Fire Mater* **1980,** *4* (2), 61.

195. Wang, L.; He, X.; Wilkie, C. A., The utility of nanocomposites in fire retardancy. *Materials* **2010,** *3* (9), 4580.

196. Babrauskas, V.; Peacock, R. D., Heat release rate: The single most important variable in fire hazard. *Fire Safety J* **1992,** *18* (3), 255.

197. Zhu, H.; Du, M.; Zou, M.; Xu, C.; Fu, Y., Green synthesis of au nanoparticles immobilized on halloysite nanotubes for surface-enhanced raman scattering substrates. *Dalton Transactions* **2012,** *41* (34), 10465.

198. Neely, A. N.; Maley, M. P., Survival of enterococci and staphylococci on hospital fabrics and plastic. *J Clin Microbiol* **2000,** *38* (2), 724.

199. Malani, P. N., National burden of invasive methicillin-resistant staphylococcus aureus infection. *JAMA* **2014,** *311* (14), 1438.

200. Takashima, M.; Shirai, F.; Sageshima, M.; Ikeda, N.; Okamoto, Y.; Dohi, Y., Distinctive bacteria-binding property of cloth materials. *Am J Infect Control* **2004,** *32* (1), 27.

201. Kong, Y.; Shi, Y.; Chang, M.; Akin, A. R.; Francis, K. P.; Zhang, N.; Troy, T. L.; Yao, H.; Rao, J.; Cirillo, S. L. G.; Cirillo, J. D., Whole-body imaging of infection using bioluminescence. In *Current protocols in microbiology*, John Wiley & Sons, Inc.: 2005.

202. Williford, J.-M.; Archang, M. M.; Minn, I.; Ren, Y.; Wo, M.; Vandermark, J.; Fisher, P. B.; Pomper, M. G.; Mao, H.-Q., Critical length of peg grafts on lpei/DNA nanoparticles for efficient in vivo delivery. *ACS Biomaterials Science & Engineering* **2016,** *2* (4), 567.

203. Chang, M.; Anttonen, K. P.; Cirillo, S. L. G.; Francis, K. P.; Cirillo, J. D., Real-time bioluminescence imaging of mixed mycobacterial infections. *PLOS ONE* **2014,** *9* (9), e108341.

204. Gamboa, D.; Priolo, M. A.; Ham, A.; Grunlan, J. C., Note: Influence of rinsing and drying routines on growth of multilayer thin films using automated deposition system. *Rev Sci Instrum* **2010,** *81* (3).

205. Bieker, P.; Schönhoff, M., Linear and exponential growth regimes of multilayers of weak polyelectrolytes in dependence on ph. *Macromolecules* **2010,** *43* (11), 5052.

206. Srivastava, S.; Ball, V.; Podsiadlo, P.; Lee, J.; Ho, P.; Kotov, N. A., Reversible loading and unloading of nanoparticles in “exponentially” growing polyelectrolyte lbl films. *Journal of the American Chemical Society* **2008,** *130* (12), 3748.

207. Choi, J.; Rubner, M. F., Influence of the degree of ionization on weak polyelectrolyte multilayer assembly. *Macromolecules* **2005,** *38* (1), 116.

208. Fou, A. C.; Rubner, M. F., Molecular-level processing of conjugated polymers. 2. Layer-by-layer manipulation of in-situ polymerized p-type doped conducting polymers. *Macromolecules* **1995,** *28* (21), 7115.

209. Itano, K.; Choi, J.; Rubner, M. F., Mechanism of the ph-induced discontinuous swelling/deswelling transitions of poly(allylamine hydrochloride)-containing polyelectrolyte multilayer films. *Macromolecules* **2005,** *38* (8), 3450.

210. Yang, Y.-H.; Haile, M.; Park, Y. T.; Malek, F. A.; Grunlan, J. C., Super gas barrier of all-polymer multilayer thin films. *Macromolecules* **2011,** *44* (6), 1450.

211. Gebhardt, J. E.; Fuerstenau, D. W., Adsorption of polyacrylic acid at oxide/water interfaces. *Colloids and Surfaces* **1983,** *7* (3), 221.

212. Van Oss, C. J.; Chaudhury, M. K.; Good, R. J., Interfacial lifshitz-van der waals and polar interactions in macroscopic systems. *Chemical Reviews* **1988,** *88* (6), 927.

213. Williams, R. E. O., Staphylococcus aureus on the skin. *British Journal of Dermatology* **1969,** *81*, 33.

214. Mitik-Dineva, N.; Wang, J.; Truong, V. K.; Stoddart, P.; Malherbe, F.; Crawford, R. J.; Ivanova, E. P., Escherichia coli, pseudomonas aeruginosa, and staphylococcus aureus attachment patterns on glass surfaces with nanoscale roughness. *Current Microbiology* **2009,** *58* (3), 268.

215. Lüdecke, C.; Roth, M.; Yu, W.; Horn, U.; Bossert, J.; Jandt, K. D., Nanorough titanium surfaces reduce adhesion of escherichia coli and staphylococcus aureus via nano adhesion points. *Colloids and Surfaces B: Biointerfaces* **2016,** *145*, 617.

216. Boukhriss, A.; Gmouh, S.; Hannach, H.; Roblin, J.-P.; Cherkaoui, O.; Boyer, D., Treatment of cotton fabrics by ionic liquid with pf6 − anion for enhancing their flame retardancy and water repellency. *Cellulose* **2016,** *23* (5), 3355.

217. Smith, R. J.; Moule, M. G.; Sule, P.; Smith, T.; Cirillo, J. D.; Grunlan, J. C., Polyelectrolyte multilayer nanocoating dramatically reduces bacterial adhesion to polyester fabric. *ACS Biomaterials Science & Engineering* **2017,** *3* (8), 1845.

218. Cui, L.; Butler, H. J.; Martin-Hirsch, P. L.; Martin, F. L., Aluminium foil as a potential substrate for atr-ftir, transflection ftir or raman spectrochemical analysis of biological specimens. *Analytical Methods* **2016,** *8* (3), 481.

219. Kim, S. H.; Misner, M. J.; Xu, T.; Kimura, M.; Russell, T. P., Highly oriented and ordered arrays from block copolymers via solvent evaporation. *Adv Mater* **2004,** *16* (3), 226.

220. Zhang, L.; Zheng, M.; Liu, X.; Sun, J., Layer-by-layer assembly of salt-containing polyelectrolyte complexes for the fabrication of dewetting-induced porous coatings. *Langmuir* **2011,** *27* (4), 1346.

221. Ghostine, R. A.; Jisr, R. M.; Lehaf, A.; Schlenoff, J. B., Roughness and salt annealing in a polyelectrolyte multilayer. *Langmuir* **2013,** *29* (37), 11742.

222. Bago Rodriguez, A. M.; Binks, B. P.; Sekine, T., Emulsion stabilisation by complexes of oppositely charged synthetic polyelectrolytes. *Soft Matter* **2018,** *14* (2), 239.

223. Lange, J.; Wyser, Y., Recent innovations in barrier technologies for plastic packaging—a review. *Packaging Technology and Science* **2003,** *16* (4), 149.

224. Gutierrez, M. M.; Meleddu, M.; Piga, A., Food losses, shelf life extension and environmental impact of a packaged cheesecake: A life cycle assessment. *Food Research International* **2017,** *91*, 124.

225. Marsh, K.; Bugusu, B., Food packaging—roles, materials, and environmental issues. *Journal of Food Science* **2007,** *72* (3), R39.

226. Dou, Y.; Pan, T.; Xu, S.; Yan, H.; Han, J.; Wei, M.; Evans, D. G.; Duan, X., Transparent, ultrahigh-gas-barrier films with a brick–mortar–sand structure. *Angewandte Chemie International Edition* **2015,** *54* (33), 9673.

227. Choi, J. H.; Park, Y. W.; Park, T. H.; Song, E. H.; Lee, H. J.; Kim, H.; Shin, S. J.; Lau Chun Fai, V.; Ju, B.-K., Fuzzy nanoassembly of polyelectrolyte and layered clay multicomposite toward a reliable gas barrier. *Langmuir* **2012,** *28* (17), 6826.

228. Qin, S.; Song, Y.; Floto, M. E.; Grunlan, J. C., Combined high stretchability and gas barrier in hydrogen-bonded multilayer nanobrick wall thin films. *Acs Appl Mater Inter* **2017,** *9* (9), 7903.

229. Song, Y.; Meyers, K. P.; Gerringer, J.; Ramakrishnan, R. K.; Humood, M.; Qin, S.; Polycarpou, A. A.; Nazarenko, S.; Grunlan, J. C., Fast self-healing of polyelectrolyte multilayer nanocoating and restoration of super oxygen barrier. *Macromolecular Rapid Communications* **2017,** *38* (10), 1700064.

230. Cramer, A. D.; Dong, W.-F.; Benbow, N. L.; Webber, J. L.; Krasowska, M.; Beattie, D. A.; Ferri, J. K., The influence of polyanion molecular weight on polyelectrolyte multilayers at surfaces: Elasticity and susceptibility to saloplasticity of strongly dissociated synthetic polymers at fluid-fluid interfaces. *Physical Chemistry Chemical Physics* **2017,** *19* (35), 23781.

231. Lindhoud, S.; Stuart, M. A. C., Relaxation phenomena during polyelectrolyte complex formation. In *Polyelectrolyte complexes in the dispersed and solid state i: Principles and theory*, Müller, M., Ed. Springer Berlin Heidelberg: Berlin, Heidelberg, 2014; pp 139.

232. Shamoun, R. F.; Reisch, A.; Schlenoff, J. B., Extruded saloplastic polyelectrolyte complexes. *Adv Funct Mater* **2012,** *22* (9), 1923.

233. Wei, Q.; Lin, J.; Shi, H.; Tang, G.; Chai, W.; Qin, L., Enhanced transparency of rough surface sapphire by surface vitrifaction process. *Acs Appl Mater Inter* **2018,** *10* (9), 7693.

234. Litmanovich, E. A.; Chernikova, E. V.; Stoychev, G. V.; Zakharchenko, S. O., Unusual phase behavior of the mixture of poly(acrylic acid) and

poly(diallyldimethylammonium chloride) in acidic media. *Macromolecules* **2010,** *43* (16), 6871.

235. Lagaron, J. M.; Catalá, R.; Gavara, R., Structural characteristics defining high barrier properties in polymeric materials. *Materials Science and Technology* **2004,** *20* (1), 1.

236. Zhang, R.; Zhang, Y.; Antila, H. S.; Lutkenhaus, J. L.; Sammalkorpi, M., Role of salt and water in the plasticization of pdac/pss polyelectrolyte assemblies. *The Journal of Physical Chemistry B* **2017,** *121* (1), 322.

237. Zhao, Q.; An, Q.; Sun, Z.; Qian, J.; Lee, K.-R.; Gao, C.; Lai, J.-Y., Studies on structures and ultrahigh permeability of novel polyelectrolyte complex membranes. *The Journal of Physical Chemistry B* **2010,** *114* (24), 8100.

238. Fares, H. M.; Ghoussoub, Y. E.; Surmaitis, R. L.; Schlenoff, J. B., Toward ion-free polyelectrolyte multilayers: Cyclic salt annealing. *Langmuir* **2015,** *31* (21), 5787.

239. Fares, H. M.; Schlenoff, J. B., Diffusion of sites versus polymers in polyelectrolyte complexes and multilayers. *Journal of the American Chemical Society* **2017,** *139* (41), 14656.

240. Fares, H. M.; Schlenoff, J. B., Equilibrium overcompensation in polyelectrolyte complexes. *Macromolecules* **2017,** *50* (10), 3968.

241. Leistner, M.; Abu-Odeh, A. A.; Rohmer, S. C.; Grunlan, J. C., Water-based chitosan/melamine polyphosphate multilayer nanocoating that extinguishes fire on polyester-cotton fabric. *Carbohyd Polym* **2015,** *130*, 227.